Geomorphology 101 (2008) 237–277

Contents lists available at ScienceDirect

Geomorphology

journal homepage: www.elsevier.com/locate/geomorph

Soil-geomorphology and "wet" cycles in the Holocene record of North-Central Mexico

Karl W. Butzer [a,*], James T. Abbott [b], Charles D. Frederick [a,c], Paul H. Lehman [a,1], Carlos E. Cordova [d], John F. Oswald [a]

[a] Department of Geography and the Environment, University of Texas at Austin, Austin TX 78712-3100, United States
[b] Environmental Affairs Division, Texas Department of Transportation, 125 E. 11th Street, Austin, TX 78701, United States
[c] 2901 FM 1496, Dublin, TX 76446, United States
[d] Department of Geography, Oklahoma State University, Stillwater OK 74078-4073, United States

ARTICLE INFO

Article history:
Received 18 August 2007
Received in revised form 9 May 2008
Accepted 9 May 2008
Available online 12 June 2008

Keywords:
Floodplain soils
"Wet" cycles
Disequilibrium events
Holocene
Soil erosion
Aridification

ABSTRACT

The distinction between the impact of climatic periodicities or land-use practices on soil erosion is an important issue for Pre-Hispanic and Colonial Mexico. That question can best be addressed by first documenting the dynamics of changing "wet" cycles during the Holocene in the central Mexican region between the northern limits of Pre-Hispanic agriculture and its southern margins in northwestern Chihuahua. Consequently the Laguna Project targeted a 125,000 km^2 sector of North-Central Mexico, 250 km from north to south and 500 km from east to west, from Saltillo to Durango. Some 40 sedimentary profiles with multiple cumulic soils were studied in the field and laboratory, supported by 163 conventional ^{14}C and AMS dates on charcoal and soil humates. We distinguish: (1) wet floodplains (with humic paleosols, redox phenomena reflecting high water tables, channel-ponding sequences, and interbedded tufas) that imply aquifer recharge, sustained base flow, and mainly low-energy conditions; and (2) high-energy pulses of discharge that mobilized cobble gravels or forced channel entrenchment ("gullying") and were tied to episodic, excessive rains that promoted valley and slope instability. In between such "wet" cycles and recurrent disequilibrium events, climate was similar to today, probably less humid, with limited geomorphologic change or slow soil formation.

"Wet" cycles were rare at the end of the Pleistocene, but prominent during the Holocene. Disequilibrium proxies became common and dramatic after 2500 BP. The drainages from the Eastern and Western Sierra Madres responded in phase, but varied in detail. Around AD 1050–1200 "natural" erosion led to loss of soil organic carbon, as alternating severe droughts and heavy rains destroyed the ground cover and led to ecological aridification, well before arrival of Spanish miners and settlers. The evidence that human activity triggered Pre-Hispanic or Colonial erosion in Central Mexico should therefore be re-evaluated. Global comparisons and interpretations are discussed, but with caution, since no single theory can explain the whole of the record. The soil-geomorphology geoarchive of North-Central Mexico primarily is an environmental history of alternating "wet" cycles, rather than of sustained wet or dry climates. The critical differences between "soaking" and "excessive" rains, with their respective impacts, may be due to switching between winter and summer storm categories.

1. Introduction

1.1. Questions

Geomorphology intersects with environmental history in a number of ways. One possible application is the delineation of changing physical environments against long-term settlement histories, to examine whether abrupt changes may induce archaeological or historical disjunctions. Conversely, changing land use may result in biotic, soil, and hydrological change, as geomorphic processes activate a chain of feedbacks that can result in degradation. Both kinds of intersection are addressed in a growing literature, some of it responsible, some of it less. That can become an unfortunate by-product of greater attention to the historic dimension and to ecological concerns. Cross-disciplinary relationships are immensely complex, in social and systemic terms, so that mere temporal coincidence does not explain cause-and-effect (Butzer, 2005).

At issue here is not, for example, the painstaking documentation that climatic forcing led to the abandonment of an irrigation network. The problems arise when big-picture authors (e.g. Sirocko et al., 1993;

* Corresponding author.
E-mail addresses: laguna@mail.utexas.edu (K.W. Butzer), phlehman@mail.utexas.edu (P.H. Lehman).
[1] For Table 1 please contact P.H. Lehman.

0169-555X/$ – see front matter © 2008 Elsevier B.V. All rights reserved.
doi:10.1016/j.geomorph.2008.06.005

Cullen et al., 2000; Drysdale et al., 2006) claim that (inferred) climatic changes caused agricultural decline and socio-political collapse over entire regions (E.K. Butzer, 1997; K.W. Butzer, 1997; see also Liu, 2007). Instead we are concerned here with the difficult middle ground, of how to distinguish the impact of secular climatic variation, on the one hand, from injudicious land-use intervention, on the other, in controlling ecological outcomes, especially in dry lands.

In Mexico, questions arise whether Spanish colonization led to ecological degradation, but also whether or not Pre-Hispanic peoples had a negative impact on the environment. Or did Spanish ecological pressures build on earlier, indigenous damage? It went almost unnoticed when Byrne and Horn (1989) published a thorough palynological study showing major deforestation in the coastal plains near Tuxtla during Classical times, well before the arrival of the Spaniards. But attention has been riveted by the limnological analysis of O'Hara et al. (1993) of multiple cores in highland Lake Pátzcuaro, demonstrating accelerated sedimentation during periods of adjacent Pre-Hispanic settlement since ~1900 BC. By comparison, soil erosion in Colonial times seemed more subdued. Fisher et al. (2003) dispute these findings, however, and instead attribute accelerated erosion to initial disturbance and landscape abandonment in the early Colonial era. We return to this important discourse in Section 9.4.

Another picture emerges in the Bajío region of Central Mexico. Here a large sedentary site is recorded at Villa de Reyes (probably Late Classic, ~AD 600–900). Intensive occupation had significant impact on rates of sedimentation in the adjacent stream, with accumulation of 3–4.5 m of alluvium in less than 400 years (dates on fill of ~AD 650–1030), with abundant cultural remains throughout. Yet the larger, Lajas drainage was unaffected, although here Colonial land use left a major and extensive record of accelerated mobilization (Frederick, 1995: 138–156, 195–197). This confirms the value of combined site-specific geoarchaeology and Quaternary watershed studies (see Butzer and Harris, 2007). Archival records further document the land cover of the Bajío during the 1500s and show widespread deforestation around older areas of indigenous settlement, especially around the large lakes—before the arrival of the Spaniards (Butzer and Butzer, 1997).

Although further studies of lake cores have been undertaken, Frederick's (1995) record for the northern Bajío suggests the need for nuanced alluvial studies, to identify the agents of soil erosion, and to compare the scale and intensity of indigenous versus Colonial disturbance. It is also critical to isolate the effects of climatic change, by examining alluvial and soil sequences north of the maximum expansion of Mesoamerican agriculture (Villa de Reyes; La Quemada [Nelson, 1997]), but south of the sedentary Casas Grandes archaeological cluster in the far northwest of Mexico. Before Spanish intrusion, except for the western Sierras, this vast area was only occupied by hunter–gatherers. It also represents a significant gap in terms of Quaternary research (see Section 9.3).

During the late 1980s and early 90s, a series of fieldtrips by Karl and Elisabeth Butzer identified promising geoarchives for study of the alluvial record of this geomorphological terra incognita. Several questions became apparent. Was the great semidesert interior of northern Mexico as bleak as it is today, when the first Europeans crossed it to Saltillo or El Paso? Did Spanish miners and ranchers degrade the vegetation and soils, or activate eolian processes? These issues led to formulation of the Laguna Project in conjunction with Charles Frederick. Fieldwork during 1996–2000 was focused in a rectangular swath of country between Saltillo and Durango (see Fig. 1), covering roughly 500 km from east to west (101°30′–105°30′ N) and 250 km from south to north (24°00′–26°30′ N).

1.2. The setting

As a matter of convenience, this area is designated as North-Central Mexico. To the east it is bounded by the folded, Cretaceous mountains of the Sierra Madre Oriental, in the west by the upfaulted igneous ranges of the Sierra Madre Occidental. In between is a characteristic mountain-and-bolson landscape, where through-streams from the east and west terminate in great endorheic basins, such as the Nazas delta plain and the shifting playas of the Mayran. Depending partly on elevation (1000–2000 m), the study area receives an annual precipitation of 250–500 cm, mainly during summer (70–85%), with frost-free winters. Given the mountainous perimeter and its rainshadows, significant moisture is derived from the Gulf of Mexico and the Pacific Ocean, frequently activated by hurricanes or tropical depressions.

Commonly referred to as the Chihuahuan Desert, over most of the region the native vegetation is dominated by semidesert shrub, thornbush, or parkland, the floristic associations and structure of which vary according to topography and substrate. Collectively grouped as *matorral*, such land cover has very low productivity and provides little raindrop interception, while the ground cover is sparse and incomplete. Various agaves, *Euphorbia*, ocotillo, and the distinctive yucca palms are mainly found on rocky slopes, while alluvial surfaces favor acacias, mesquite, and mimosaceae. On sandier surfaces, creosote, mesquite, and prickly pear may be more characteristic. In the playa environments with highly alkaline soils and gypsum, woody chenopods such as saltbush (*Atriplex*) are dominant, with scattered acacia and mesquite on less extreme substrates.

Riverine vegetation is more luxuriant, with ash, oak, willow, cottonwood (*Populus*), pecan or mesquite and considerable grass; dominants differ between eastern and western sectors (ash versus cottonwood). The foothill ranges have open mosaics of live oak and pine scrub, and at higher elevations grade into montane woodlands of pine, where juniper is a subdominant in the western sectors.

1.3. Objectives

From the beginning, the project design included a comprehensive picture of the variable evidence from the eastern, western, and central sectors of the study area. But the initial results were surprising: aridification appeared to predate European intrusion, an assessment that continued to be affirmed, even as the project focused on the stacks of paleosols identified in alluvial contexts of each sector. The time frame was accordingly pushed back, from the Late Holocene to the terminal Pleistocene, given alluvial records that were accessible without coring.

The most striking and informative sedimentary sequences are found in deeply entrenched stream valleys, and marked by sets of buried cumulic soils, many of them "black mucks" that appear somewhat anomalous in a low-productivity environment with little soil organic carbon (SOC). Amenable to radiometric dating, these alluvial sequences proved to be the centerpiece of the investigation, documenting repeated equilibrium cycles and allowing comparison of soil chronostratigraphies across different drainage basins, from east to west. Access to the great, exotic Nazas delta plain was less satisfactory, as a result of few good exposures and multiple distributaries of varying age, reflecting singular flood surges rather than systematically documenting channel evolution.

The playas, fed by various Nazas distributaries at different times, can be examined at a reasonable number of incidental quarry sites, typically dug down to water table at 4 or 5 m. These reveal interplays of eolian, paludal, lacustrine and alluvial depositional environments, with a rudimentary temporal structure available through dating of prominent paludal soils. But the rapid lateral shifts of facies indicate large-scale, Holocene changes in topographic definition of the playa floors, in response to episodes of strong sediment influx, deflation, differential autocompaction, and possible tectonic impulses. To effectively document the Holocene environmental history of the Mayran playa will entail another major project, but the materials presented here do elucidate the interfingering of local and long-

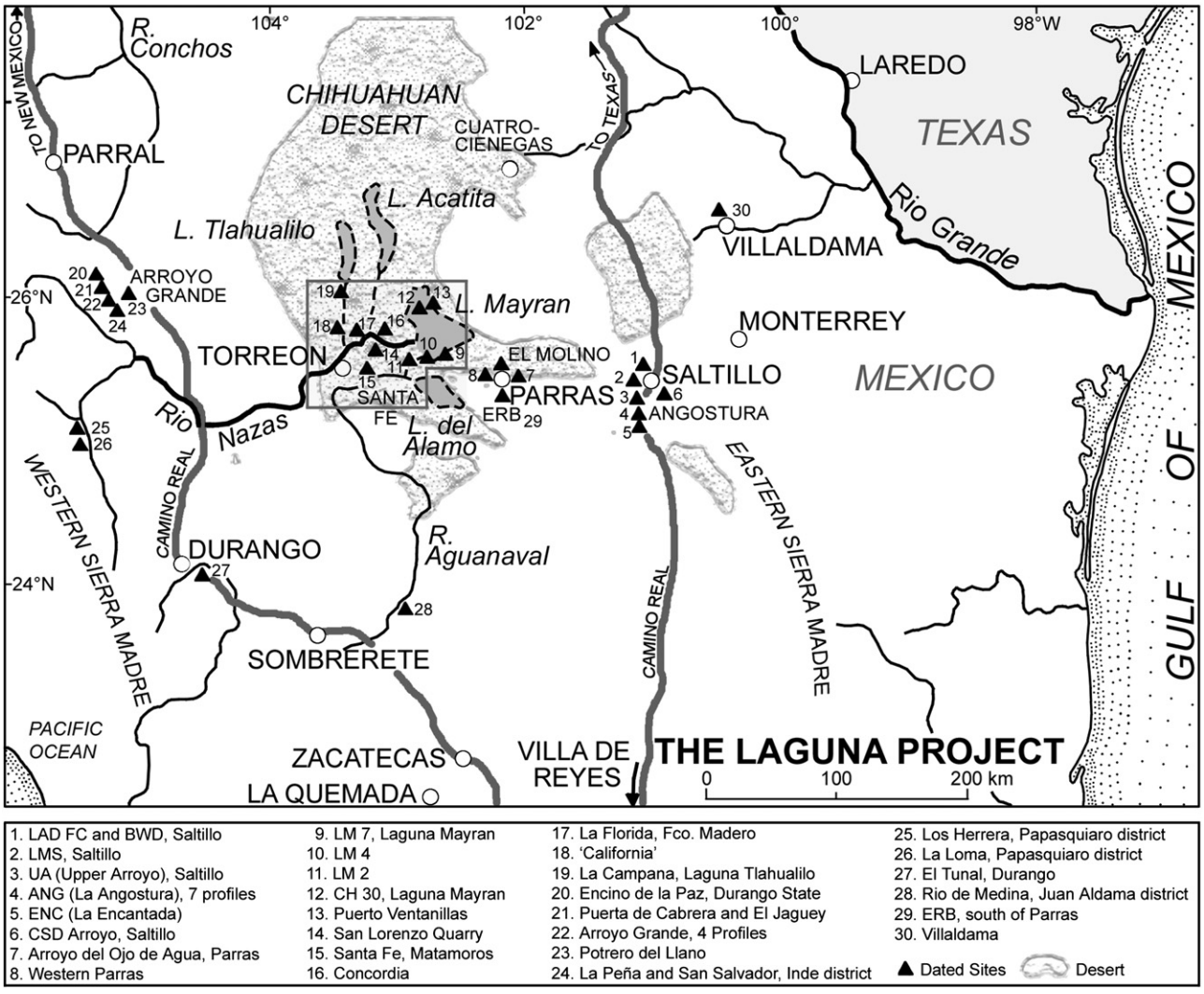

Fig. 1. The Laguna Project in northern Mexico, showing the major sites studied. The internal frame is shown with detail in Fig. 16. Casas Grandes and Babícora are located northwest of the map, north of latitude 29°.

distance sediments between the eastern and western sectors of the study area.

The final objective of the project was to develop a Holocene record for this little-studied area, so as to (1) better understand the linkages between the U.S. Southwest and Central Mexico; (2) re-examine the premises for human-induced degradation in Mexico; and (3) consider the place of this vast region in current discourse on global climatic change.

1.4. Methods

Some 40 sedimentary profiles were recorded, including stratification and contacts, structure, consistency and cementation, carbonate morphology, and illuvial features, nodules, mottling or ferruginous concentrations. Over 430 samples were processed at the University of Texas Laboratory of Applied Geomorphology and Geoarchaeology, with textural analyses by hydrometer and sieving, the results of which were graphed and converted to the standard analytic parameters. Organic matter was approximated by loss on ignition (LOI), after first removing matric and hygroscopic water, the results of which co-vary with those of the chemical Walkley–Black procedure (Schulte and Hopkins, 1996). Calcium carbonate equivalent (CCE) was approximated by the Chittick technique, although this method tends to under-represent CCE when values nominally exceed 20 or 30%. Magnetic susceptibility and pH were also determined, the latter fluctuating in a fairly narrow range from 7.0–8.6. An additional suite of over 200 samples was run by Frederick at the University of Sheffield, using Cilas laser textural techniques on cube-based samples.

Because clays and silts are the key diagnostic textural variables here, and relatively clean sands are rare, textures are reported in the international soils terminology; this also lends itself well to initial field approximation. In cases where precise textural parameters are material, φ and σ values are listed in the graphical representation. Horizons are designated according to common Quaternary and Soils usage (see USDA, 1999). Colors are dry Munsell readings.

Suites of samples for diatoms and ostracods were collected from many profiles and analyzed by Barbara Winsborough and M. Palacios-Fest (private consultants) respectively, but preservation was mainly poor and the results limited, much like Holocene diatoms were also rare at Babícora in northern Chihuahua (Metcalfe et al., 2002). Small gastropod shells and less common bivalves are present in the k-horizons beneath many soils, but have not yet been consigned to a specialist, because such sporadic units are not representative. The charaphytes (green algal silicic skeletons) encountered in many beds at Saltillo also deserve specialist study. Sporadic finds of animal bone were identified courtesy of Ernest W. Lundelius (University of Texas). Archaeological materials at the surface or within the profiles were recorded and photographed, as possible, but were not removed, in compliance with Mexican antiquity laws. Vegetation cross-sections were recorded by Carlos Cordova. A comprehensive palynological

Table 1
Radiocarbon ages from the Laguna project in North-Central Mexico organized by profile as presented in the text and figures

Site (figure)	Stratigraphic unit	^{14}C Age bp (uncalibrated)	Calibrated age BP (two sigma)	Median probability calibrated age (BP)	δ^{13}C (‰)	Lab number	Material
UA (Fig. 4)							
	G.1	370 ± 55	510-310	420	-25.3	AA 33471	Ch
	G.1	565 ± 45	650-520	590	-24.9	OS 15517	Ch
	F.2	610 ± 80	710-510	610	-23.5	A 11116	Hu
	F.2	1140 ± 35	1160-970	1040	-25.1	OS 15412	Ch
	F.2	1210 ± 50	1240-1030	1140	-22.6	TX 9153	Hu
	F.1	1880 ± 75 *	1990-1680 (95.2%)	1820	-24.0	OS 15413	Ch
			1670-1620 (4.8%)				
	E.5	1620 ± 65	1660-1370	1520	-24.3	A 11117	Hu
	E.5	1670 ± 75	1760-1410	1580	-24.9	A 11118	Hu
	E.1	1550 ± 40 *	1530-1360	1440	-23.9	TX 9170	Hu
	D.11	2280 ± 60	2410-2130	2300	-23.1	TX 9150	Hu
	D.5	2795± 40	3000-2820	2900	- 25.2	AA 40250	HuA
	D.3	2820 ± 60	3110-2810	2940	- 24.3	TX 9154	Hu
	D.0	3800 ± 60	4370-4010	4190	- 17.9	TX 9151	Hu
	C.6	4205 ± 120	5060-4400	4740	- 19.3	A 11128	Hu
	C.6	7600 ± 130 *	8700-8670 (0.5%)		- 18.8	OS 16100	Ch
			8660-8150 (98.4%)	8410			
			8100-8050 (1.1%)				
	C.3	5840 ± 150 *	7030-6330	6660	- 24.5	A 11122	Hu
	C.2	5670 ± 60	6620-6580 (5.4%)		- 27.8	OS 14142	Ch
			6570-6310 (94.6%)	6460			
	C.2	5880 ± 60	6860-6540	6700	- 24.6	OS 14143	Ch
	B.5	7640 ± 45	8520-8360	8440	- 22.1	AA 40612	HuA
	B.4	7410 ± 65 *	8370-8150 (90.7%)	8250	- 12.1	OS 17841	Ch
			8130-8050 (9.3%)				
	B.3	8990 ± 60	10,250-10,110 (61.3%)	10160	- 24.0	OS 17058	Ch
			10,090-9920 (38.7%)				
	B.2	8820 ± 110	10,180-9570	9890	- 23.1	AA 33477	Ch
	A.6	9065 ± 80	10,490-10,460 (1.4%)		- 24.0	AA 33478	Ch
			10,430-10,120 (86.2%)	10,230			
			10,070-9920 (12.5%)				
	A.6	9240 ± 50	10,550-10,260	10,410	- 24.1	OS 15416	Ch
	A.6	9100 ± 75	10,510-10,150 (99.7%)	10,270	- 23.7	AA 33479	Ch
			9980-9970 (0.3%)				
	A.5	8605 ± 55	9680-9480	9570	- 22.8	AA 40251	HuA
	A.5	8675 ± 65	9880-9840 (4.3%)		- 24.0	AA 33480	Ch
			9830-9530 (95.7%)	9640			
	A.3	9820 ± 100	11,630-11,000 (95.7%)	11,250	- 22.5	TX 9152	Hu
			10,960-10,830 (4.3%)				
	A.1	9845 ± 95	11,700-11,670 (1.2%)		- 25.0	AA 33481	Ch
			11,640-11,080 (97.2%)	11,280			
			10,930-10,880 (1.6%)				
LAD (Fig. 5)							
	LD.1	2640 ± 40	2840-2720	2760	-27.7	OS10558	Ch
	LD.0	3790 ± 55	4330-4020	4170	-24.2	TX 9164	Hu
	LC.7	4130 ± 55	4830-4520	4670	-24.5	OS 10548	Ch
	LC.3	5150 ± 65	6170-6150 (0.7%)		-11.4	OS 10178	Ch
			6110-6070 (2.2%)				
			6020-5720 (97.0%)	5900			
	LC.0	6080 ± 40	7150-7110 (6.3%)		-24.7	OS 10545	Ch
			7060-7060 (0.2%)				
			7030-6800 (93.5%)	6940			
	LB.5	6100 ± 80	7180-6750	6980	-23.8	OS 10177	Ch
CSD (Fig. 7)							
	DH	700 ± 40	710-610	660	-17.4	TX 9173	Hu
	DF	4170 ± 110	4960-4420	4690	-22.5	OS 10179	Ch
	DE	5795 ± 150	6970-6290	6610	-20.6	A 10401	Hu
	DE	8380 ± 250	10,130-10,060 (1.4%)		n/d	OS 10560	Ch
			10,010-10,000 (0.1%)				
			9940-8630 (98.4%)	9340			
	DA	12,915 ± 90	15,620-14,970	15,260	-22.2	AA 34476	HuA
Saltillo (BWD) (Fig. 6)							
	Interbedded organic and algal beds, at –2.6 m	2510 ± 35	2740-2470	2590	n/d	OS 10557	Ch
ANG 1 (Fig. 11)							
	Horse Inset	2310 ± 50 *	2430-2210	2330	-18.3	TX 9323	Hu
	Horse Inset	Fm = 1.0022 ± 0.0059	1699-1720 AD (8.2%)	n/d	-10.4	CAMS 59590	Collagen
			1818-1834 AD (5.9%)				
			1879-1916 AD (81.3%)				
	Horse Inset	6550 ± 90 *	7590-7290	7470	-24.4	OS 15411	Ch

Table 1 (*continued*)

Site (figure)	Stratigraphic unit	^{14}C Age bp (uncalibrated)	Calibrated age BP (two sigma)	Median probability calibrated age (BP)	δ^{13}C (‰)	Lab number	Material
ANG 1 (Fig. 11)							
	Horse Inset	7220 ± 80	8220-7890	8050	-18.7	TX 9319	Hu
	Santa Ana soil	495 ± 85	640-380	530	-21.1	A 10398	Hu
	Santa Ana soil	780 ± 40	770-650	710	-16.4	TX 9149	Hu
	Santa Ana soil	Fm = 0.978 ± 0.015	modern	n/d	-21.3	A 10399	Hu
	Santa Ana soil	880 ± 45	910-710	800	-23.1	AA 33482	Ch
	Santa Ana soil	880 ± 45	910-710	800	-23.2	AA 33483	Ch
	Santa Ana soil	640 ± 45	670-550	610	-21.0	AA 33484	Ch
	Gray Colluvium	1660 ± 95 *	1800-1370	1570	-22.8	OS 14139	Ch
	Gray Colluvium	745 ± 45	750-650 (98.1%) 590-570 (1.9%)	690	-24.4	AA 33485	Ch
	Gray Colluvium	1130 ± 35	1140-960	1030	-22.9	OS 15415	Ch
	Soil D2+E+F1	2620 ± 45	2830-2670	2760	-19.0	AA 34475	HuA
	Soil C+D1	4185 ± 135	5090-4330	4710	-15.0	A 11123	Hu
	Soil C+D1	5250 ± 90	6270-5890 (97.1%) 5810-5770 (2.9%)	6040	-20.8	OS 10550	Ch
ANG 2 (Fig. 13)							
	Soil E+F1	915 ± 105	1030-6601	840	-16.5	A 10396	Hu
	Soil E+F1	1470 ± 40	450-1300	1370	-15.9	TX 9163	Hu
	Pink Alluvium	9020 ± 70	10,370-10,360 (0.5%) 10,290-9910 (99.5%)	10190	-13.0	AA 33475	Ch
	Banded Alluvium	7075 ± 70	8020-7740	7900	-11.1	AA 33476	Ch
	Banded Alluvium	7000 ± 45	7940-7720	7840	-13.6	OS 15414	Ch
	Channel Fill	7760 ± 120	8930-8350	8570	-17.7	TX 9324	Hu
	Channel Fill	8360 ± 80	9510-9150	9360	-17.6	TX 9320	Hu
	Pond Sequence	10,500 ± 110	12,760-12,090	12,460	-22.8	TX 9148	Hu
La Angostura Main Insets (Fig. 8)							
	Top of fill (- 50 cm)	2470 ± 45	2690-2410	2550	-19.9	AA 34475	HuA
	Carbon from same level	50,500 ± 1180	n/d	n/d	-26.2	OS 15516	Lignite
	Banded alluvium (-4 m)	8150 ± 260	9580-8410	9070	-13.2	OS 10646	Ch
	Lower fill, above conglomerate (- 4.5 m)	9700 ± 190	11,720-10,510	11,050	-11.9	OS 10556	Ch
La Encantada (Fig. 14)							
	Tufa oolites	14,370 ± 95	17,730-16,730	17,230	-6.6	A 10441	Carbonate
Villaldama (Nuevo Leon) (Fig. 1)							
	Main 5m fill, unit II (- 1 m)	685 ± 100	810-520	660	-23.4	A 10394	Hu
	Main 5m fill, unit I (- 2.5 m)	1480 ± 50	1480-1300	1380	-20.8	AA 34156	HuA
Parras (El Molino) (Fig. 15)							
	MG	755 ± 65	800-600	700	-18.7	A 11125	Hu
	MF	1030 ± 50	1050-840	950	-19.7	A 10392	Hu
	MF	1995 ± 50	2070-1830	1950	-6.0	A 10440	Carbonate
	ME	1805 ± 95	1940-1510	1730	-18.8	A 11126	Hu
	MD	3425 ± 40	3790-3580	3690	-20.5	AA 40252	HuA
	MD	6080 ± 40	7260-6660	6960	-24.7	OS 10545	Ch
	MC	7170 ± 140	8310-8240 (3.6%) 8220-7700 (96.4%)	8000	-18.2	OS 10661	Ch
	MC	7890 ± 130	9030-8420	8750	n/d	OS 10559	Ch
Parras (East) (Arroyo del Ojo de Agua) (Fig. 15)							
	OA.2	770 ± 35	750-650	710	-18.0	AA 40613	HuA
	Reconstruction of dam #2	Fm= 1.0267 ± 0.0042	> modern	n/d	-21.6	TX 9373	Wood
Parras (West) (Arroyo del Capulin) (Fig. 1)							
	Organic soil capping fill	570 ± 100	720-430	580	-22.6	A 10393	Hu
Parras (South) ERB (Fig. 1)							
	Low fill with hearths	250 ± 25	420-390 (7.1%) 320-280 (82.9%) 180-150 (8.2%) 10-modern (1.8%)	300	-21.3	OS 15515	Ch
Concordia (Quarry) (Fig. 16)							
	Unit 3 (-0.6m)	1440 ± 65	1510-1440 (7.9%) 1440-1270 (92.1%)	1350	-24.5	OS 9504	Ch
	Unit 8 (-2.4m)	1450 ± 40	1400-1290	1340	-24.8	OS 9501	Ch
	Unit 9 (-2.55m)	1630 ± 45	1680-1670 (1.1%) 1620-1400 (98.9%)	1520	-26.2	OS 8688	Ch

(*continued on next page*)

Table 1 (*continued*)

Site (figure)	Stratigraphic unit	^{14}C Age bp (uncalibrated)	Calibrated age BP (two sigma)	Median probability calibrated age (BP)	δ^{13}C (‰)	Lab number	Material
Santa Fe (Vega del Caracol) (Fig. 16)							
	Section 1, upper soil (-0.45m)	440 ± 55	550-420 (81.0%)	490	-25.2	OS 10549	Ch
	Section 1, lower soil (-0.85m)	240 ± 35	400-320 (19.0%) 430-380 (10.4%) 330-270 (53.5%) 210-140 (28.4%) 20-modern (7.7%)	290	-25.1	OS 10862	Ch
	Section 2 (-1.0m)	1420 ± 40	1380-1280	1330			
	Section 2 (-1.55m)	1960 ± 25	1980-1860	1910	-24.6	OS 10863	Ch
	Section 2/3 hearth site	3340 ± 35	3680-3660 (2.5%) 3650-3470 (97.5%)	3580	-23.7 -24.3	OS 9495 OS 9496	Ch Ch
Rio Florida (Fig. 16)							
	Weak soil (-1.55m)	655 ± 220	190-150 (1.1%) 1060-270 (98.6%) 10-modern (0.3%)	640	-26.2	OS 17842	Ch
	Strong soil (-1.75m)	1460 ± 50	1460-1280	1360	-17.1	TX 9321	Hu
	Base of section (- 3.35m)	2120 ± 50	2250-1970	2100	-21.2	TX 9322	Hu
	Lateral organic bed	2230 ± 85	2440-2410 (1.2%) 2370-1990 (98.8%)	2230	-22.5	OS 10860	Ch
California (Fig. 16)							
	Thin-bedded fill (-2.3m)	7570 ± 70	8500-8250	8380	-18.7	TX 9318	Hu
Puerto Ventanillas (Fig. 17)							
	VC	9760 ± 100	11,400-10,750	11,160	-10.2	OS 11315	Ch
	VB	16150 ± 900	21,410-16,950	19,330	-16.4	OS 9958	Ch
San Lorenzo (Fig. 17)							
	Below burnt rock	1200 ± 30	1250-1200 (6.4%) 1190-1050 (93.6%)	1130	-24.9	OS 8686	Ch
	Above hearth	9720 ± 900 *	13,300-8970 (99.6%) 8910-8870 (0.2%) 8830-8790 (0.2%)	11,180	-23.0	OS 9956	Ch
	Hearth	8230 ± 80	9420-9020	9210	-21.9	TX 9166	Hu
	Hearth	8350 ± 90	9530-9110	9350	-14.6	OS 9505	Ch
	Hearth	8520 ± 160	10,120-10,070 (1.6%) 9940-9080 (98.2%) 9050-9040 (0.3%)	9520	-13.8	OS 9959	Ch
	Interbed	8780 ± 90	10,130-9590	9820	-23.0	TX 9155	Hu
	Burnt rock and bone	15,300 ± 660 *	19,810-16,660	18,360	-14.8	OS 9962	Ch
	Alluvial fan	15,400 ± 1600	19,810-16,920	18,510	-20.1	OS 9960	Ch
Cuota LM4 (Fig. 18)							
	4.F	340 ± 55	500-300	400	-11.0	OS 10547	Ch
	4.C	5090 ± 100	6170-6160 (0.4%) 6110-6080 (1.3%) 6020-5600 (98.3%)	5830	-10.8	OS 15410	Ch
Cuota LM7 (Fig. 18)							
	7.H	1160 ± 50	1200-990	1080	-26.2	AA 34038	HuA
	7.G	2145 ± 70	2310-1960	2140	-26.7	AA 34155	HuA
	7.D	8820 ± 75	10,150-9640	9880	n/d	AA 34037	HuA
Cuota LM2 (Fig.19)							
	2.Ia	3780 ± 45	4340-4340 (0.2%) 4300-3990 (99.8%)	4160	-26.0	OS 10552	Ch
	2.Ia	4370 ± 40	5050-4860	4950	-19.4	TX 9169	Hu
	2.H	5000 ± 60	5890-5630	5750	-21.6	TX 9167	Hu
	2.B	5690 ± 80	6670-6330	6490	-24.2	TX 9156	Hu
CH 30 (Fig. 19)							
	CH.6	1380 ± 50	1380-1210	1300	-22.7	TX 9165	Hu
	CH.6	3320 ± 100	3820-3370	3560	-18.5	OS 10864	Ch
Tlahualilo (Fig. 20)							
	T11	230 ± 40	390-160 (92.4%) 120-100 (0.9%) 20-modern (6.7%)	290 2750	-15.0	TX 9347	Hu
	T10	2620 ± 50	2850-2640	13,520	-18.2	TX 9348	Hu
	T3	11,650 ± 240	14,000-13,070		-23.6	TX 9349	Hu
AG 5 (Fig. 23)							
	Pond, upper AG.D	5090 ± 85	6000-5630	5820	-12.5	OS 8689	Ch

Table 1 (*continued*)

Site (figure)	Stratigraphic unit	^{14}C Age bp (uncalibrated)	Calibrated age BP (two sigma)	Median probability calibrated age (BP)	δ^{13}C (‰)	Lab number	Material
Near AG 1(Fig. 23)							
	Below pond, AG.D	5670 ± 50	6580-6350	6460	-18.3	TX 9171	Hu
	unit AG.D, above	5245 ± 70	6260-6250 (0.5%)		-27.0	AA 33470	Ch
	conglomerate		6210-5890 (99.5%)	6030			
AG 4 (Fig. 23)							
	AG.M	240 ± 30	370-230 (97.5%)	300	-15.0	TX 9354	Hu
			10-modern (2.5%)				
	AG.L	1180 ± 50	1220-1000	1110	-15.6	TX 9159	Hu
	AG.L	1600 ± 40	1590-1400\	1500	-15.7	TX 9353	Hu
	AG.K	2210 ± 40	2320-2110	2220	-15.9	TX 9351	Hu
	AG.J	2270 ± 40	2380-2190	2290	-15.7	TX 9352	Hu
	AG.G	2840 ± 40	3080-2850	2960	-15.0	TX 9168	Hu
AG 2 (Fig. 23)							
	AG.K	15,000 ± 460 *	19,050-16,760	18,100	-18.7	OS 9955	Ch
	AG.G	2760 ± 60	3020-2770	2880	-15.0	TX 9145	Hu
	AG.D	5110 ± 60	5980-5710	5870	-17.9	TX 9158	Hu
	AG.D	5410 ± 85	6390-6360 (2.0%)		-24.0	OS 9957	Ch
			6350-5990 (98.0%)	6200			
	AG.D	5715 ± 80	6670-6320	6510	n/d	AA 33799	Ch
	AG.D	5890 ± 50	6840-6580	6710	-16.8	TX 9167	Hu
	AG.C	6140 ± 80	7230-6820	7030	-15.2	TX 9148	Hu
	AG.C	6160 ± 80	7240-6840	7060	-15.2	TX 9146	Hu
	AG.B	7250 ± 80	8240-7930	8080	-13.6	TX 9147	Hu
Puerta La Cabrera (Fig. 21)							
	Black mucks at bridge (- 1.35m)	2340 ± 50	2500-2240	2360	15.0	TX 9162	Hu
	Black mucks 500m east of bridge (- 1.4m)	2680 ± 50	2890-2720	2800	14.9	TX 9160	Hu
	Cumulic soil below lag surface (- 1.6m)	16,630 ± 1220	22,700-16,700	19,880	23.3	TX 9161	Hu
Portrero del Llano (Fig.21)							
	Baseof Holocene soil (- 2.1m)	4185 ± 90	4950-4940 (0.2%)		n/d	AA 33798	Ch
			4880-4440 (99.8%)	4710			
La Peña (Fig. 21)							
	Prismatic soil (-2.2m), 3m above horse bone	15,990 ± 170	19,470-18,900	19,180	17.2	TX 9172	Hu
San Salvador (Fig. 21)							
	Weak soil in youngest fill (- 1.8m)	155 ± 35	290-70 (82.8%)	160	-26.3	10551	Ch
			40- modern (17.2%)				
	Donkey mandible, same level	Fm = 0.9940 ± 0.0043	1691-1730 AD (23.4%)	n/d	n/d	CAMS 68024	Collagen
			1810-1922 AD (72.0%)				
La Loma (Papasquiaro District) (Fig. 1)							
	Soil (-1.8m)	620 ±40	660-560	610	-16.8	TX 9175	Hu
	Base of soil (- 4.0m)	2585± 55	2790-2480	2710	-23.3	AA 33469	Ch
Los Herrera (Papasquiaro District) (Fig. 1)							
	Below prismatic soil (- 2.1m)	5720± 70	6680-6370	6520	-15.1	TX 9174	Hu
El Tunal (Durango District) (Fig. 1)							
	Late Holocene fill (- 1.1m)	680 ± 40	690-620 (63.2%)	650	-23.2	OS 14141	Ch
			610-560 (36.8%)				
	Late Holocene fill (- 1.7m)	825 ±40	890-870 (2.2%)		-26.1	OS 14140	Ch
			800-680 (97.8%)	740			
	Late Holocene fill (-2.85m)	715 ±35	720-640 (93.6%)	670	-24.1	OS 10553	Ch
			590-570 (6.4%)				
	Pueblito Formation (-1.5m)	7510± 130	8550-8040	8310	-24.3	OS 10546	Ch
	Pueblito Formation (-5.3m)	7250 ± 609	8180-7970	8080	-25.1	OS 10554	Ch

(*continued on next page*)

Table 1 (*continued*)

Site (figure)	Stratigraphic unit	^{14}C Age bp (uncalibrated)	Calibrated age BP (two sigma)	Median probability calibrated age (BP)	δ^{13}C (‰)	Lab number	Material
Rio de Medina (Juan Aldama District) (Fig. 1)							
	Inactive channel bar (- 0.5m)	200 ±20	300-270 (27.4%) 210-150 (57.4%) 10-modern (15.2%)	170	-26.5	OS 868	Ch
El Jaguey (Fig. 25)							
	Soil A2+B	7230± 80	8230-7910	8060	-14.6	TX 9350	Hu
Encino de la Paz (Fig. 26)							
	EP.7	970 ±30	970-820	890	-13.2	A 10387	Hu
	EP.6	3140± 65	3500-3200	3360	-15.8	A 10386	Hu
	EP.4	5350± 60	6270-5990	6140	-14.8	TX 9355	Hu
	EP.3	10,830 ± 75	12,930-12,740	12,840	-18.7	AA 34036	HuA
Canutillo Road (north of Encino de la Paz [Fig. 1])							
	?Historical colluvium	Fm = 1.0057± 0.0048	1696-1726 AD (14.3%) 1814-1835 AD (9.9%) 1847-1851 AD (0.6%) 1877-1918 AD (70.5%)	n/d	n/d	CAMS 680257	Collagen

All dates (with 3 exceptions) are calibrated with CALIB 5.1 using the IntCal04 dataset (Reimer et al., 2004).
All charcoal dates were calibrated with a 30 year moving average, and all humate and carbonate dates a 200 year moving average.
The 3 exceptions are dates from CAMS whose calibrations are provided by T. Stafford (using OxCal and IntCal04).
Material codes: Ch = charcoal AMS; Hu = conventional humate; HuA = AMS humate.
Dark gray background indicates dates not presented in the article. Medium gray background indicates dates discussed in the text, but not shown on a figure.
* Indicates out of sequence dates.

program is nearing completion by Bruce Albert, and will be reported separately, as will results for the stable carbon isotopes.

A total of 163 radiometric ages were obtained by the Project, in an effort to achieve precision dating that would allow close comparison for the large number of profiles. The Wood's Hole Oceanographic Institute reactor [NOSAMS] provided 79 AMS ages on charcoal, while the University of Texas and University of Arizona laboratories determined 79 ages on bulk humates, in good part by AMS, as well as two assays on calcareous tufas. A further three AMS ages on bone collagen were processed by Stafford Research Laboratories. Although the charcoal ages are occasionally out of sequence as a result of erosional reworking, and some of the humate ages may be slightly too old because of allogenic organic matter, an effort was made to select samples to provide for cross-checking of results; stratigraphically-associated ages on the charcoal and humate samples are usually surprisingly consistent. A limited number of optically stimulated luminescence (OSL) ages from the Mayran area were run at the Sheffield Centre for International Drylands Research luminescence laboratory, courtesy of Mark Bateman. These are reported in calendar years from measurement (2001), but we lack sufficient parallel sequences to test them. Full details of the OSL data and associated technology will be reported separately.

The dates quoted are shown in the graphics, all in δ^{13}C corrected but uncalibrated radiocarbon years (bp), with charcoal or humates specified. This deliberate choice was made to allow listing of a simple, if somewhat arbitrary number. The full corpus of dating information, with error and calibration ranges is presented in the supporting dates collated in Table 1) at the end. Uncalibrated dates evidently distort Holocene time scales, and are badly compressed between 2400 and 4700 bp, arbitrarily "shortening" mid-Holocene time. In the concluding discussions of cyclic environmental changes, however, calibrated dates (BP) are used in their proper place, with reference to the supplementary data of Table 1.

Finally, this study comprises a large corpus of primary, field and laboratory data from a little-studied area, to provide the necessary depth and breadth. For publication that has required a compromise between minimal reporting, on the one hand, and detail, on the other.

2. The Saltillo Basin

2.1. Introduction

Saltillo is a rapidly growing city in a semiarid rainshadow of tectonic origin. The defining feature is a major SSW–NNE transverse fault (Fig. 2). To the east, strongly folded limestones of the Lower Cretaceous and Jurassic, broken by W–E linear faults, dip under a body of late Cenozoic conglomerates toward the transverse fault, to continue beneath folded, Upper Cretaceous shales and sandstones. The major drainage line, the Arroyo del Pueblo, parallels the same fault for some 40 km, tapping an artesian aquifer that explains the ecology of urban location. With a mean channel gradient of 0.0133, this low-sinuosity stream commonly exposes 10–15 m of Holocene alluvium.

Five geoarchives were recorded in the basin (Fig. 2), three of them analyzed in detail. The Arroyo del Pueblo has some base flow of spring origin, downstream of profile LMS, but further upstream discharge is episodic while the proportion of bedload in the alluvial sequence increases. From BWD upstream to La Angostura, late Quaternary floodplain width typically is 500–700 m, but much narrower elsewhere.

2.2. The Upper Arroyo profile (UA)

The hallmark sedimentary profile of the Saltillo Basin, designated as UA (Figs. 3–4) and with a thickness of 8–12 m, is anchored at its southern end by an early Colonial diversion dam. A 140 m-long profile was drawn of the natural face, which cuts the channel obliquely as it comes out of a bend. Such a wide exposure provides a significant sample of the floodplain and insight into the processes that operated there. The lowest units, dated at >9900 bp, rest either on schistose bedrock (fault contact alteration) or on 1.5 m of visible, cemented Pleistocene deposits (colluvium, redox sands, and a calcified sandstone conglomerate, capped by a scoured pavement).

At UA, six beds (A.1–A.6) are grouped as *Unit A* and include a set of low-energy deposits dominated by channel-ponding, with weak cumulic paleosols, several redox horizons, and three zones of

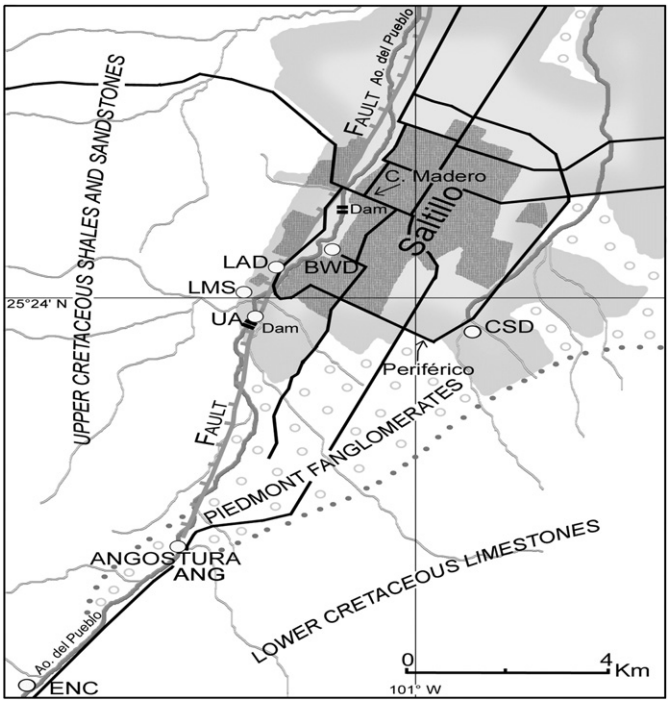

Fig. 2. Southern part of the Saltillo Basin. Lighter gray shows growth of the city during the last 35 years.

interbedded, laminated tufas (A.1, A.4, A.6, see Fig. 4) (see Butzer et al., 1978 on tufa formation). In A.1 the thick tufa is part of a larger, subchannel spring vent and points to active artesian spring discharge, implying higher rainfall in the basin. Some 3.5 m of deposits are preserved and apparently accumulated discontinuously across about a millennium, although the dates are inconsistent, probably as a result of minor vent eruptions or squeeze-ups (see Table 1).

Unit B is marked by limited facies variation and minimal changes of LOI, CCE, or χ. Two isochronic dates suggest charcoal eroded from Unit A and imply previous channel cutting and partial removal of Unit A, which is supported by laterally interdigitated gravels of low-grade schists. A long erosional break is present between A.6 and B.1, so that Units B.1–B.3 probably accumulated rapidly in the wake of bank undermining. Towards 7600 bp the new channel stabilized, judging by the reappearance of tufas and development of Soil B. Up to three Ab-horizons, visible along the outcrop but not illustrated in Fig. 4, suggest episodic cumulic soil formation.

As documented at site LAD (Fig. 5), seven beds, which at LAD represent 5 m of deposit and perhaps a millennium of time, are missing from above B.5 of UA as a result of channel entrenchment. Indeed, when the sedimentary record resumes near UA, it is only found in a tributary entrant 500 m downstream. In this segment of Fig. 4, Cilas laser granulometry was applied to 5 cm intervals in *Unit C*, but the sand fraction appears to be underrepresented by that method. The 3 m of deposit are dominated by laminated silt loams (or sandy loams), with interlaminations of organic muds, charaphytes, and occasional tufas. Two cumulic soils and the basal bed C.1 record channel pools, interbedded with a sandier bedload. The inconsistent ^{14}C dates (see Fig. 4) suggest derived charcoal and organic matter from the missing units, and only the terminal date of 4205 bp is considered applicable.

The upper 5.5 m of the UA profile are representative, and begin with a strong paleosol, Soil D1 of Fig. 3, with A/Bk/Ck horizons. Structure is prismatic and considerable decalcification is apparent across at least several centuries ~3800 bp.

After an erosional break, *Unit D* varies from 2–7 m in thickness, and represents a channel >150 m wide, with periodic ponding near its center (see Fig. 3). The thin-bedded axial deposits alternate between dark gray, organic muds (mean LOI 4.7%) and white, chalky and charaphytic beds of low-density; the latter are laminated, with slack-and-swirl micro-structures, but less organic matter (mean LOI 3.0%). Green algae (*Chara* sp.) require moderately deep and semi-permanent waters, suggesting sustained base flow or an active artesian aquifer, and a moister regional environment. The humate dates represent a period of 700 years, but depositional breaks are likely.

Unit E marks a dramatic hydrological change, with the intrusion of cobble gravels, moved by a high-energy flood regime that is unprecedented during the preceding Holocene record of UA. The cross-section (see Fig. 3) shows disposition of the clasts as poorly sorted, mid-channel gravel bars and channel-margin lenses within a

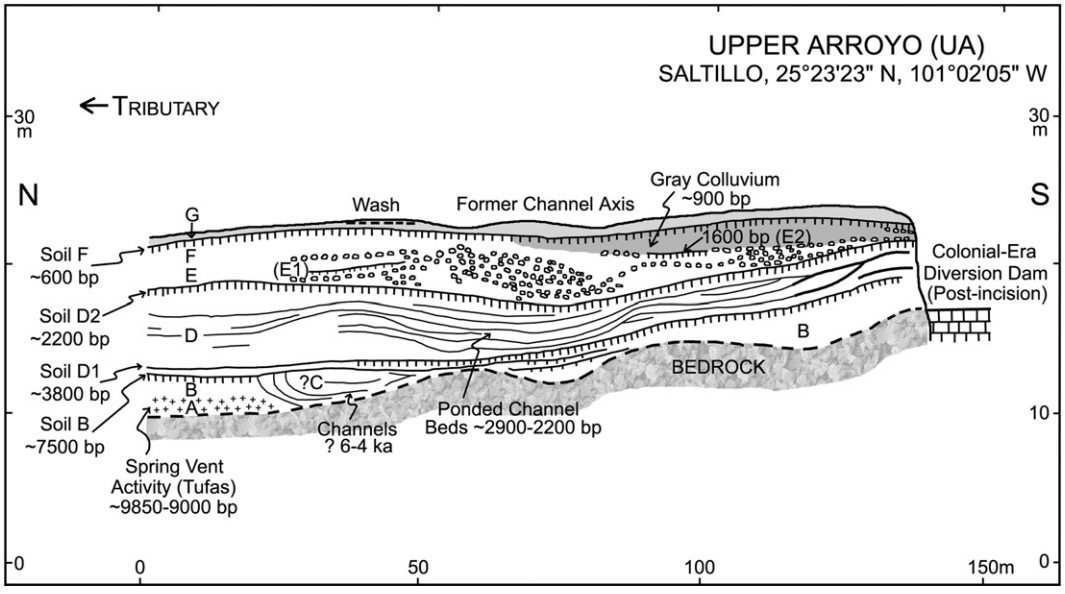

Fig. 3. Cross-section of the Upper Arroyo exposure and position of the Colonial dam.

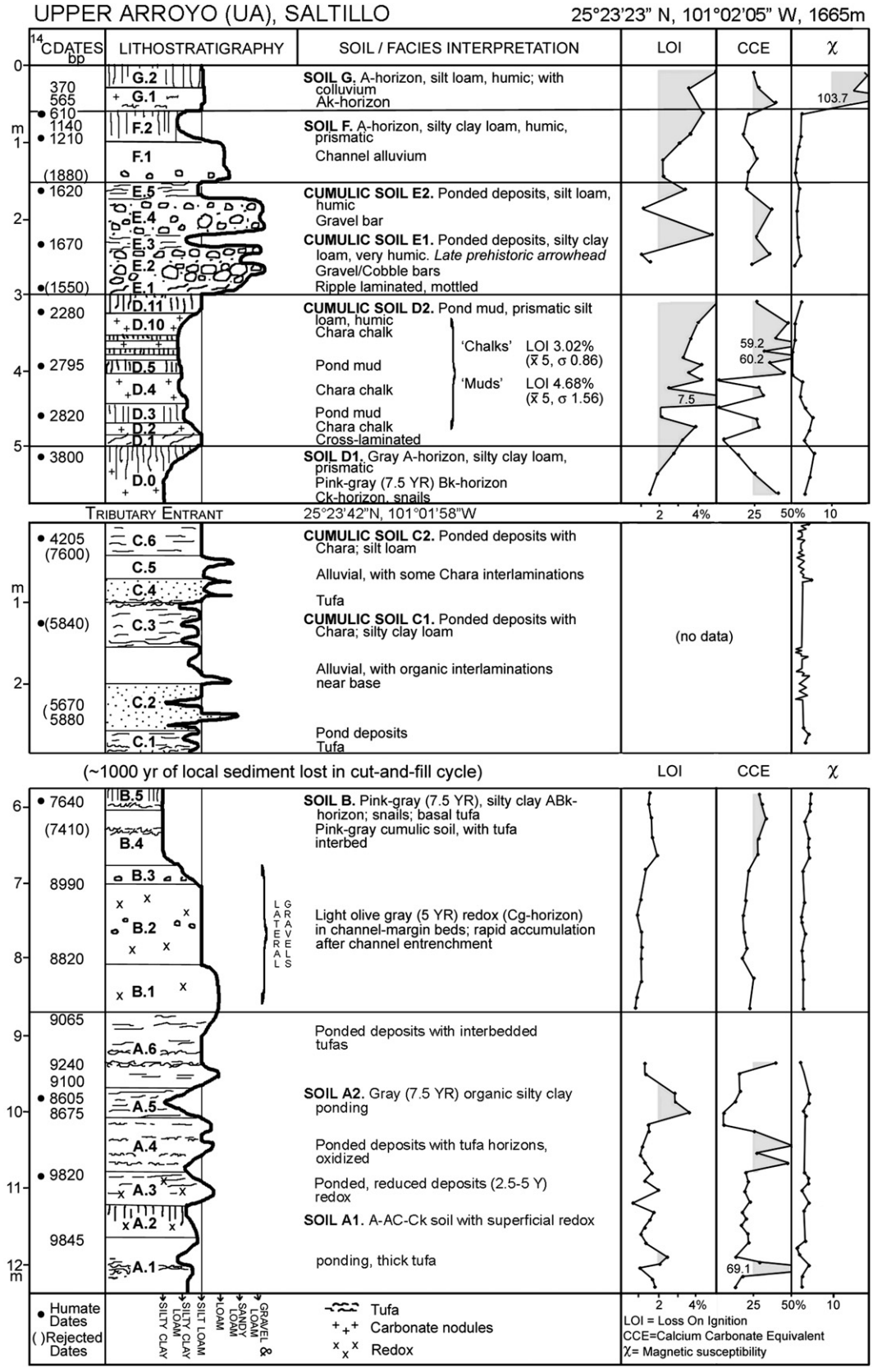

Fig. 4. Analytical profile of the Upper Arroyo site, Saltillo. The Tributary Entrant segment comes from a different profile, 500 m downstream.

wide channel course dominated by sands and loams (1.5–4 m thick). In the measured section, the unit begins with ripple bedding because of accelerating flow, before introduction of cobbles (to 30 cm diameter) as a paleoflood climaxed. Subsequent gravel bars are interwoven with cumulic soils, namely thin-beds of fine texture and high organic content and represent periods of mid-channel ponding. The limestone clasts of *Unit E* are likely to have been eroded from Pleistocene suballuvial gravels a little further upstream. Accumulation

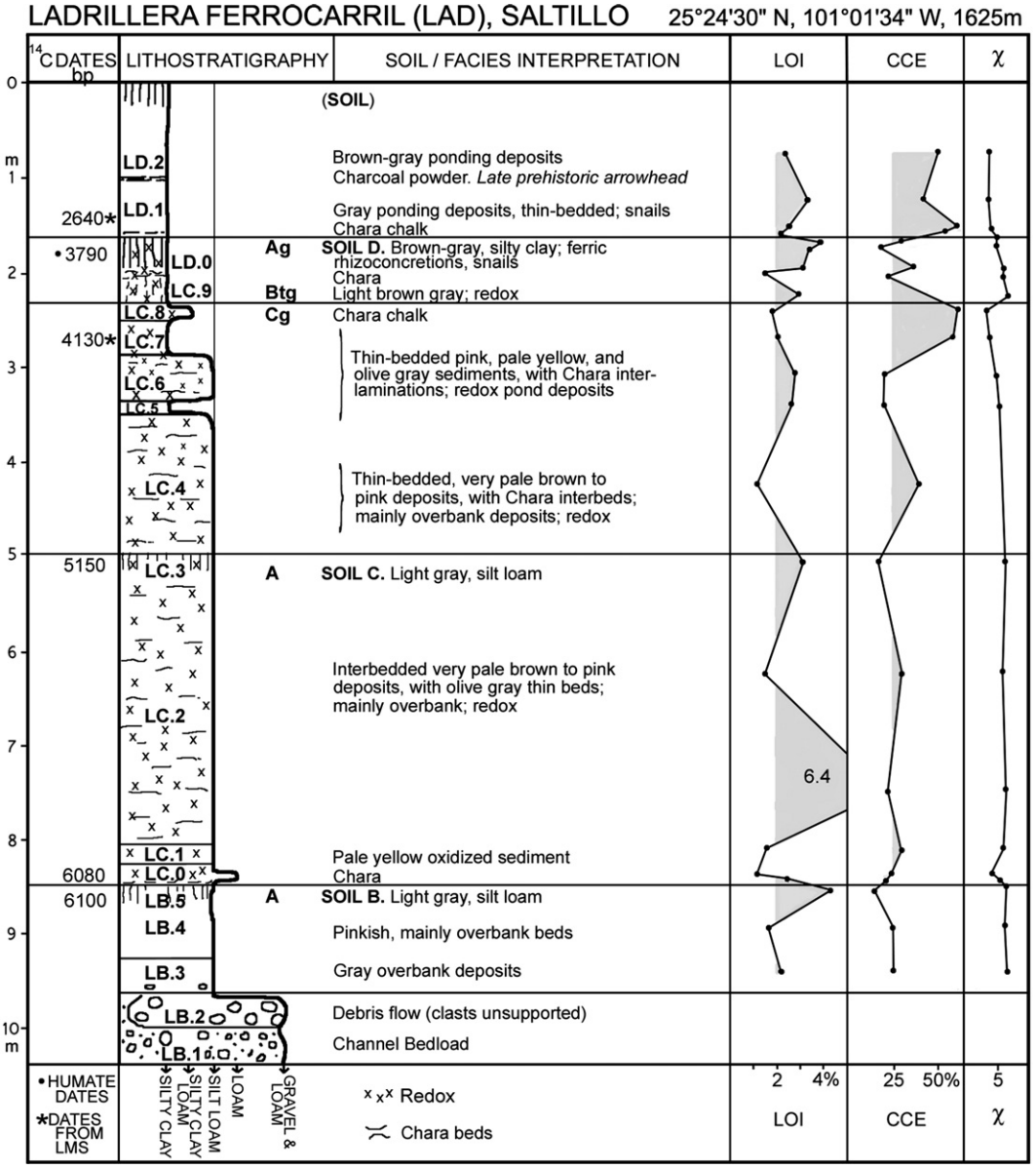

Fig. 5. Analytical profile of Ladrillera Ferrocarril site, Saltillo.

was episodic, with strongly fluctuating energy conditions, during several centuries prior to 1600 bp.

From a basal, gravelly loam, *Unit F* shifts upwards to a silty clay loam and forms a strong terminal Soil F with 3.5–4.0% LOI. Ages of 610, 1140 and 1210 bp suggest slow accretion of Unit F2 (30–40 cm) by overbank episodes and colluviation on a moderately wet floodplain.

Thinly interbedded loams and silty clay loams in the uppermost *Unit G* have mean textures of silt loam. Distinct Ak-horizons preclude human disturbance (as opposed to colluvial components) and two humate dates for the Ak appear to favor a date prior to Spanish intrusion (first land grants AD 1577). The most striking feature is the abrupt increase of magnetic susceptibility, discussed in Section 8.3. High χ values probably reflect allogenic eolian components derived from magnetite in coarse silt introduced from the upper Nazas catchment (see Fig. 1). Shortly after formation of *Soil G*, the Arroyo del Pueblo was abruptly entrenched some 8 m, but prior to construction of the early Colonial dam. The temporal constraints for this unprecedented gullying are refined upstream at La Angostura (Section 3 and discussed further in Section 8.1); they are replicated at other sites as far west as Durango City (Section 7.5).

Explanation for the cut-and-fill cycles at UA, as complemented by other sites in the Saltillo area, is deferred to Section 8. The alternation of low and high-energy reflects shifting equilibrium modes. Unit E and, to a lesser degree, Units B.1–B.3, stand out as examples of abrupt disequilibrium, in contrast to the modest cyclicity of Units A, C and D. The UA profile offers a useful index of regional moisture, through increased influx from artesian water sources. These are recorded by channel tufas (in part structured as subchannel spring vents) and as substantial base flows (recorded by channel-ponding or redox). For this to happen, the standing water table at UA would have to be 8–10 m higher than at present, because the Arroyo del Pueblo currently does not intersect the water table from 350 m downstream to 150 m upstream of the hard bedrock sill at UA. Such a higher water table would be necessary to generate the features of Unit A, bed B.4, most of Unit D, and beds E.3 or E.5.

But the mid-Holocene record at UA is incomplete, and for this we turn to the LAD section downstream.

2.3. The Ladrillera Ferrocarril Brickyard (LAD)

Active and abandoned brickyards extend along the Arroyo del Pueblo for ~20 km, mainly on the western side, before the exposed thickness of Holocene alluvium rapidly tapers off north of latitude 25°25′. Although obscured by recent construction on top of exhausted brickyards, the last downstream outcrops were observed near the Calle Madero bridge. Quarries for brick kilns and "Saltillo tiles" exploit silty clay loams or silty clays, rich in organic matter and CCE. Informants stressed that the raw material was used without admixing tempers. The deeper silt loams are not systematically excavated, probably because they include too much sand or too little organic matter. Early Holocene levels are, therefore, exposed only where a brickyard operates by stepping-back steep, high outcrops, such as at LAD.

A brickyard SW of the railroad crossing over the Arroyo del Pueblo (LAD, see Figs. 2 and 5) exposes a more or less complete Middle Holocene record. Topping at 15 m above modern floodplain, the composite profile is ~10 m thick. An intricate warren of small workings, targeted at selected seams, was shown us through the courtesy of the foreman, Juan Rivera Iracheta.

The sequence begins with a gravelly channel-floor (LB.1), partly covered by a debris flow of unsupported clasts (LB.2). This dramatic initiation of a new cycle of sedimentation was followed by ~6 m of silt loams (LB.3–LC.4), representing thin-bedded slackwater deposits, with two weak cumulic soils (B and C), many *Chara* interbeds, and prominent redox phenomena, ranging from gray or olive gray to pale yellow or pink in color (Munsell hues 5Y to 7.5YR). Changes in CCE or χ are subdued, but the LOI curve fluctuates considerably, up to 6.4%.

Variability increases in levels LC.5–LC.9 (1.6 m thick), with texture ranging from silt loam to silty clay. Mottling is more conspicuous, and bed LC.9, in between *Chara* chalks, is a 40 cm Btg horizon that preserves the thin-bedding of the parent material. Above that is a conspicuous, 25 cm Ag-horizon (LD.0) with reddish yellow, ferric rhizoliths.

Beds LD.1–2 are 1.5–2.5 m thick. These are dark silty clays, thin-bedded, with considerable organic matter, attributed to ponding in a marginal sector of the former floodplain. A late prehistoric arrowhead was observed in a charcoal-rich lens between the two levels.

The Ag/Btg profile at the contact of Units LC and LD is 70 cm thick, with evidence of oxide segregation, strong redox conditions, and formation or accumulation of a heavy clay. The clay fraction of the Ag-horizon is 53%, that of the Btg 57%, and the Cg 35%. This is a gleyed Alfisol, but one retaining cumulic properties. The water table fluctuated within a meter of the surface, and was sufficiently acidic to allow iron mobilization (pH is presently 7.53–7.71). That suggests rich floodplain vegetation, a channel of low relief, and artesian waters that rose to the coeval floodplain level of the Arroyo del Pueblo. Although occasionally inundated by overbank waters, the pedogenesis responsible for Soil D of Fig. 4 was primarily linked to a high, standing water table, as observed today further downstream.

This soil at LAD is contemporary with Soil D1 at UA, but they are fundamentally different in character. At UA a 60 cm A/Ak horizon is present over a 20 cm Ck with snails, and the A-horizon is a dark gray, silty clay loam with prismatic structure. In contrast to the Alfisol at UA, this is a Rendoll (Mollisol) with cumulic attributes, developed on an active, free-draining channel-margin, accessible to secondary CCE from discharge gathering in a more distant watershed. Soil D at UA developed after downcutting of the floodplain to a level 5 m below the persisting "terrace" surface at LAD. The contrasting pedogenic trajectories for Soil D at UA and LAD reflect different elevations, substrates, and geomorphic processes.

2.4. The Las Miñitas Brickyard (LMS)

Holocene sediments are well developed near the confluence of the Arroyo del Pueblo and its tributary, the Agua de las Mulas. A similar section is found in the Las Miñitas Brickyard (25°24′01″ N, 101°02′08″ W, 1640 m), ~1.2 km SW of LAD.. This analysis is limited to the more salient features, because of difficulty in securing permission to access the site upon return visits.

Much of the topmost unit (MC) at LMS had been cut back, but 1.6 m remained (in 1996), with aquatic snails and some bivalves (1–3 mm). Recalling bed LD.1 at LAD, this carbonate-rich base at LMS preserves a major channel structure and dips towards the arroyo. It has an AMS charcoal date of 2640 bp (see Fig. 5).

The intermediate unit MB is capped by a strong cumulic soil of 60 cm thickness (Soil D), with horizontal, ferric rhizoliths. MB consists of ~2 m of overbank deposits with snails and a pedogenic overprint.

The lowest unit exposes ~3.5 m of reduced pond beds. Two organic horizons have abundant fine charcoal and horizontally-bedded plant remains enriched with iron; the higher has an AMS date of 4130 bp. This unit has many snails, and thickens toward the valley axis.

On its eastern side, the whole LMS profile has slumped toward the arroyo, and a fault disrupted the strata of MA and MB prior to

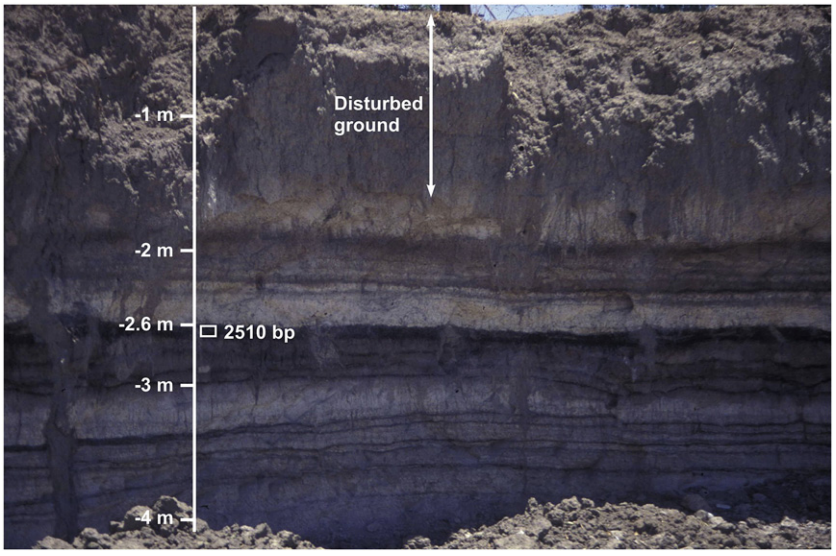

Fig. 6. At BWD, 1.5 m of light gray spoil rest on alternating beds of white, carbonate mud with *Chara* fragments and black, organic microbial mats, analogous to the ponded channel beds at UA (Unit D) The thick black horizon at −2.6 m has an AMS age of 2510 bp.

accumulation of MC. In effect, the two older units were undermined by channel incision of the Arroyo del Pueblo, just after development of Soil D at LMS. In combination, LMS and LAD record stable and wet conditions from before 6100 to 3800 bp, prior to downcutting by 5 m.

2.5. Ponding at site BWD

In a recreational area modified by mechanical grading, an interesting exposure is present on the eastern bank at 25°24′42″ N, 101°01′09″ W (BWD). The top 1.5 m is suffused with trash, including the tibia and astragulus of a domesticated horse (Texas Memorial Museum [TMM] No. 43547). Below that are >2.5 m of alternating, thin-beds of white or light gray *Chara* chalk and black organic mats (Fig. 6).

These two facies, which replicate those of UA Unit D, were studied by Barbara Winsborough. She describes the low-density, light colored, porous material as a carbonate mud, consisting of small fragments of a green macro alga (*Chara* or *Nitella*), encrusted with micritic calcite. These suggest rapid deposition in shallow, alkaline ponds. The dark horizons are formed as microbial mats impregnated or encrusted with iron, laid down in muddy water undersaturated in bicarbonate.

The alternating beds may, therefore, be partly explained by waters alternatingly supersaturated or undersaturated in calcium bicarbonate. In the latter case, iron compounds would be mobilized by cyanobacteria (blue–green algae), and Winsborough found abundant red bacteria in sediment samples from LAD. These features pose issues for more specialized analysis. Equivalence with UA Unit D is supported by an AMS date of 2510 bp at 2.6 m depth.

2.6. The CSD Arroyo, eastern Saltillo

The piedmont alluvial plain east of Saltillo represents a very different sedimentary environment. When first visited by Butzer in 1982, this semidesert setting was dominated by at least two surfaces of fanglomerates, the higher of which was topped by petrocalcic horizons and red paleosols. In 1998 rapid urban expansion had already obscured the gross stratigraphy, and today this geoarchive has been largely lost. Fortunately, a study site (CSD) had been selected to elucidate the Holocene strata exposed along one of the deep arroyos draining the mid-fan. It lies directly east of the *periférico* highway around Saltillo. The schematic and unconventional composite profile (Fig. 7) incorporates several irregular faces along a narrow, 7 m-deep channel, then a semicircular gravel quarry, and finally a long cut next to the road. With five dates, it records 2.5 m of Holocene deposits and almost 4 m of uncemented Pleistocene beds that fill a drainage line cut into the fanglomerates.

This site illuminates processes affecting the semidesert margins of the Saltillo floodplain. At the base are ~2 m of soil sediment, terminated by a truncated Bt-horizon of yellowish red (5YR), silty clay loam with strong columnar structure; this has a humate date of 12,915 bp, which probably represents mean residence and, therefore, provides a minimum assay. The channel was reactivated with a mass of channel gravel (Unit DB), grading laterally into a gravelly sand, with a columnar Bw-horizon (DC, see Fig. 7). After further alluviation (DD), a strong, calcic paleosol had developed by 8380 bp and suggests correlation with Unit A at UA.

The mid-Holocene record at CSD comprises up to 2 m of loamy fill, with gravel horizons and at least three pale brown, cumulic Ak-horizons (see DE in Fig. 7). The earliest of these has a humate date of 5795 bp (Soil B?), the youngest a charcoal assay of 4170 bp (Soil C?). Several modest cut-and-fill episodes (DG.1–2) preceded a general fill (DH) capped by a conspicuous soil. This A-horizon of grayish brown, silt loam has a humate date of 700 bp and matches Soil F at UA. It was abruptly followed by 7 m of entrenchment of a narrow gully into unconsolidated fill and calcified Pleistocene units. Downcutting apparently took place prior to veneering of the surface by a sweep of coarse gravel.

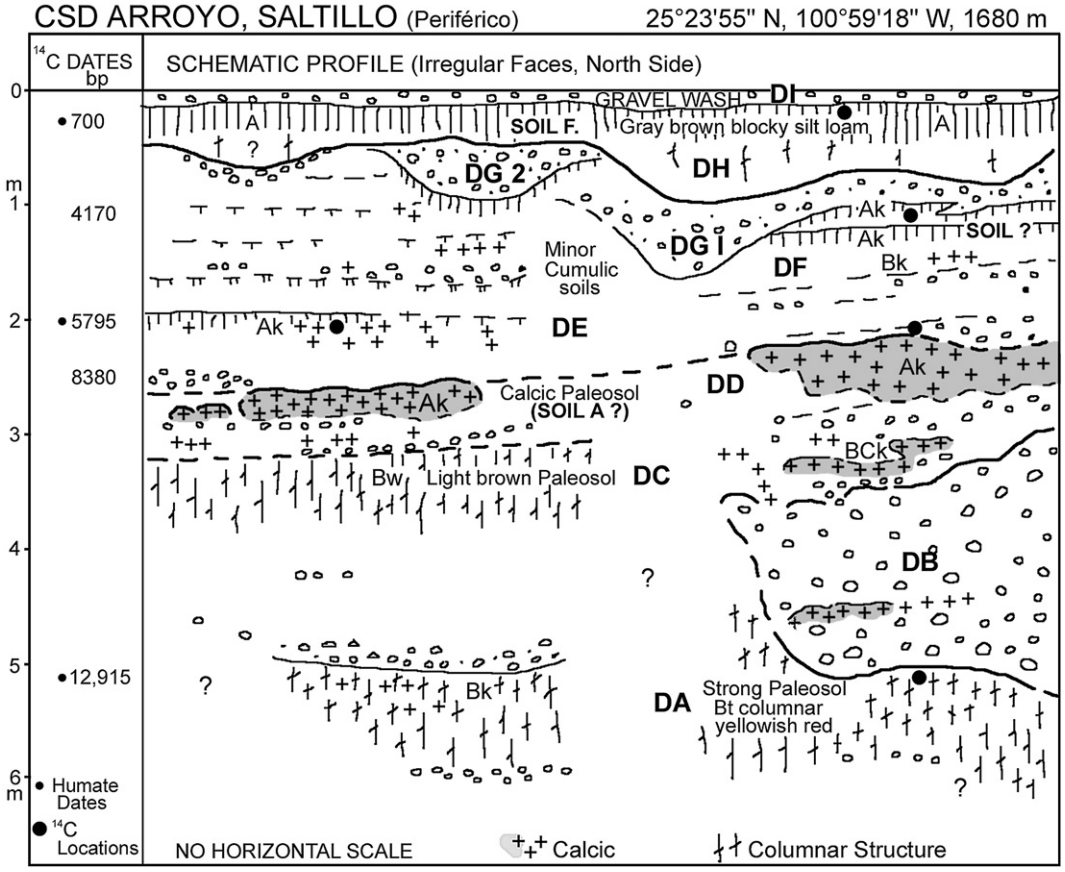

Fig. 7. The CSD Arroyo site, Saltillo.

The CSD profile indicates that major activation of the piedmont dates back to Late Pleistocene times. The Holocene record is more modest and has been simplified by the attrition of many minor cutting episodes. But it does suggest that the basic pulses of fluvial response were analogous to those of the Arroyo del Pueblo—even though the CSD Arroyo drains into a piedmont stream, which in turn runs northward for 15 km before turning west toward the main floodplain. Thus, the CSD profile should primarily reflect climatic inputs rather than base level changes.

3. The Angostura badlands

3.1. Introduction

At the southern end of the Saltillo Basin, the Arroyo del Pueblo, the highway south, and the railroad tracks to Mexico City or Zacatecas all converge to run through the pass at La Angostura ("the Narrows"). On the eastern side over 100 m of Plio-Pleistocene fanglomerates mantle the foot of the Lower Cretaceous limestones, and steep-sided arroyos interrupt these low cliffs, exposing coarse, well rounded clasts of limestone and chert, embedded in an indurated calcrete. The western side of the valley has gentler slopes, rising up over similar conglomerates, abutting the foot of Upper Cretaceous shales and limestones. The valley floor is virtually impassible because of a maze of deep (9–12 m) gullies, along a stretch 2.5 km in length and 150–400 m in width (Fig. 8). This may be the most dramatic example of gully badlands in Mexico, and it defined the strategic context for the battle of La Angostura or Buena Vista, during February 1847, between generals Santa Ana (Mexico) and Taylor (USA).

Various published sketches of the battlefield (see Smith, 1919), and especially a map of Benham (1847), show the labyrinth of gullies, which was much the same then as now. At the suggestion of Dean Lambert (UT Geography doctoral student), the site was briefly visited by Butzer in 1987. Selected as a key objective of the Laguna Project, it proved to be a complex lithostratigraphic puzzle, incorporating a full Holocene sequence of sediments, soils, and cut-and-fill cycles.

3.2. Sedimentary units at La Angostura

Lithostratigraphy at Angostura is not provided by a quasi-continuous column, as at Upper Arroyo, but by a number of discrete segments exposed around our "Santa Ana Profile" (Figs. 9–11), immediately below a modern culvert that drains the Arroyo de las Terneras under the highway. In 1847 there would have been a gully here, behind which a U.S. artillery unit was emplaced. Located at the interface between fanglomerate hills and valley floor, slope and floodplain components are interdigitated. The slope elements include derived limestone and chert cobbles of the original fanglomerates, together with calcite-cemented sands and coarse silts reworked from disaggregated matrix that has been incompletely decalcified. What follows is a synthetic description of the mainly Holocene stratigraphic units studied in a number of profiles (Figs. 9–13).

The dominant sedimentary body of the Angostura Badlands is a 7–9 m fill of pink (5YR) silt loam and silty clay loam. When wet and

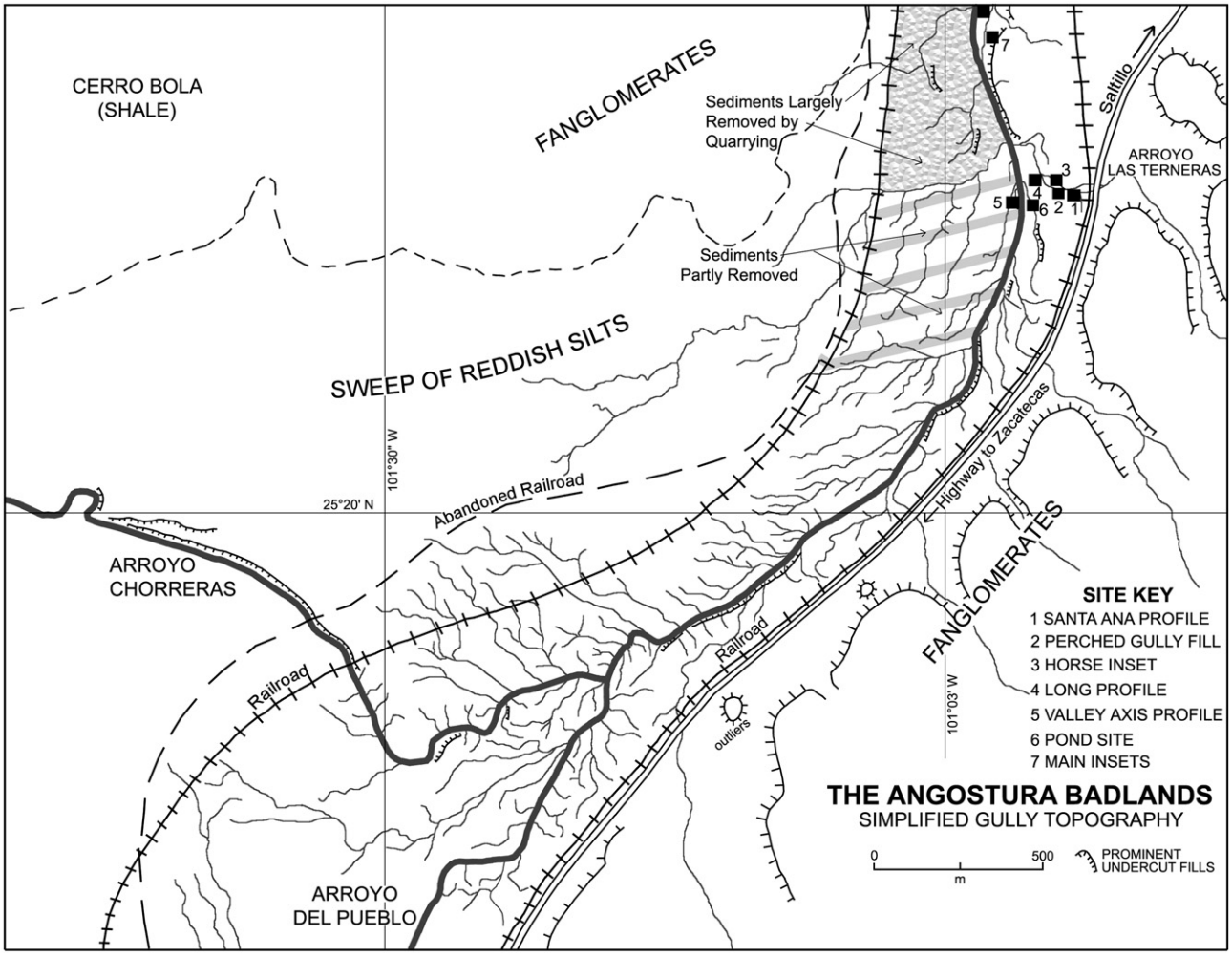

Fig. 8. Topography of the Angostura Badlands.

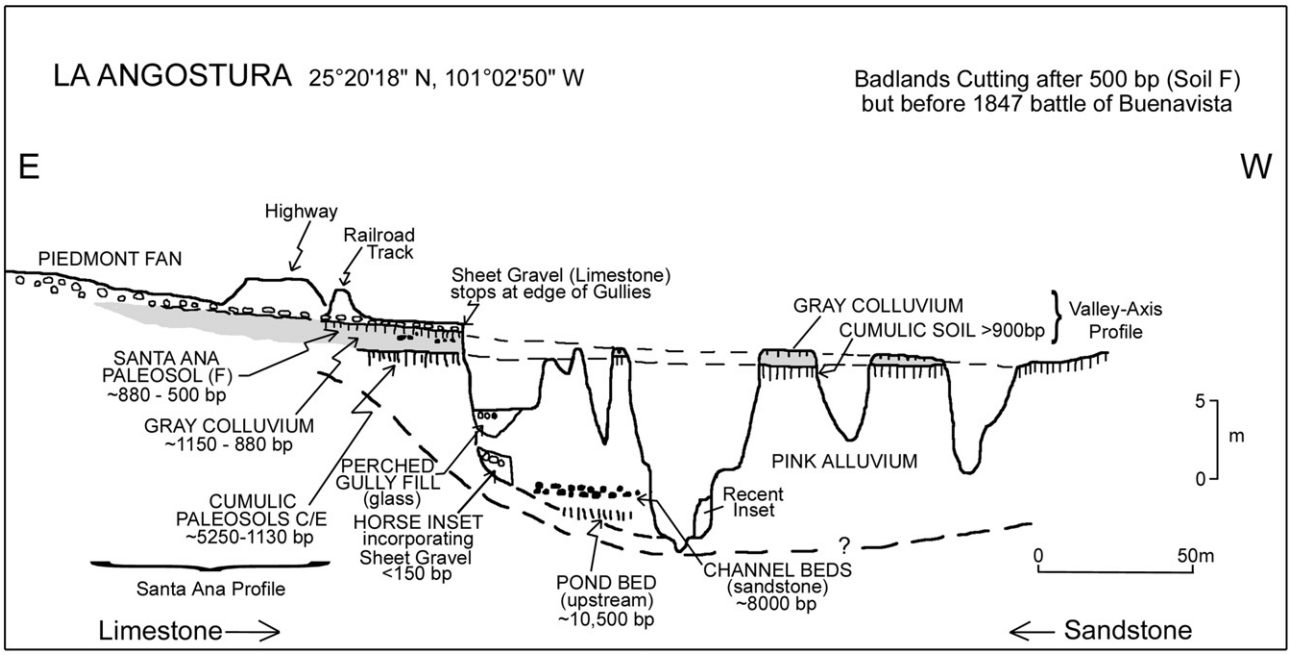

Fig. 9. La Angostura cross-section.

undermined by water, this material collapses to form near-vertical cliff faces. Informally designated as the *Pink Alluvium*, these are time transgressive deposits, with conflated, terminal cumulic soils (dating between 5250 and 915 bp) at the top, and a variable configuration of overbank, bedload, or ponded beds near the base (dating between ~10,500 and ~7000 bp), resting directly on conglomerates (Fig. 13). This "Lower Complex" reflects several cut-and-fill cycles that are incompletely exposed, but the components lack identifiable slope materials, which only begin to appear towards ~3000 bp (Fig. 13). The typical Pink Alluvium shows minor alternations of sandy or clayey thin-beds or interlaminations, and occasional disconformities, but internal stratification is weak and barely visible. The unifying process of the Pink Alluvium was an overwhelming influx of reddish silts, derived from breakdown of Upper Cretaceous shales, and swept into the axial valley by floods of a single major, western tributary, the Arroyo Chorreras (see Figs. 10, 13).

On top of Pink Alluvium is a package of *Cumulic Soils* that suggest an A/Bt-horizon, based on color, structure, LOI, CCE and texture. But the dates argue for a conflation of cumulic soil processes, at intervals, across as much as 4 ka (see Figs. 12–13), during which pedogenic material was formed, mixed and locally eroded in the valley bottom. Near the top of the unit, calcite sand and silt begin to appear (up to 7.5% of the fraction total), recording a slow incorporation of slope components into the valley floor soil.

The ensuing *Gray Colluvium* signals a more rapid accretion of slope facies and a change of slope ground cover and runoff. High LOI ranges (3.5–4.5%) imply attrition of upslope humic soils, and doubled CCE values indicate a strong influx of calcite sand and silt (to 20%), suggesting selective erosion of C-horizon material. Accumulation began somewhat later than 1130 bp (basal charcoal, derived from the Cumulic Soils), with apparent slope stabilization near 880 bp. Significant colluvial transfer probably took place between AD 1050 and 1200 (see Section 9.1). A trebling of the magnetic susceptibility above background values suggests an influx of eolian silts, as argued below (Section 8.3). The Gray Colluvium is well preserved on top of

Fig. 10. The Angostura Badlands at the confluence of the Arroyo Chorreras, mainly exposing the Pink Alluvium.

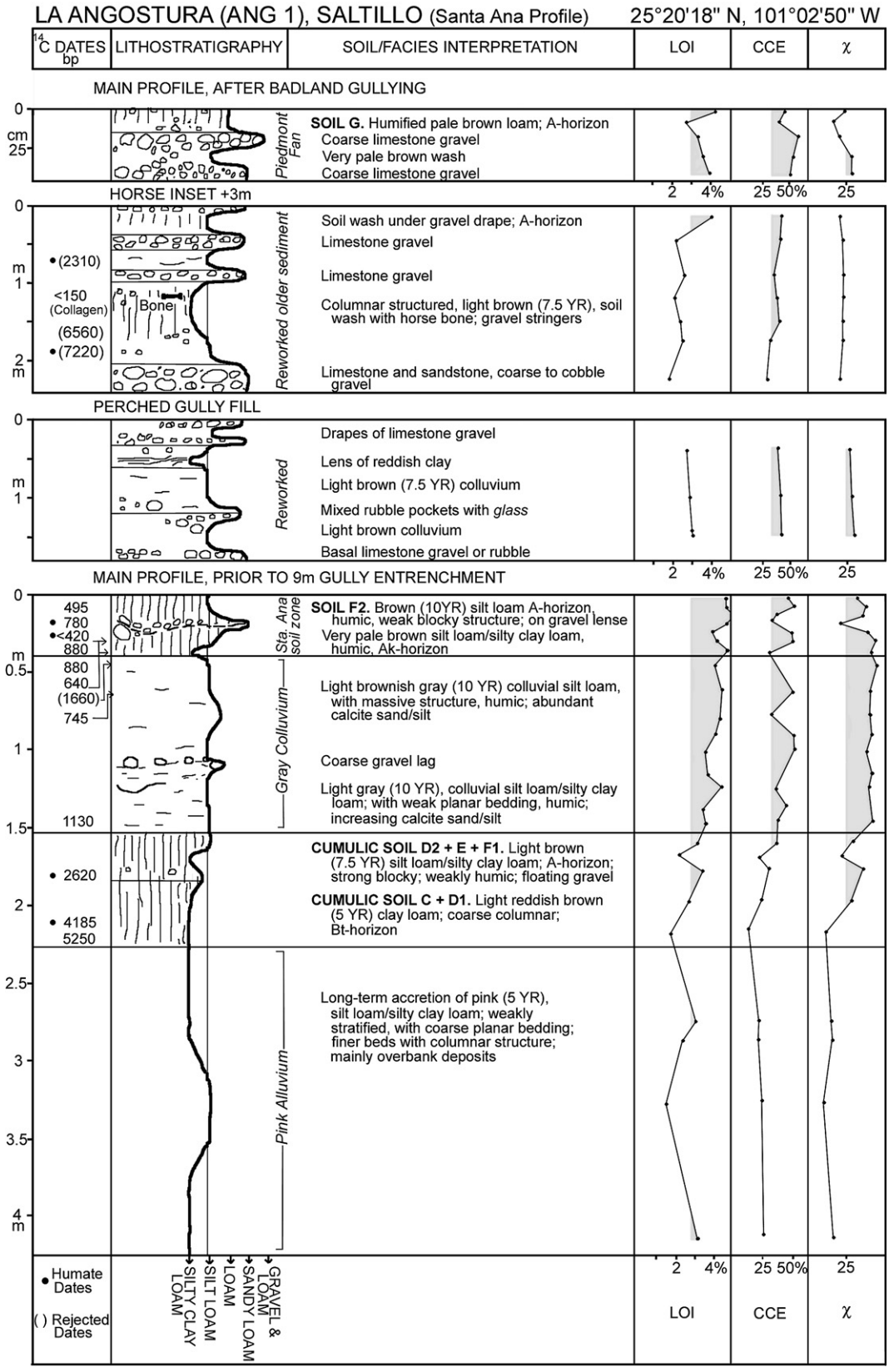

Fig. 11. La Angostura analytical profile (1).

various outcrops within the maze of gullies, so that the gully system had not yet formed.

Soil F or the *Santa Ana soil zone* is represented by humic A or Ak-horizons on top of the Gray Colluvium, interrupted by a lens of limestone gravel (Figs. 9, 11). This 40 cm zone represents a cumulic soil with a mollic epipedon. LOI values are high (4.0–5.3%), χ variable (17–39), and calcite sand/silt inconsistent (1.4–18.8%), while CCE within the Ak reaches 54%. This suggests periodic

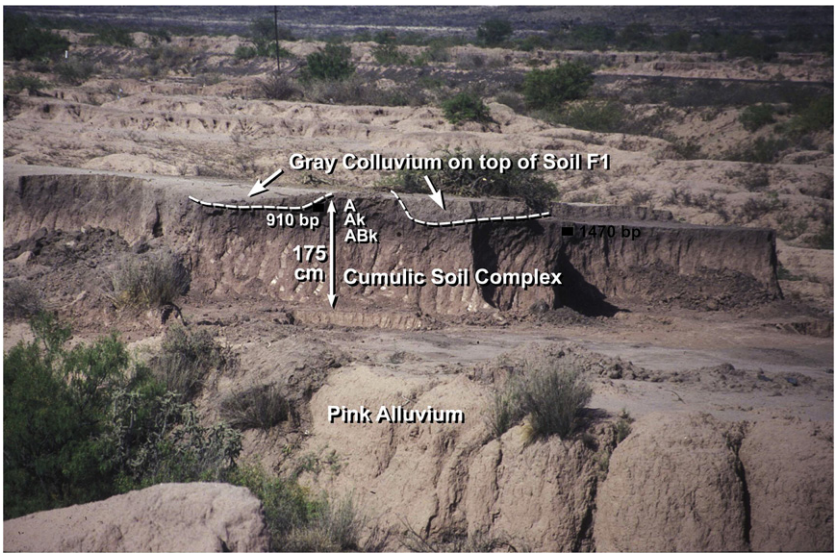

Fig. 12. The Valley-Axis Profile, Angostura, during commercial excavation, April 1998. The position of the 1470 bp sample, collected May 1996, was slightly higher than shown.

colluvial additions, alternating with periods of relative slope stability. Effective ages at ANG for Soil F are 780, 745, 640 and 495 bp, which fits with the dates for the same soil at UA, CSD, and Parras, giving a median calibration probability of ~AD 1300 (see Table 1).

The final unit of Angostura is the *Piedmont Fan* (see Figs. 9, 11). This is extensive east of the highway and locally includes 40 cm of coarse limestone gravel, with an intermediate level of soil wash, terminated by a humic soil (Soil G, 10–15 cm). Activation of the mountain drainage on such a scale has not happened since the Late Pleistocene (see Section 3.3). Even more remarkable is that the fan was preceded by creation of the Angostura Badlands, with 9–12 m of gully entrenchment during a relatively short period of time.

3.3. Stratigraphic controls for 9 m entrenchment

The field evidence at ANG identifies how entrenchment and badland formation fits into the stratigraphic sequences. Whereas the Gray Colluvium and the superimposed Soil F continue to the western side of the main channel undisturbed, the Piedmont Fan and its gravel sweeps do not extend beyond the gully system (see Fig. 9). Instead they drape down some gully walls to connect directly with late inset fills. These insets fix the age of the containing gullies more precisely.

The "Perched Gully Fill" (Figs. 9, 11), embanked against the Main Profile in a minor gully, includes 1.8 m of unconsolidated colluvium with rapid facies changes. This is dated by a piece of machine-molded, "modern" glass at ~1.2 m.

The 3 m Horse Inset (see Figs. 9, 11), found at the bottom of a broad, 9 m-deep gully, is more complex. The basal gravels include limestone and sandstone, whereas the closing gravels link directly to drapes of limestone rubble extending downslope from the Piedmont Fan. In between are colluvial beds and minor gravels, with an animal long-bone embedded deep within firm sediment. Identified as the proximal radius of a relatively small horse, but larger than a burro (E. Lundelius, pers. comm. 1998; TMM 43544-1); collagen from this bone yielded an AMS date of younger than 250 years (see Table 1). If the horse was a victim of the 1847 battle, which seems likely, the Piedmont Fan is younger and the gullying event somewhat older.

The other, highly discordant dates from this inset (see Fig. 11), combined with a flat magnetic curve, point to charcoal and soil/sediment organic matter reworked by rapid collapse of gully walls, with insufficient time to generate a new humic imprint in the accumulating sediment. The properties of the fine sediment match those of the Pink Alluvium exposed in the gully walls.

The "Main Insets" (see Fig. 8) represent fills at 5–6 m above channel-floor, ~300 m downstream on either side of the main channel. Fabrics consist of irregular thin-beds of sand, loamy sand, and silt loam, with reactivation surfaces, and basal lenses of sandstone and limestone gravel. Compaction is minimal, even though a humate date at ~50 cm yielded 2470 bp and a charcoal date near the base 8150 bp. The dating incongruences resemble those of the Horse Inset, but the bedding precludes quasi-instantaneous sedimentation. In addition a 2–3 m, modern floodplain inset exits at these locations.

The land-use implications of the final geomorphic events at La Angostura can be seen ~900 m downstream of ANG, where a minor eastern tributary has cut an entrant, now partly filled by a 5–6 m inset, its surface cultivated by the local campesino. But his field is littered with limestone cobbles of the Piedmont Fan, verifying that it post-dates 9 m entrenchment and remained active for a while after accretion of the inset.

In sum, badland entrenchment predates the 1847 battle, with greater stratigraphic precision provided by the disjunct *Inset Fills*, accumulated at 3–6 m above broad gully bottoms by a combination of high bank collapse, channeled floods, and lateral, colluvial activation. In part, these fills date to before the mid-19th century, consonant with the historical cartography. Sweeps of fan gravel feed directly into the top of the Horse Inset and the Perched Gully Fill at ANG, but prominent limestone clasts at the base here and in the Main Inset indicate that the Piedmont Fan was active earlier. In other words, the Inset Fills and the Piedmont Fan overlap in age. Although some gravel continued to debouch from the fan thereafter, the surface soil G at ANG is well enough defined (Fig. 11) that it would argue for more recent (19th or 20th century) stability of the larger watershed.

The Inset Fills record multiple, discrete events, with repeated changes of energy conditions. The amplitude of variability exceeded that of the prior Holocene record, implying a lower threshold of disequilibrium, coupled with a degraded ground and land cover. That would also explain simultaneous activation of the Piedmont Fan. Although the Angostura evidence illuminates the processes of entrenchment and partial refilling, it leaves the time span between the Inset Fills and the Santa Ana Soil undefined. Greater temporal precision is provided at Parras (Section 4.2).

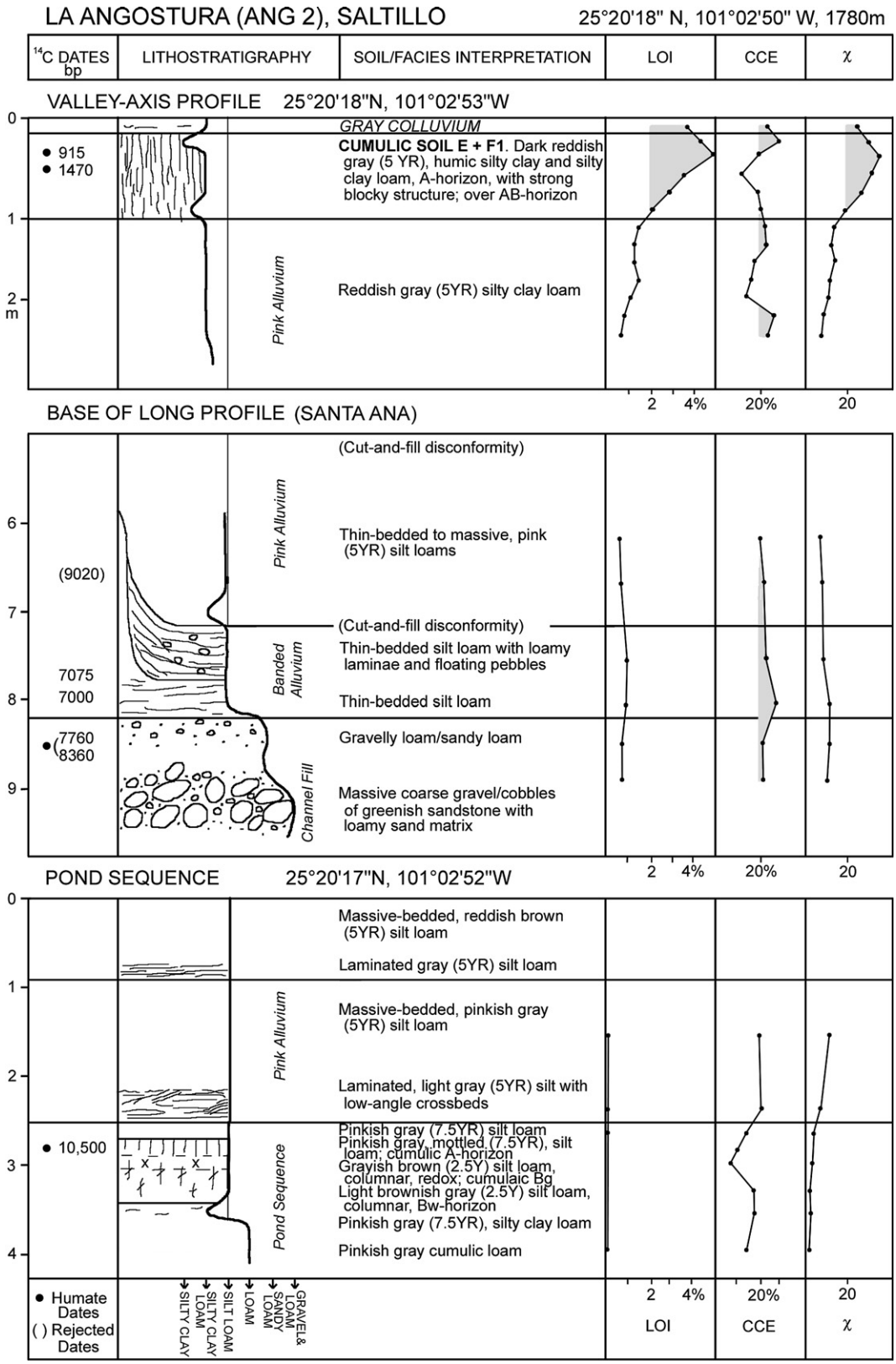

Fig. 13. La Angostura analytical profile (2).

3.4. La Encantada railroad station (ENC)

The Angostura profile is complemented 4.2 km upvalley, in several shallow quarries and a deep gully near the old railway station of La Encantada (ENC) (see Fig. 2). A roadside sign proclaims that Pleistocene mammoth remains were found nearby, but the importance of ENC is that it is unaffected by either the artesian aquifer or the sediment influx of the Arroyo Chorreras and, therefore, represents a clearer relationship between a semiarid, axial channel and its mountain periphery. The composite profile

(Fig. 14) telescopes several non-contiguous sections, so that the horizontal scale is only approximate, and standard laboratory processing was not carried out.

The surface (Unit EG) is formed by an equivalent to the Gray Colluvium at ANG, resting on Soil E (EF), and the base is given by spring tufas (EC) with plant structures and a ^{14}C assay of 14,370 bp on clean oolites, presumably incorporating "dead" carbon and probably with a true age closer to that of UA Unit A or Soil A at CSD. So defined, the Holocene record here also includes overbank silts (EE) and ponded channel beds (ED), that form a shallow counterpart to the Pink Alluvium at ANG.

Of particular interest is the visible Late Pleistocene record of calcrete cobble conglomerates (EB1, EB3), fingering out next to the Holocene channel and postdating a body of cienega marls (EA). These conglomerates have frequent scour-and-fill structures that represent shifting, ephemeral streams that drain a steep piedmont slope only 4 km from the 2700 m crestline of the adjacent sierra. This argues for vigorous slope transfer with extreme rainfalls promoting cobble displacement. The cienega marls (EA), on the other hand, indicate a ponded axial channel, supersaturated with carbonates, but grading upslope into a redox mottled silt loam; they indicate an interval of low-energy runoff and less concentrated rains. Evidently the parameters of Pleistocene hydrology were quantitatively different than those of the Holocene.

Also noteworthy is the 7–8 m channel entrenched into Pleistocene and Holocene beds, following directly upon slope erosion, colluvial transfer and cumulic soil formation (Unit EF). As at LA, ANG and CSD, this channel entrenchment documents an extreme, regional climatic impulse.

4. The Parras district

4.1. El Molino or Boca de San Francisco

El Molino marks the northern gateway to the basin of Parras (Fig. 1). Here the catchment waters drain through a narrow bedrock pass at 1245 m elevation, interrupting a steep ridge of Cretaceous sandstone that rises westwards to a crestline above 1500 m. Profiles of 4 m are exposed on both sides of the stream, the base obscured by a 1.5 m sandy inset. The western side, at the base of the steep, rocky hillside, includes several lenses of coarse slope wash. Otherwise, the sections are dominated by calcic ponded deposits (30–55% clay fraction, 30–60% CCE), with several tufa zones, and five prominent paleosols. Fig. 15 represents our only profile with common, interbedded archaeological features, not surprising in view of the strategic location at a narrow pass, and in the presence of numerous petroglyphs among the boulders above the western bank.

The basal Unit MA is poorly exposed and cemented by tufa lenses, but represents a cumulic A-horizon. Unit MB marks another soil with a truncated B-horizon, good soil structure, mottling, and carbonate nodules. The overlying bed MC is coarser and interdigitated with slope wash, resting on a disconformity. Charcoal from the unit was dated to 7890 and 7170 bp and suggests that the earlier units are of Late Pleistocene age.

Unit MD begins with massive tufas and pulses of slope scree, and closes with a prominent, vertic soil. Dates of 6080 and 3425 bp, and strong textural variation, suggest that this record is incomplete. Unit ME has basal tufas and a thick, highly humic, cumulic soil, with strong redox mottling and carbonate nodules; the clayey A-horizon yielded a humate date of 1805 bp.

A shorter cycle is recorded by MF, with strong laminar tufas and another cumulic soil, dated to 1030 bp, while a 1995 bp assay on the tufa itself reflects an older carbonate reservoir. A distinct surface unit (MG) represents a weaker soil, dated to 755 bp. The repetitive soils and high clay fractions imply that waters were repeatedly ponded at this site and for long periods of time.

The interstratified archaeological remains are primarily represented by carbon-encrusted, fire-fractured limestone rocks, often found in association with charcoal residues (MB, ME), supplemented in several cases with lithic debitage (MC, MD), or concave charcoal stains that suggest small hearths (MD). A boulder embedded in the top of MF has prominent geometric petroglyphs, identical to those of the hillside, but they are only present on the exposed surface of the rock, implying that the petroglyph site is in the order of a millennium old. A tentative but inconclusive case can be made for sporadic prehistoric

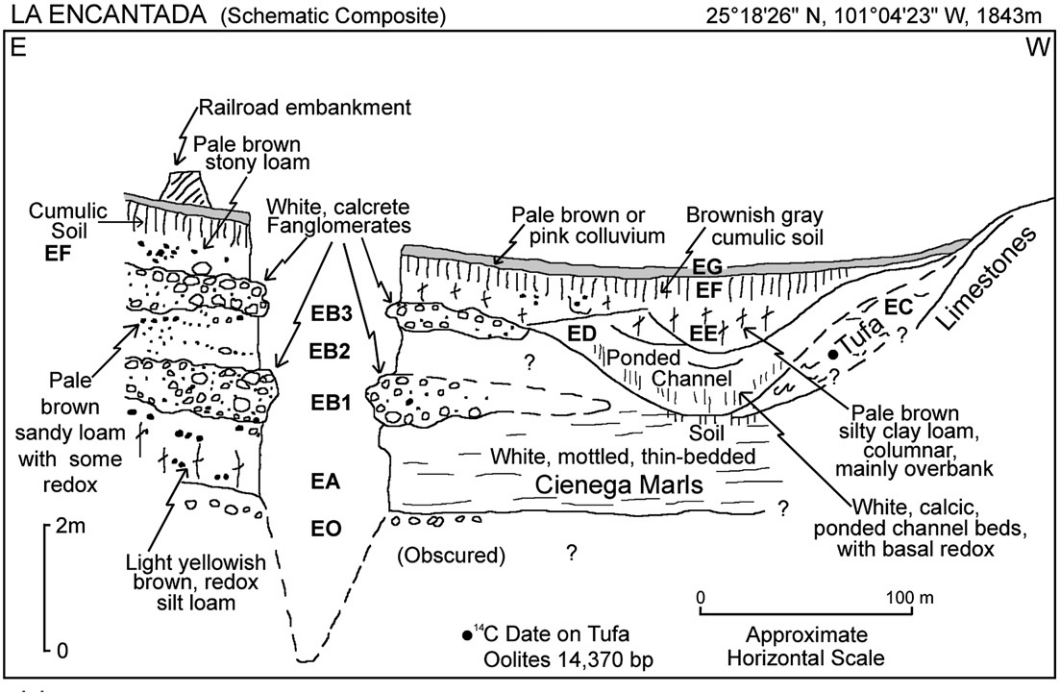

Fig. 14. La Encantada composite cross-section.

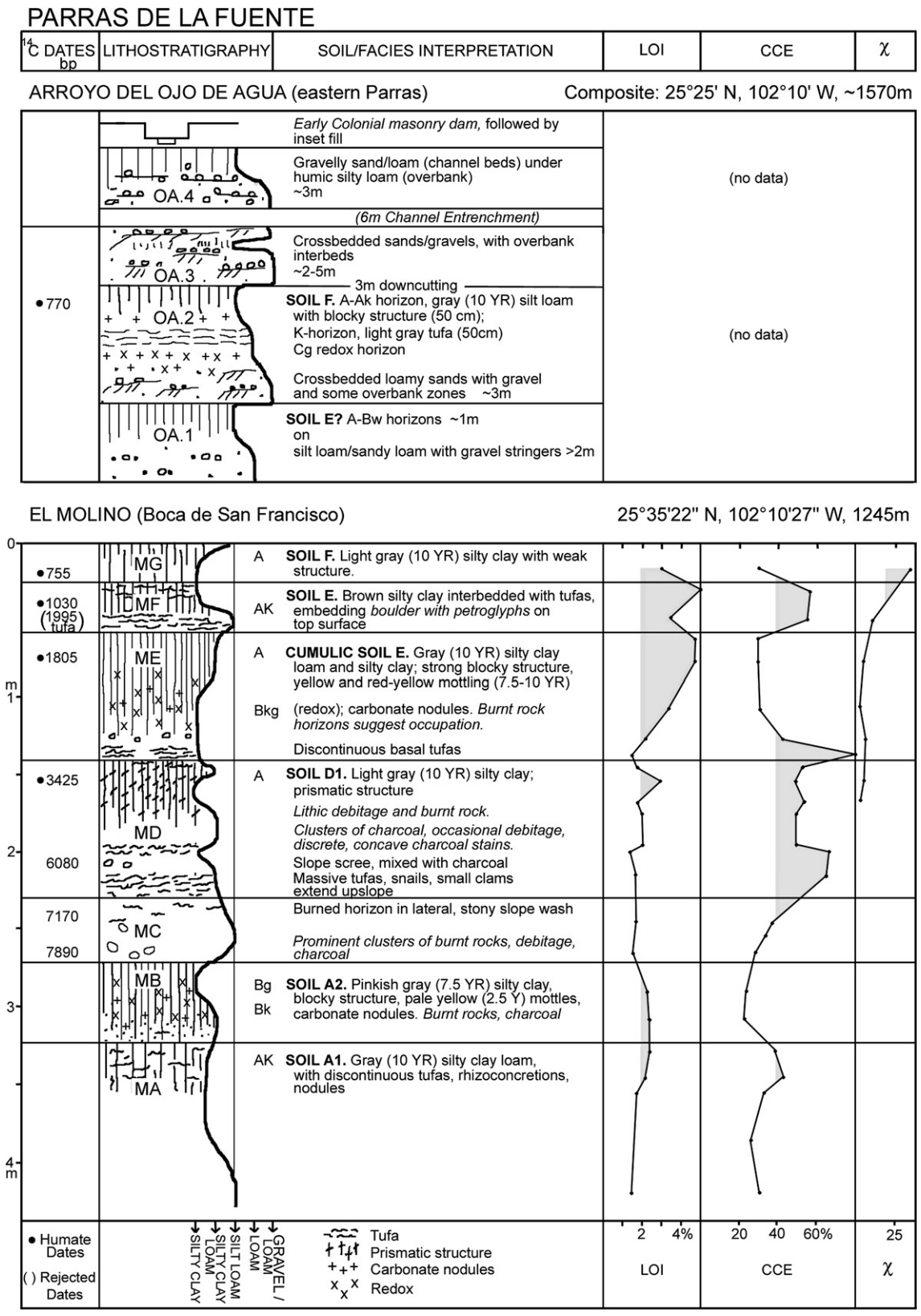

Fig. 15. Profiles at Parras and El Molino. The OA segment is a composite and not drawn to scale.

occupance at and around El Molino across more than 9000 cal. years, presumably to take advantage of a reliable waterhole, with abundant plant growth and attractive to game. Pollen is preserved, but diatoms and phytoliths are not present.

4.2. Exposures near Parras

Parras is situated on the footslope of the Sierra de Parras (1712 m), a block of Cretaceous limestones. A half dozen lobes of Pleistocene

tufas are spread along the upper margin of town, and prior to the modern water supply, many of the houses tapped a relatively shallow aquifer with private wells. The first hacienda, however, was set up in 1595 east of the Arroyo del Ojo de Agua (OA) that runs down the eastern margin of town and contains a number of old irrigation works. The lowest dam directly next to Parras (Presa 1), is the oldest, and a ruined weir at this site supplied water to the hacienda, the Jesuit mission, and the new town by around 1600 (Butzer, 1999). It was subsequently rebuilt and reinforced at least twice, at unknown but early dates, judging by a flurry of litigation after a competing Presa 2 was built 800 m upstream in 1618, to channel most of the water to the hacienda. This stretch of the arroyo exposes a succession of Late Holocene beds, schematically shown in upper Fig. 15.

Unit OA.2 is of interest because it initiates a period of rapid facies changes and channel instability. Basal cross-bedded sands were followed by finer beds and formation of a dense tufa or caliche (as in MF at El Molino), leading to redox conditions in the substrate. Eventually a gray cumulic soil developed around 770 bp, equivalent to Soil F at El Molino.

Shortly afterward, this unit was abruptly undercut by 3 m of entrenchment, then followed by rapid accretion of large-scale, low-angle cross-bedded sands and gravels (Unit OA.3), in two phases. Yet another cut-and-fill cycle intervened, but at a larger scale, now with 5–6 m of channel entrenchment, reminiscent of the incisive gully-cutting at Angostura and in the Saltillo Basin. But at OA a new, ephemeral fill, reflecting rapid, high-energy accretion occurs but without soil formation prior to the hydrological crash. That suggests one or more phenomenal floods, the volume of which exceeded channel capacity and triggered quasi-instantaneous entrenchment. The overdeepened floor of the arroyo began to refill almost immediately, with alternating sands and gravels, derived from mobilization of slope screes that were funneled in by lateral chutes. The result was a new floodplain terrace with 1.5 m relief (Unit OA.4).

Presa 1 provides a *terminus ante quem* for these events, because the dam is connected to the higher surface of OA.3 by a buttressed, deflecting wall while it is anchored on an earthen dam built atop OA.4. In other words, the components of Presa 1, initiated by the first European colonists around AD 1600, post-date or are contemporary with Unit OA.4. In other words, the 6 m entrenchment was Pre-Hispanic.

In the upper Arroyo del Ojo de Agua, 17 km south of Parras, three generations of sandy alluvium are present at site ERB (see Fig. 1): a) a complex 6–8 m fill recalling Units OA.2 and OA.3; b) a compact 2–4 m fill, embedding a hearth lined with charcoal fragments, dated 250 bp by AMS; and c) a recent floodplain deposit at 1.5 m. These features appear to replicate the OA sequence.

The two disequilibria at OA also have dramatic counterparts west of Parras (Arroyo del Capulín, or Morón). Upstream of the 1904 bridge are two thick fills, separated by 11 m of entrenchment. The cumulic soil on top of the younger fill here has a humate date of 570 bp, before yet again being entrenched by 11 m. Two further inset fills are found within the overdeepened valley, the older of which is modified by a Colonial irrigation weir.

The channel instability of the Parras arroyos can be attributed to steep channel gradients, high catchment relief, and abundant available sediment. As a result, the dynamics of the last millennium played out here step-by-step and left a detailed record of the responsible processes.

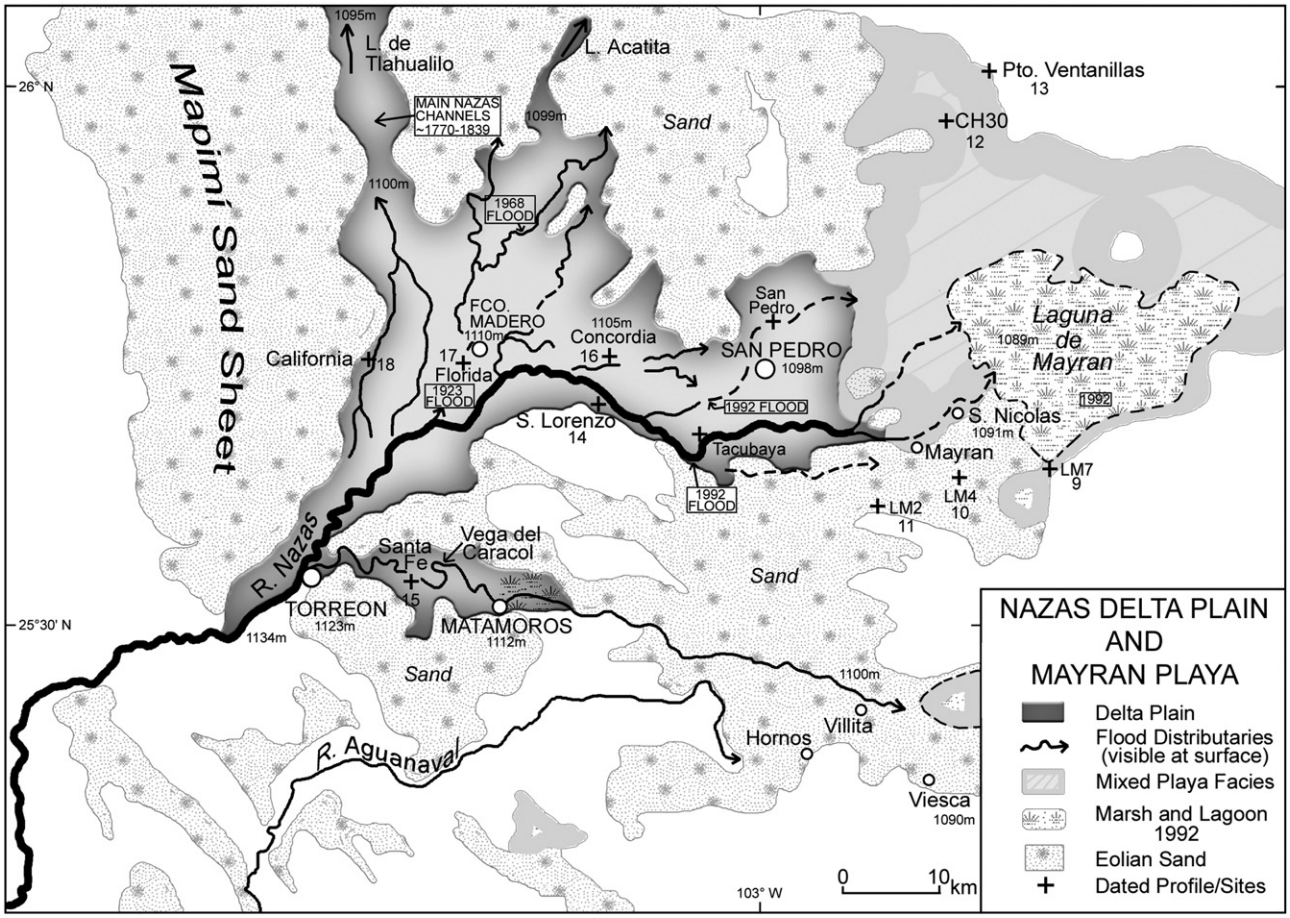

Fig. 16. Nazas delta plain and the Mayran playa. Historical information after E.K. Butzer (1997) and local informants. Numbers 9 to 18 refer to dated profiles (also Fig. 1). A selection of elevations is given in meters.

5. Alluvial fans of the Laguna margins

The Saltillo Basin, Angostura, and Parras give access to the medium-scale Holocene environmental history of the eastern half of the study area. Fragments of a Late Pleistocene record suggest that dominant processes were different than during the Holocene, but the bigger picture does not emerge. For this purpose we turn to the big-canvas landscape of the Mayran–Nazas plains (Figs. 1 and 16), alternatively known as the Desierto or Laguna del Mayran. Three examples are singled out.

5.1. The Parras Laguna fan

Large-scale alluvial fans are uncommon around the Laguna, where basin margins usually are delimited by playa and eolian deposits. An exception is the drainage from the complex, mountainous catchment of Parras, with a great fan projecting 25 km beyond El Molino. Diverging across a front of 35 km, its surface area is ~450 km^2, with five major channelways that feed calcium-charged waters to the eastern Mayran. In sharp contrast to the fine-grade Holocene deposits at El Molino, 3–4 m-deep quarries in the fan reveal little other than alternating, meter-thick lenses of compact coarse cobble gravel and eolian sand. Most of this probably is of Pleistocene age, but a veneer of gravelly sand loam appears younger. No marker horizons to merit dating were observed.

The scale of the Parras fan probably reflects Pleistocene detrital production in the Cretaceous fold-mountains of the Sierra de Parras (crestlines ~2500 m, highest peak 2880 m), suggestively known in early Colonial times as the Montes Pirineos or Pyrenean Mountains. Today remnants of oak–pine woodland occur above ~2300 m, but degraded oak–acacia–yucca scrub is more widespread. Episodic, high-energy fluvial processes are indicated by thick, compact or cemented

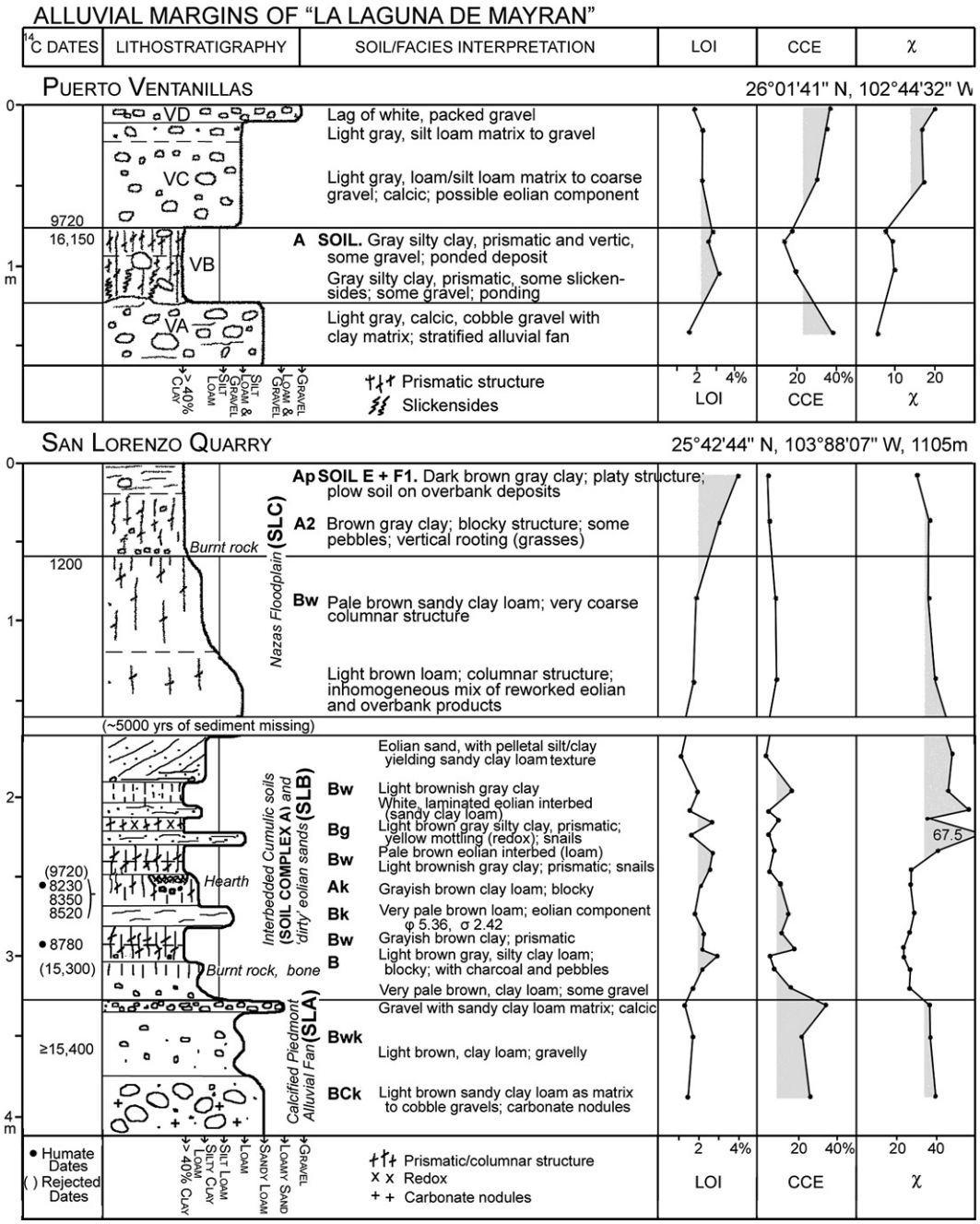

Fig. 17. Profiles from the alluvial margins of the Mayran.

slope screes, and by thick, stratified conglomerates that form ~20–25 m alluvial terraces down and upstream in the Arroyo del Ojo de Agua. Fragments of another such fill are present at intermediate elevations. We assume that the great Parras fan was part of this wider Pleistocene system.

5.2. Puerto Ventanillas fan complex

At the northeastern corner of the Mayran, Coahuila Hwy. 30 ascends from the playa flats to the mountains via the Ventanillas Pass on its way to Cuatrocienegas (Fig. 17). Here a set of superposed, petrocalcic fans is exposed in a number of 5 m-deep quarries for gravel (Unit VA). A calcic, but uncemented, fan also spreads a sheet of limestone cobbles to the edge of the mudflats (Fig. 16); the distal part preserves pockets of paludal deposits (>40% clay fraction) (VB) in hollows. Above that is a matrix-supported gravel (VC) that suggests a sporadic beach deposit to ~1086 m. A lag gravel (VD) veneers the surface.

The lower part of the paludal palimpsest designated VB has slickensides, while the upper is vertisolic, with a charcoal AMS date of 16,150 bp. A charcoal fragment embedded atop VB is dated 9720 bp. Given the discrete shore zones around the mudflat (with a surface sample of calcic, silty clay loam; LOI 2.6%), Unit VB indicates a low-energy body of water, episodically present in the adjacent playa, after fan accumulation had terminated. Part of Unit VC represents a storm beach.

5.3. An alluvial margin near San Lorenzo

Located at the contact of the Nazas floodplain and a footslope of minor alluvial fans, a suite of Late Pleistocene to Late Holocene beds is exposed in quarries east of San Lorenzo (see Figs. 16–17). Three gross units are displayed: 1) the sedimentary architecture of a Late Pleistocene alluvial fan (suite SLA); 2) an interfingering of Nazas overbank deposits, cumulic soils, and eolian sands during the Pleistocene–Holocene transition (SLB); and 3) a body of Nazas floodplain sediments, beginning with reworked eolian sands and terminating with overbank clays (SLC), dating to ~1200 bp.

The fan deposits of Unit SLA are exposed to a thickness 2–5 m and, towards the base of the exposures, include the prominent, medium-scale, low-angle cross-bedding of former ephemeral channels. Finer interbeds of sandy clay loam or clay loam, and gravel, vary in color from very pale brown (10YR hues) to light brown (7.5YR hues). Calcification, with respect to a former phreatic level, includes micritic calcite and $CaCO_3$ nodules. A charcoal AMS date of ~15,400 bp, in combination with an aberrant date of ~15,300 bp reworked in SLB, suggests termination of high-energy, local alluvial activity by ~15 ka, i.e., midway in Marine Isotope Stage (MIS) 2. The finer, end-Pleistocene components of SLA represent reworking of Nazas overbank material, or incorporation of fresh or old eolian pelletal silt/clay.

SLB is a thin-bedded complex of Nazas overbank deposits, cumulic soils, and eolian components, mainly of pelletal aggregates blown out of the Nazas floodplain. Only the youngest subunit has eolian cross-bedding. A number of archaeological features, including a small hearth pit, are dated at ~9–8 ka bp.

Macro-unit SLC follows a sedimentary hiatus of some 5 ka, and suggests culmination of Nazas delta plain accretion towards 1200 bp. Subsequent overbank discharge did not crest quite as high.

The Ventanillas and San Lorenzo profiles suggest that the smaller piedmont alluvial fans around the Laguna basin were active during mid-MIS 2 but ceased activity towards ~15 ka. Local precipitation had become ineffective. By ~9700 bp Nazas river influx had increased to the point that it supported periodic, local playa lakes in the Mayran—at about the same time that the Pink Alluvium began to aggrade at La Angostura, and only slightly later than the activation of the channel-floor artesian springs at Saltillo (UA, Unit A). In other words, Holocene hydrology was inaugurated simultaneously, shortly after 10,000 bp (~11,500 cal. BP), in the western and eastern Sierra Madre. That seems a reasonable working definition for the Pleistocene–Holocene boundary in the study area.

6. Interpretation of facies and paleosols in the Mayran playa

6.1. The problem

The Nazas delta plain and Mayran playa represent a very large place, where productive exposures are widely spaced, equilibrium is a dicey concept, and facies are not always what they appear to be.

Fine-grained flood deposits do not provide many useful sedimentological indices. Silts and clays are commonly aggregated by calcite, clay–humic compounds, gypsum or common salt; if deflated, such pelletal, silt/clay aggregates can be transported and deposited much like quartz, and may qualify as an eolian facies. But if pretreated in acid, calcic aggregates dissolve into the basic constituents, while gypsum will, to some degree, dissolve in water. As in the case of macro-unit SLB at San Lorenzo (see Fig. 17), textural analyses then give spurious results. This can be avoided by not decalcifying samples, but other than thin-sections, little can be done to diagnose eolian components in beds of gypsic aggregates.

The textural qualities of several suites of samples from quarry profiles were studied, including distributary levees and the 1992 flood deposits on the Nazas delta plain, although no salient quantitative parameters were detected. Sediments are overwhelmingly in the silt fraction (typically 60–65%, up to almost 80%), so that even exceptional floods leave only a localized or diluted fine sand fraction, as discharge promptly goes into overbank mode. When such surges of silt are deposited into the playa zone, they accumulate in sheets or shallow depressions, and may subsequently be deflated to blow as dust into standing waters or marsh to form loess; a cycle later, coagulated and dried pellets of silt bound by calcite or gypsum can be remobilized and deposited as eolian pseudo-sands.

Four Mayran profiles are selected to illustrate the problems of separating eolian, paludal, lacustrine or alluvial beds in the Mayran. They also inform the climato-stratigraphic record by virtue of the dated paleosols. Oxidation is often slow, and burial rapid, so that some pollen is preserved except in more extreme geochemical micro-environments.

6.2. Cuota site LM4

Along the southern side of the Mayran the toll-road (*cuota*) from Torreón to Saltillo is accompanied at intervals by large borrow pits. Nine of them were examined along a 30 km stretch east of the San Pedro tollgate, three of these studied in detail. Site LM4 (km 76.9, see Fig. 18) was selected as an example of clean quartz sand with eolian cross-bedding; 30 samples were examined by Cilas laser, four by traditional hydrometer and sieving. One charcoal and three OSL dates suggest that such eolian sands have been active at intervals for much of the Holocene. Sands are primarily developed in the southwestern Mayran, derived from the main Nazas channel between the small towns of Tacubaya and Mayran, mainly by deflation (compare Muhs et al., 2003). The thickest mantle runs southward to the village of Villita (see Fig. 16) while near LM4 sands take the form of shallow W-dunes, under a scatter of coppice dunes.

Construction crews had bulldozed a roadway here, to reveal a shallow but primary archaeological site. We deepened the section to expose the pre-occupation levels. The basal unit (4.A) begins with a thin-bedded silt loam, marked by repeated alternating beds of 5–30% sand, and a reducing environment with traces of gypsum. A permanently wet subsoil with periodic movement of fresh surface water is suggested for the Early Holocene.

Unit 4.B is poorly structured and sorted, mainly a sandy loam, without abrupt internal boundaries. It suggests a transitional eolian-

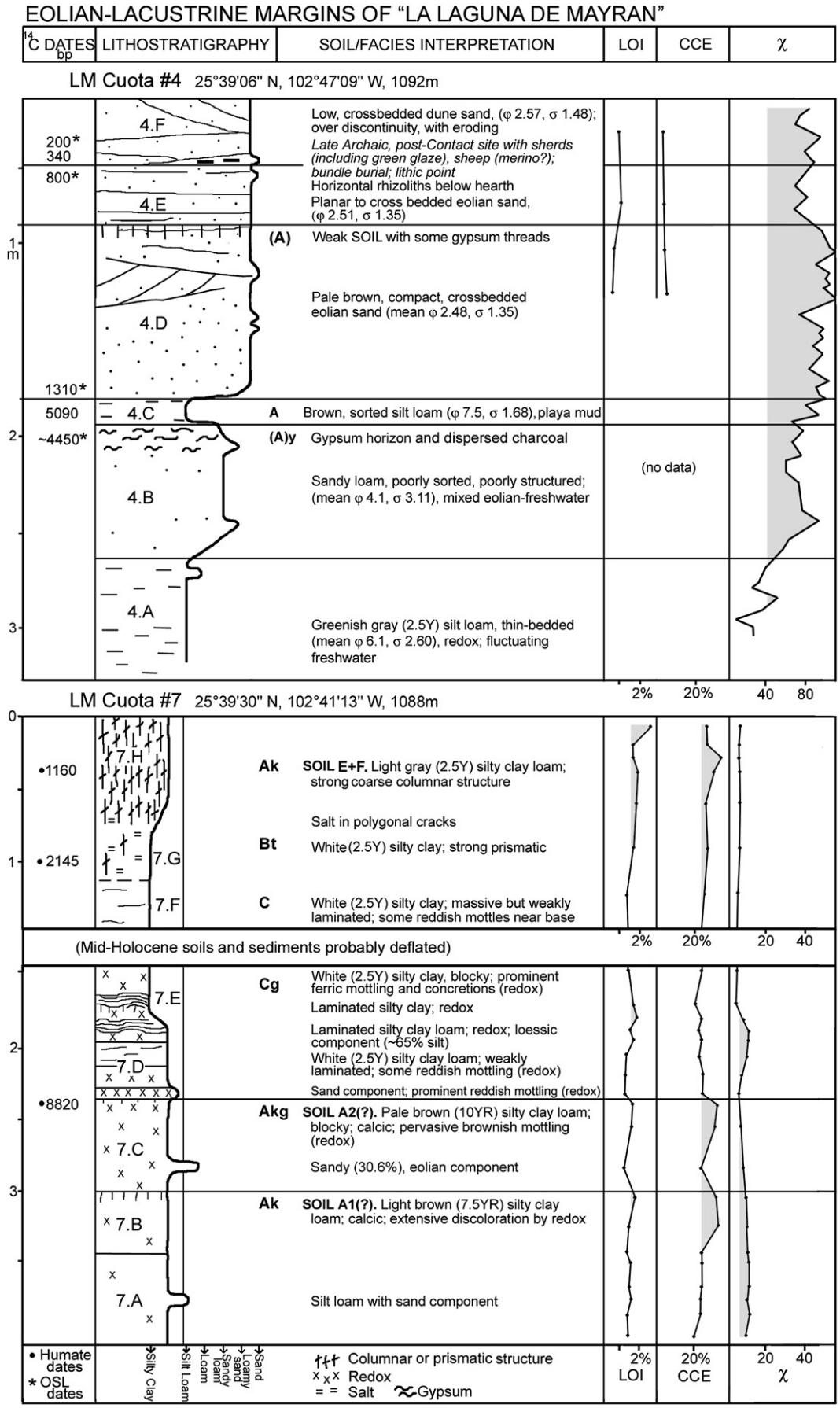

Fig. 18. Profiles from the eolian–lacustrine margins of the Mayran.

freshwater deposit (with 20–30% silt and 4–7% clay), reflecting rainwater ponding within interdunal swales or occasional freshwater influx from the adjacent piedmont zone.

Unit 4.C has only minor gypsum threads, but the 30 cm below it are heavily impregnated with gypsum (15–20% fillings in 3–5 mm pores), with a gypsum crust at the top of 4.B. Unit 4.C is a deflated palimpsest of playa mud, rather than a cumulic soil. The OSL date directly above it is 1310 BP and below it 4450 BP, the latter younger than a charcoal AMS date of 5090 bp.

The top three units (175 cm) are homogeneous, low-angle, cross-bedded eolian sands with very high magnetic susceptibility (Units 4.D, E, F). They rest on 15 cm of well-sorted silt loam bounded by straight contacts.

The archaeological site was occupied on top of a low dune, at the disconformity between units E and F (Fig. 18), and between bounding OSL dates of 800 and 200 BP. This protohistoric site includes the horn core of a domesticated sheep, possibly merino (according to E. Lundelius; TMM 43546); a hearth with charcoal and burnt rock; abundant fragmented animal bone; many poorly-fired potsherds, two with interior green (lead) glaze; lithics, including two thumb scrapers and a triangular bird point; perforated mussel shells; and an adjacent, extended, human "bundle" burial, which had been badly damaged by the time of our second visit. The hearth has an AMS date of 340±55 bp (with a median calibrated probability age of AD 1650), and the $\delta^{13}C$ of −11.0‰ implies that semidesert shrubs (saltbush?) served as fuel. If the mussels came from the Nazas River, the paleoecological implications could be significant.

The Spanish intrusion began during the 1590s (Jesuit missions along the Nazas and a hacienda at Parras), arguing for an early 17th century frame to account for contact phenomena such as sheep or lead glazes. The presence of this site at this time means that eolian sands were active at the time of Spanish intrusion—and had been dominant here for many centuries before that. Surface sites are fairly common in this sector and call for salvage archaeology and test excavations before they are lost.

6.3. Cuota site LM7

Site LM7 (at km 86.9, see Fig. 18) is located adjacent to playa beds, on flats with more vegetation (saltbush, *Suaeda*, scattered acacias) and lacking eolian veneers. Not surprisingly, the 4 m quarry profile is dominated throughout by silty clays and silty clay loams, but a mid-Holocene record is missing and probably has been deflated.

The Early Holocene part of the profile is heavily gleyed and includes two weak soils, as well as two wavy, laminated beds with a chalky feel, but without CCE peaks. They may reflect running water. The sandy thin-beds record brief eolian intrusions of the playa flats; the basal subunit may go back to the terminal Pleistocene.

The Late Holocene segment represents a prominent paleosol with an Ak/Bt-horizon of 120 cm and humate ages of 1160 and 2145 bp. The topmost 10 cm are more organic and have 62% silt, suggesting recent modification and blowing dust. The strong columnar structure of the light gray A-horizon grades down into a polygonal cracking zone, with prismatic structure and salt, but with >40% clay fraction, probably a Bt-horizon. Below that is a massive-bedded silty clay, with strong redox features, separated by a disconformity.

The dates and changing environment suggest a conflated, cumulic soil, perhaps representing Soils D2, E2 and F. The salt crystals, mainly halite, reflect post-depositional penetration of soil cracks, down to the top of the massive-bedded silty clay.

LM7 provides a discontinuous record of the evolution of a typical playa environment in the Mayran.

6.4. Cuota site LM2

The third site is LM2 (at km 69.5, Fig. 19), which is preserved under a veneer of fine sand. A 4 m profile is exposed in a large borrow pit, and 24 samples were studied in the laboratory. Two paleosols are visible within what appears at first inspection to be a dominantly sandy profile of very pale brown (10YR hues) color, with a mix of eolian and water-reworked eolian facies. Considering that Unit 2.J has 25–50 cm of steeply cross-bedded deposits, and that the lateral equivalent of Units 2.D to 2.F at nearby site LM1 (km 68.6) comprises 1.5 m of cross-bedded eolian sands, that interpretation is technically correct.

But the sands are mainly pellets, aggregated by gypsum. In water or a phosphate solution they slake into silt loams, clay loams or loams that flocculate in the hydrometer unless the gypsum is first removed. These pellets clearly derive from fine-grained playa deposits that have partially disaggregated, been deflated, and subsequently deposited downwind as eolian pseudo-sands. Such sands are only found above the lower soil, which is a gypsic and reduced clay (ABgy-horizon), with an apparent, terminal date on humates of 5690 bp. Periodic flooding by gypsum-rich waters probably goes back beyond 6 ka, and we suggest that a much thicker playa deposit at this level was largely destroyed by wind erosion and then reworked into a shallow dune field of pelletal muds. These gypsic materials were reactivated at various times, up to the present.

This original "gypsum phase" seems to be of Early Holocene age and localized, because it is not apparent at LM7 or at LM2, where the "saline phase" is Late Holocene.

The soil palimpsest of Unit 2.B and the thicker soil of Unit 2.H are strikingly dark, but like the capping soil at LM7 have very little organic matter. Evidence exists for occupation at the Unit 2.H/2.I contact, namely a hearth with burned rock and a charcoal age of 3780 bp. The humate age from 5 cm below the top of 2.H is 5000 bp, while humates 5 cm above the base of 2.I are dated 4370 bp. Pedogenesis had effectively stopped before 3780 bp, probably between 5000 and 4370 bp. That would leave no more than 800 calibrated years for soil formation and previous accumulation of 200 cm of sediment, perhaps as a result of migrating pelletal dunes, partly trapped in standing waters.

No mid-Holocene hiatus is evident other than the almost complete erosion of Unit 2.B. Unit 2.I suggests a mixed environment and may represent a period of incipient soil formation or the base of another eroded soil.

6.5. Coahuila Highway 30

Site CH30-2 is located next to the highway from San Pedro to Cuatrocienegas, 9.5 km SW of Puerto Ventanillas. The features of this profile (Fig. 19) can be summed up from top to bottom, so as to highlight their dissonances.

As in many sites along the Cuota, a prominent paleosol is present near the surface, consisting of an A/Ak profile 55 cm thick. The top 20 cm (CH.6) is gray, enriched with organic matter and yielded a charcoal age of 1380 bp and a humate age of 3320 bp. The lower part of the soil (CH.5) is light brownish gray with decreasing LOI.

The soil rests discomformably on ~25 cm of white, silty clay loam (CH.4-4a) that suggests periodic playa flooding. It follows a 70 cm sequence of sorted sand and silt (CH.2-3) that grades upward into a heavy silt, while the magnetic susceptibility is halved. The silt has a loessic texture and appearance, including a large krotovina, or vertical rodent burrow. The basal OSL assay of 7130 years comes with a wide error range.

At the base of the section is a reduced, pale yellow silt loam, exposed for 40 cm, with low χ values. This gleyed playa mud (CH.1) emphasizes that Units CH.2–3 are long-distance sediments, introduced by running water or wind. Today the closest sand veneers and coppice dunes are located >5 km to the SW. It is, therefore, possible that the sands were introduced by a powerful flood surge, with the silt accumulating when discharge waned. This seems more plausible than an eolian explanation, given that the 1992 Nazas flood undermined the highway north of San Pedro as it shot sweeps of muddy water 20 km and more into the playa environment (Enrique Fernández, pers. comm. 1996).

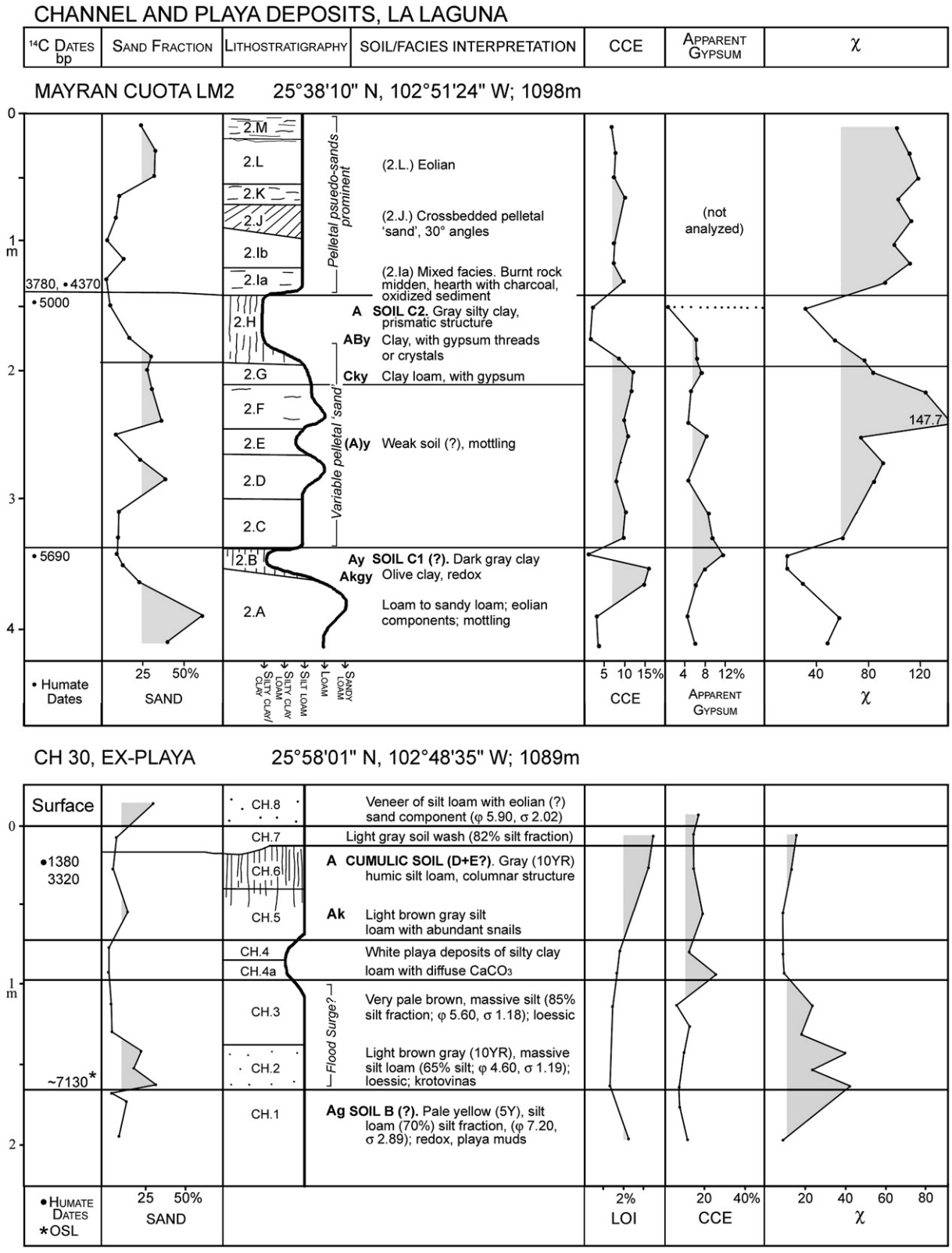

Fig. 19. Channel and playa profiles of the Mayran.

6.6. La Campana, Laguna de Tlahualilo

At the northwestern end of the Nazas delta plain is another playa, the former lake of Tlahualilo, occupying a long valley between fault-block mountains. Historical records show that much of the Nazas water flowed into here ~AD 1770–1839, after sediment had blocked the main channel (E.K. Butzer, 1997). Several narrow overflow-type channels remain quite visible, converging toward La Campana at the southern end of the playa. A 4.5 m profile (TLA) is exposed in a quarry here (Fig. 20).

The lower half (Units T1–T7) has interbedded playa muds, fluvial sands, and eolian components or dune sands, indicating shifting environments in a fluvio-lacustrine setting. The basal beds define an Ag/Bgy soil profile. Dated to 11,650 bp, that soil developed at the edge between the playa and a larger stream (T1–T3). Superposed on this is a cross-bedded alluvial horizon with reworked eolian sands (T4). It was followed by lake expansion and playa sedimentation (T5). Thin-bedded silt loams and loams indicate subsequent stream proximity (T6), and the analogous sequence at 'California' (Fig. 16) has a date of 7570 bp on this distinctive bed. Dunes then developed as the playa shrank and the stream dwindled, allowing subsequent deflation of the Middle Holocene record.

The second half of the column begins with a playa mud (T8), followed by accretion of a major, clayey cumulic soil in two phases, with dates of 2620 and 230 bp (T9–11). This probably is the same prominent soil visible within the Nazas delta plain, thus at La Florida (date of 1460 bp), Concordia (dates of 1450 and 1630 bp), and Santa Fe (dates of 1420 and 1960 bp) (see Fig. 16 for location of these sites). Nothing akin to the minor terminal soil has been recognized in the Mayran, but in-channel features of similar age are found at La Florida (655 bp) and Santa Fe (240 and 440 bp).

The Campana profile points to episodes of strong fluvial activity, accompanying repeated fluctuations of the lake shoreline, during terminal Pleistocene and Early Holocene time. According to this geoarchive, a good part of the Late Holocene was marked by more stable and comparatively moist conditions. That is not supported by the alluvial stratigraphies of Saltillo, Angostura, Parras or Arroyo Grande (Section 7), which commonly responded to disequilibria by cut-and-fill cycles. But in an endorheic basin with a floor elevation of ~1090 m, no significant option exists for distributary incision: a) streams can shift laterally and destroy older sediment by limited lateral erosion; and b) shallow playa lakes will evaporate to mudflats at much the same elevation, while beach development is rudimentary, and deflation may become the main process of sediment removal.

In other words, the playa and delta record of the Mayran cannot be interpreted by the same criteria as the alluvial histories emphasized in this study. It has a different dynamic, amplitude, and equilibrium mode, because gradients become insignificant and base level is essentially fixed.

6.7. Where is the mid-Holocene record?

Without recourse to alluvial and paleosol histories from adjacent geoarchives, our Mayran and Tlahualilo records are inadequately dated. Technically, that could be partially remedied by greatly

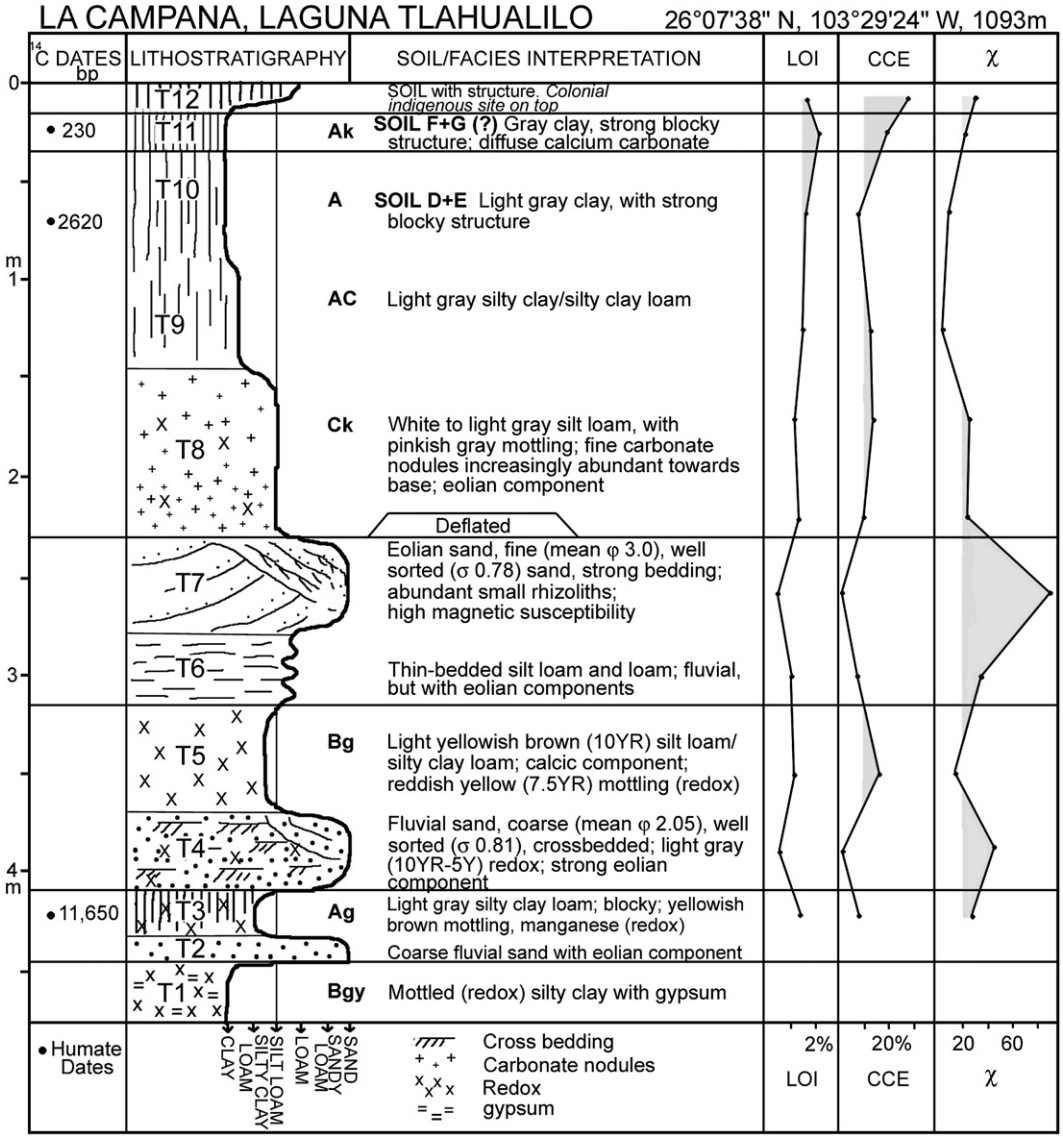

Fig. 20. Profile at La Campana, former Lake Tlahualilo.

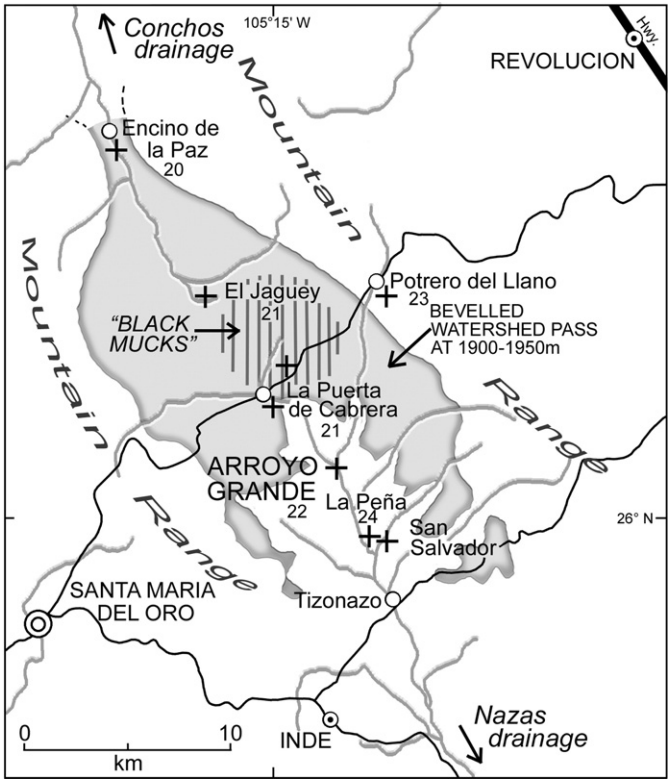

Fig. 21. The Nazas–Conchos watershed, with location of studied sites. The beveled watershed (in gray) is an ancient erosional surface.

increasing the number of AMS dates. But organic carbon is scarce, and particularly the mid-Holocene and older segments would require an OSL dating program. A second problem is the presence of major sedimentary discontinuities and many minor erosional breaks that are often difficult to detect. In effect, to document the Holocene environmental history of the Mayran playa would entail another major project, grounded in scores of drill core profiles. At this stage the import of understanding the environmental history of this area is primarily systemic, rather than comprehensive.

We must, therefore, consider the five previous profiles within a broader geomorphic and lithostratigraphic context. That is provided by seven other, undated profiles, not described here; various sediment-sampling sites; study of satellite imagery; and transverses of the Mayran margins. Sites on the perimeter, such as San Lorenzo and El Molino, provide a frame of reference.

The common stratigraphic marker is a strongly structured grayish soil, up to 120 cm thick. Frequently it is near or at the surface, under a veneer of calcic mud or loose sand. Elsewhere it may be at 50–175 cm below the surface, under colluvial wash or eolian beds. This dominant, regional paleosol has diverse dates ranging from 1160 to 5000 bp, a time span that includes *three* distinct soils at El Molino (see Fig. 15). Pedogenesis was intermittent and cumulic, in combination with short or long-term deflation, so as to simulate a single soil profile. Local conditions may also have favored subaquatic muds—dense and calcic or gleyed—instead of pedogenesis. Nonetheless we informally designate this complex feature as the *Mayran soil zone*, for the sake of convenience.

The second stratigraphic marker is a "lower soil," preserved or visible as a palimpsest at a limited number of sites: LM2 (5690 bp), CH30 (before 7130 OSL), LM7 (8820 bp), PV (9720 bp), and TLA T6 (? 7570 bp). It too represents but a fragment of several millennia, as suggested by the interbedded soil and eolian lenses of Soil Complex A at San Lorenzo (see Fig. 17). The playa environment has not been favorable for preservation of Early Holocene paleosols, that once may have been as prominent as the Mayran soil zone.

The beds between these two marker horizons may be 1–2 m thick, recording mixed facies or prominent eolian sands, in addition to breaks because of substantial deflation. But no trace exists of another soil in between. That is not just a matter of deflation, because the delta plain also lacks significant soils below the Mayran soil zone, in a sedimentary environment without large-scale deflation. Indeed, during part of the mid-Holocene, flooding of the Mayran was uncommon and limited in extent.

A final question concerns the paleoenvironmental significance of the Mayran and "lower" soils. They did not record, for example, a set of three, 500-year periods of abundant water. Instead it would be better to posit periods with a reasonable recurrence of strong floods, perhaps once a decade. Even floods might not occur for decades at a time. What our study did show was frequent evidence for anoxic soil environments. Even today the water table in a marginal sector of the Mayran, such as LM1 and LM2, is at less than 4–5 m below the surface. The degree of gleying at some of our sites suggests long-term water tables within 100–150 cm of the surface. High water tables can persist for decades after a surge of water, but sheets of open water will evaporate within a year or two. The former offer greater stability for certain biological communities.

Fig. 22. Main exposures of Arroyo Grande, looking southwest.

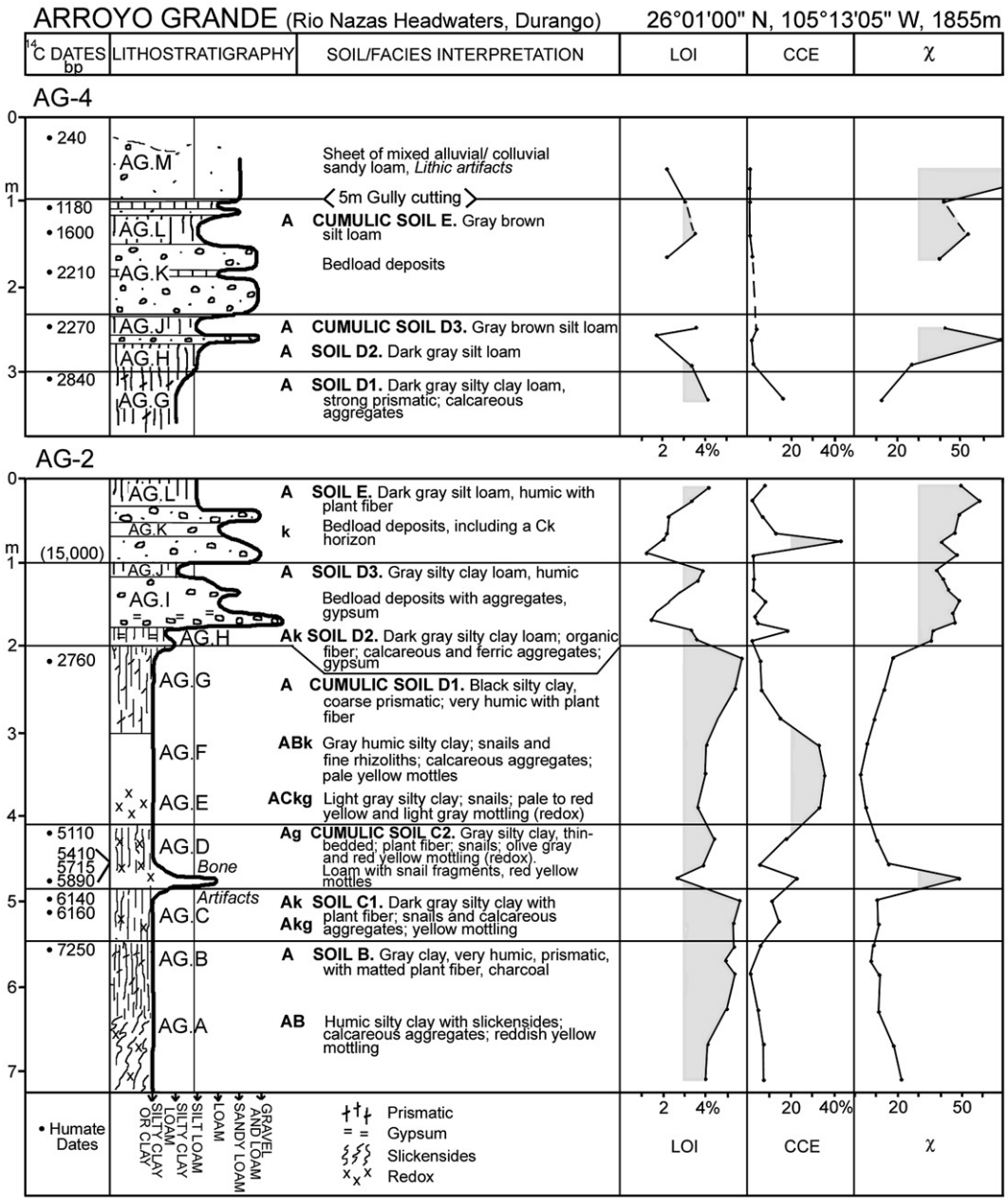

Fig. 23. Arroyo Grande analytical profiles: AG-2 combines ages from AG-1 and AG-5.

Beyond inhibiting deflation, higher water tables would favor a richer vegetation of halophytes or grasses, belts of wetland plants, and more trees—widely scattered, yes, but also taller, and perhaps including taxa other than acacia and mesquite. Pollen preservation in the four Mayran sites is reasonably good, and Bruce Albert (University of Texas) is preparing to publish the profiles. Together with provisional study of stable carbon isotopes, this may help diagnose whether a different quality of ground cover facilitated development of the Mayran soil, versus the "lower" soil, given that anoxic substrates were more common during the Early Holocene.

7. The Rio Nazas headwaters, Durango

7.1. The issue of the "black mucks"

The Nazas and Conchos drainages meet not as steep mountain catchments, but at 1920 m on a smooth erosional surface near Puerta de Cabrera, Durango (26°4′ N, 105°16′ W) (Fig. 21). Within a longitudinal valley of the Sierra Madre foothills, this beveled plain is cut across extensive rhyolites, between parallel fault-blocks. Before the upland plain breaks up in the gorges of the upper Nazas, it delimits large tracts of unimproved grassland that support dark gray or brown Mollisols.

These "black mucks" have much the same properties as the dark cumulic soils identified in floodplain profiles around Saltillo and at El Molino, and they feature prominently in our profiles from Arroyo Grande, Puerta de Cabrera, and Encino de la Paz (see Fig. 21). Remarkable in this Durango watershed is that remnants of these mucks occupy upland surfaces and dominate an area of over 10 km^2. It is, therefore, possible to link the cumulic Mollisols of dated local alluvial sections with such relict, upland terrestrial soils.

The hypothesis formulated in 1993 when Butzer examined these features was that a soil organic carbon (SOC) budget could be estimated for the period during which these black mucks formed, so as to quantify the extent to which the contemporary SOC reserves have been degraded. This is a significant issue for the paleoecology of

North-Central Mexico. The present paper attempts to study the temporal and spatial parameters for such a future investigation—with the requisite biological and geochemical expertise to capitalize on these findings.

We first examine the complex profiles at Arroyo Grande (Figs. 22–24), which anchor the western end of the study area. Additional profiles are then drawn in to expand on the local Pleistocene record and the black mucks.

7.2. The Early to mid-Holocene record

The lithostratigraphy of Arroyo Grande is assembled from several profiles, two of them directly adjacent: AG-1 (7.2 m with 17 sediment samples from 16 subunits, but not illustrated here) and AG-2 (7.2 m with 31 samples from 10 subunits. Basal contacts are revealed at AG-3 (1.2 m with 3 samples) and AG-5 (2 samples). The Early and Middle Holocene units can be summarized, with respect to Fig. 23 and its key soils.

Cumulic Soil B (>1.8 m). Gray/olive/dark gray clays (AG-2) and silt loams (AG-1); highly organic (>5% LOI); very coarse prismatic, but with slickensides at AG-2; redox overprinting; a humate date of 7250 bp is the oldest for black mucks of the watershed.

Soil C1 (0.5–1.0 m). Similar to Soil A, but more calcic and with snails; humate ages of 6140 and 6160 bp. A large, retouched side-scraper and a flake were found embedded on top.

Cumulic Soil C2 (0.7–1.0 m). Olive to gray silty clay; strong prismatic structure and redox mottling; less organic (~4% LOI) than soils A or B; snails; humate dates of 5110 and 5890 bp, and charcoal counterparts of 5245, 5410, and 5715 bp at AG-1/2 and AG-3. *Lateral variants*: At AG-5 the unit is capped by 5 cm of laminated pond muds with an age of 5090 bp (charcoal) and traces of leaf impressions. These rest on 100 cm of gray loams, enclosing 15 cm of loamy fine gravel, and continuing upslope to light gray, gravelly loams with redox mottling, related to a small lateral channel. The olive gray organic horizon immediately below yielded a humate age of 5670 bp. The AG-5 detrital zone, younger than the loam lense of AG-2, indicates that the coeval channel must have had substantial bedload.

Cumulic Soil D1 (1.5–2.1 m). Black silty clay (AG-2), silty clay loam (AG-4) or silt loam (AG-1); highly organic (5.8% LOI); strong and very coarse prismatic structure; clear horizonation, with a gray ABk horizon of silty clay and a light gray ACkg of silty clay loam. The base cuts into Soil C along a wavy boundary. Humate ages of 2760 bp (AG-1) and 2840 bp (AG-4) indicate that this final black muck is equivalent to the >1.5 m of black, slickensided fill at Puerta la Cabrera (see Fig. 21) (2340 bp at the bridge profile, and 2680 bp in the roadside ditch 600 m E).

Continuous Sedimentation at Arroyo Grande? On the mountainside at Potrero del Llano (see Fig. 26), the Arroyo la Boquilla (which joins the Arroyo Grande at AG-4) exposes a more modest, 160 cm profile for Soil D1; a basal charcoal date of 4185 bp was obtained from the ACk horizon above an underlying gravel. Such a linkage draws attention to the problem of equating the age of an A-horizon with the full time span of its sedimentary hemicycle. But if the Potrero del Llano date were applicable, it would suggest that the ~2 m accumulation of AG Units E through G took very roughly 2300 cal. years (see Table 1 for median probability calibration dates for 4185–2340 bp).

To continue the speculation, it would give a rate of sedimentation of 1.15 cm/year for AG.E–AG.G, and 1.0 cm/year for AG.D (Soil C2) to imply a hiatus of ~900 years between Soils C2 and D1, and of ~1200 years between C1 and C2. Applying 1.0 cm/years to the sediment thickness of Soils B and C1, the dates would leave no hiatus between those hemi-cycles. In short, the apparent continuity of the main profiles at Arroyo Grande is deceptive, and major breaks occur during the mid-Holocene, before and after Soil C2. Its strong lateral variability in AG.5 suggests that Soil C2 is the telescoped record of a stream system marked by considerable instability, and perhaps on the brink of disequilibrium.

7.3. Mid-Holocene bedload eruptions and piedmont paleosols

The true dynamic of the mid-Holocene environment becomes apparent on the gently inclined watershed surface, rather than in an arroyo meander bend. Fig. 25 for El Jaguey is a schematic section representing 450 m of exposure along a small arroyo recording a Late Quaternary environmental history of this piedmont.

The bulk of the sediments are Pleistocene clays and silty clays, in part with slickensides or coarse prismatic structure. The lower part is heavily redox-modified, and $CaCO_3$ has been mobilized and segregated into large (10–30 cm), irregular concretions. Resting on ancient, decomposing rhyolite flows, this sheet of sediments has two major paleosols (Units 2a/3 and 5c/upper 5b), suggesting a weathering residuum of piedmont fans or rhyolite bedrock, or both. Gravel lenses or laminar stratification (Units 4/5a) near a subsurface rhyolite discontinuity indicate fan-like reworking at this break of gradient.

The Holocene at El Jaguey is mainly represented by sheets of fine debris (Units 6–10) with strong Munsell chromas, overlying slickensided, low-chroma clays (Units 5a/b/c). Exceptions are two massive

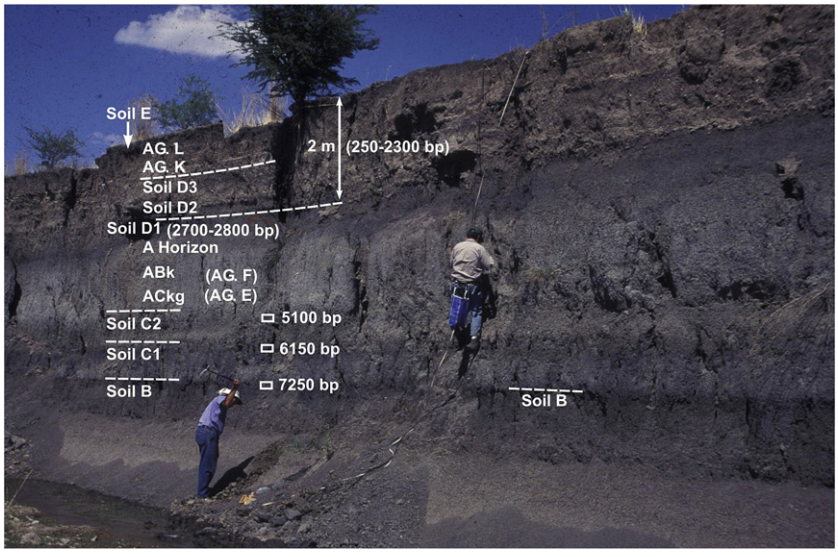

Fig. 24. Rappelling on and measuring AG-2 at Arroyo Grande. The lowest, dark gray Horizon is Soil B, ~7250 bp.

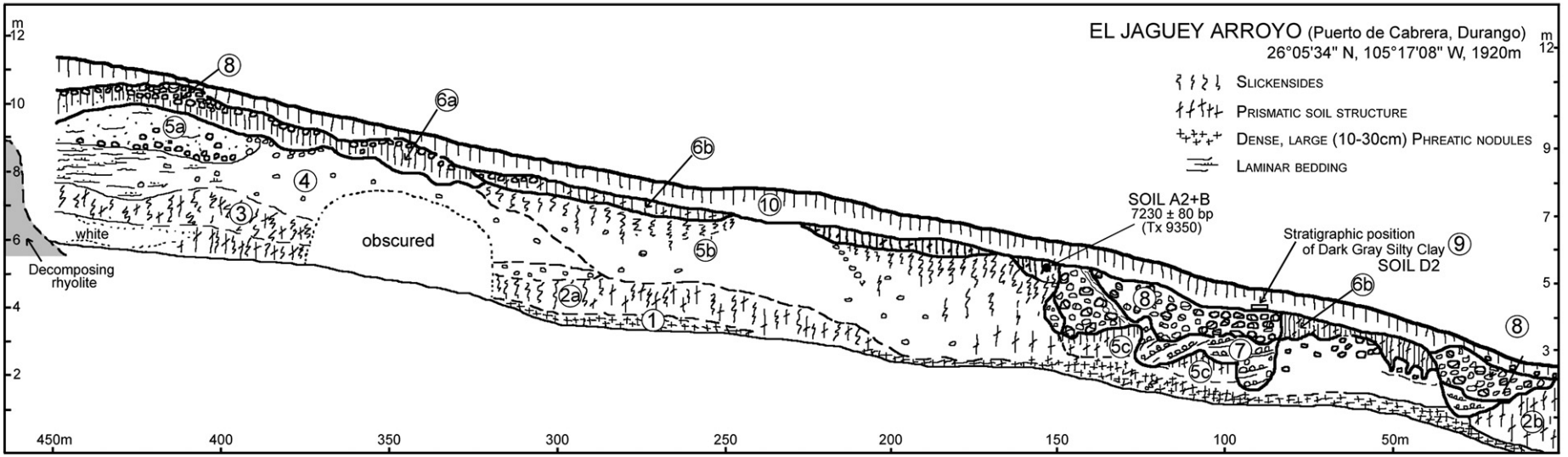

Fig. 25. Longitudinal profile of El Jaguey, showing inferred Pleistocene deposits (Units 1–5) and Holocene features (6–10).

bodies of coarse-to-cobble-grade gravel packed into former channels that intersect the recent gully diagonally. At issue is the age and significance of these rubbles.

The basal contact is given by a well-developed paleosol (Unit 6b, see Fig. 25) with a strong brown (7.5YR), organic (>4.0% LOI), very coarse prismatic, A-horizon (50 cm) of clay texture. Traces of a yellowish red (5YR) Bt-horizon (25 cm) exist; some floating pebbles have ferric cutans, while soil pipes extend as much as 75 cm into the substrate. This qualifies as a vertisol (Chromic Haplustert), with a humate date of 7230 bp, i.e. coeval with Soil B at Arroyo Grande.

The gravel channel tore through the paleosol in two places, up to 80 m in cross-section. The main outcrop of this gravel has a cumulative thickness of 2.5 m, beginning with current-bedded coarse clasts in a sandy loam matrix (0–125 cm) (Unit 7 in Fig. 25). A massive body of coarse-to-cobble-grade gravel followed (150 cm), with a silt loam matrix. After a break, a new eruption deposited coarse-to-cobble-grade gravel (Unit 8), with interbedded sandy loam (100–150 cm); the upper half becomes a lag, with much boulder-size material in a silt loam matrix, and illuvial clay recorded by cutans beneath some clasts.

On the facing, north side of the gully, a palimpsest of black mucks rests directly on this gravel complex, under the truncated Bt-horizon (30–60 cm) of another paleosol (Unit 10, Fig. 20). This is a yellowish brown (10YR hues), organic clay loam/loam with angular blocky structure, and would probably classify as an Alfisol. The illuvial clays from this Bt-horizon have penetrated this upper Gravel Complex (Unit 8, Fig. 25). The surface supports a cumulic Mollisol, with an A-horizon of dark brown clay loam, organic (4.1–4.5% LOI), and gravelly towards the base.

The Vertisol (Unit 6b) under the Gravel Complex has inherited some characteristics from the Pleistocene base, but the soil pipes, the anomalously high clays (61–66%), and the LOI values argue for extended and intensive pedogenesis on the piedmont surface, probably going back into the end-Pleistocene. With tighter dating and work on the clay minerals and soil micromorphology, a case could be made that the Vertisol–Alfisol–Mollisol sequence differs primarily in terms of time and stability, rather than pedogenic direction.

For the black mucks, we propose that these are cumulic soils reworked from the initial Vertisol, emplaced in wet declivities on an almost unentrenched valley floor, where organic matter continued to accumulate. Incremental erosion and redeposition would initially have diluted the clay fraction, which then was augmented by a higher component of authigenic smectite. Periodically, this “bank” of black mucks in storage on the piedmont was drawn down to supply the basic substance of the Holocene paleosols coming together in low-energy stream valleys like Arroyo Grande.

This interpretation appears applicable at Puerta de Cabrera where, at the bridge, black mucks rest on 120 cm of a similar gravel complex. These are torrentially bedded, very coarse gravels with a matrix of sandy loam, intensively gleyed (yellowish red 5YR) in their lower part. Near the base is a columnar structured silt loam, under a cobble lag and in turn resting on another lag of coarse-to-cobble-grade clasts with extensive red (2.5YR) and pinkish gray discoloration. A humate date from the basal redox horizon gave 16,630 bp. The black clay, exposed nearby to 1.5 m thickness, has a humate age of 2340 bp. This is the greatest thickness of black mucks observed, and the two dates bracket the gravel complex. But the gravel body and the basal red silt loam are separated by a disconformity, the redox alteration of the latter being much more intensive.

A last profile to elucidate both the Pleistocene and Holocene records was studied from an old meander bend near Encino de la Paz (EP) (Fig. 26). The dominant feature is a long, calcrete ridge developed

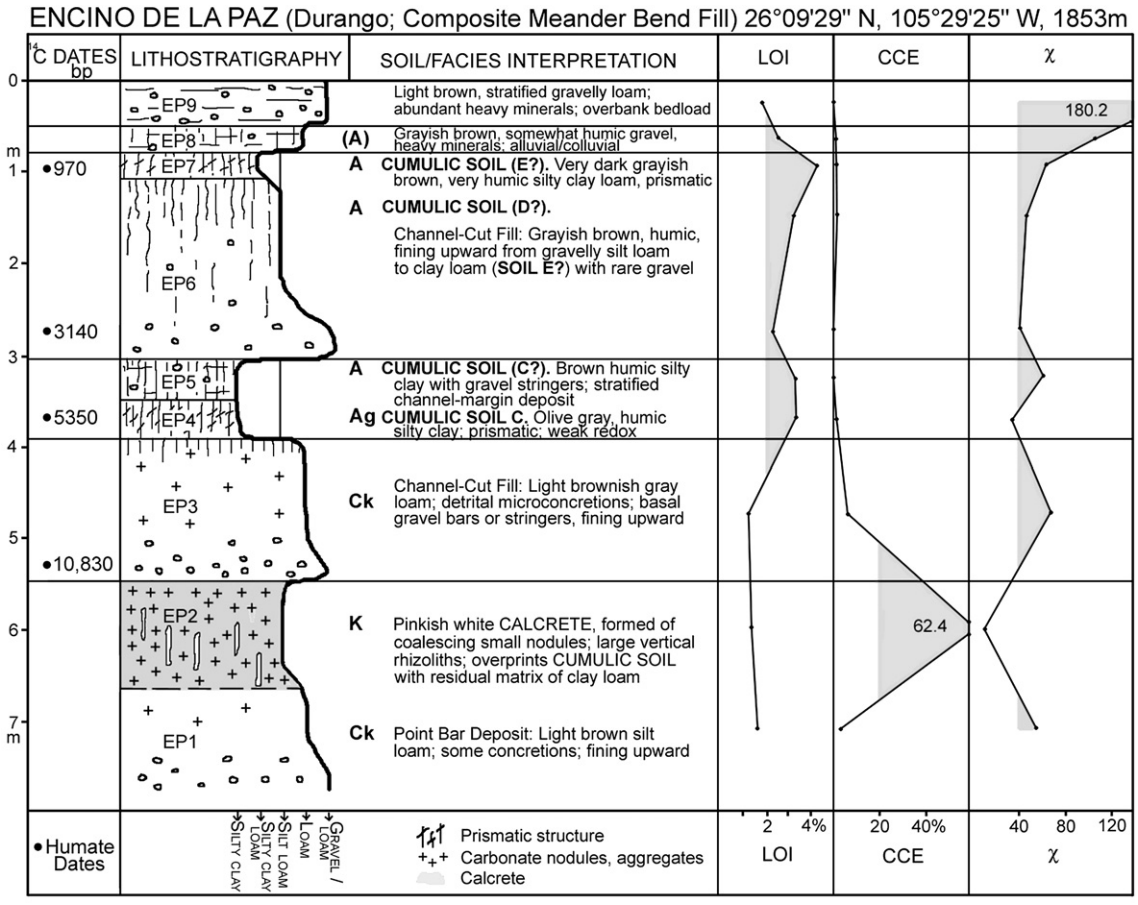

Fig. 26. Profile of Encino de la Paz. Compare the calcrete with Pleistocene features of Fig. 25.

on channel beds; the petrocalcic cap (EP2) was formed by coalescing of small calcareous nodules and large vertical rhizoliths, to overprint a cumulic soil of clay loam.

At a later point, after extensive erosion, a channel-cut fill (EP3) was embanked against the calcrete, beginning ~10,830 bp. After renewed entrenchment, two distinct cumulic soils (EP4, 5) of organic silty clay formed upon a channel-margin slope. The older of these has a date of 5350 bp. Following further cutting there was deposition of another channel-cut fill (EP6), once more fining upward from a basal date of 3140 bp. This is capped by a third cumulic soil (EP7), a prismatic, blackish silty clay loam with a date of 970 bp. The sequence is terminated by two superficial deposits, EP8 with colluvial components, and EP9 a channel-margin overbank deposit, with strongly increasing magnetic susceptibility.

Encino de la Paz seems to have a different Holocene rhythm than Arroyo Grande, but its 10 units are compressed within 3 m, recording four or five cut-and-fill cycles in a low-gradient channel conducive to graded bedding. Three black mucks are found there, the last representing the Late Holocene, and Unit EP6 has terminal pedogenic features consonant with a fourth cumulic soil of humic clay loam (see Fig. 25). This profile demonstrates the dynamism of the mid-Holocene.

The basal calcrete recalls the poorly-drained, terminal Pleistocene units at El Jaguey, but is identical in facies and aspect to a pre-Holocene, petrocalcic fill at Potrero del Llano—where it is found in a well-drained context.

7.4. The Late Holocene at Arroyo Grande

For roughly 6 ka (>7250 to ~2500 bp) the Arroyo Grande at the holotype appears to have been in dynamic equilibrium, even as shallow streams on the plain of the watershed were interrupted by cut-and-fill cycles or surges of bedload. The active channel shifted almost imperceptibly within a ~70 m-wide valley axis. But then, over a space of ~1200 years, sands and gravels were periodically injected into the channel, leading to rapid alternations of bedload deposits and more modest cumulic soils during the Late Holocene. In that time span, seven distinct beds were deposited at AG-1, nine at AG-4, and 14 at AG-2, each with a cumulative preserved thickness of 2 m. That compares with 9 or 10 subunits during the Early to mid-Holocene, with a thickness of 5.5 m: the rate of sedimentation had almost doubled.

Profiles AG-1, AG-2, and AG-4 record the Late Holocene lithostratigraphy, with humate ages of 2270, 2210, 1600 and 1180 bp (in AG-4, see Fig. 19), although the earliest subunit (AG.H) is undated. Anomalous is "desert rose" gypsum in AG.H and at the base of AG.I. The ostracods of AG.1 and AG.H indicate "saline" conditions (M. Palacios-Fest, pers. comm.). But the diatoms of AG.G and AG.H point to "fresh, flowing water", less alkaline than today (B. Winsborough, pers. comm.) (modern pH of AG.G to AG.I ranges from 7.82 to 8.03). The absence of gypsum in other profiles or units indicates a very local and perhaps temporary situation, in a stream where base flow was minimal and floods episodic. Alternatively the gypsum penetrated AG.H from above. After ~2500 bp the valley bottom appears no longer to have been stabilized by a dense aquatic or marshy vegetation.

Events subsequent to ~1000 bp (Soil E) recall La Angostura but are more difficult to date or fix stratigraphically. Initially the arroyo was incised by ~5–6 m.

A *major inset* of ~3 m accumulated in the newly incised channel of Arroyo Grande. It has planar cross-bedding, with lenses fining upwards from gravelly sands to sandy loams. Accretion took place after a finite number of high-volume floods, so that carbon recycling is likely and precluded an attempt at dating.

After renewed incision, a *minor inset* was deposited, with shifting facies, including well-stratified muds, sands, and gravels, older than a ~2.5 m cobble point bar. The complexity of these subrecent deposits is evident 3.7 km downvalley at the mouth of Arroyo San Salvador (see Fig. 21). Here dark muds are interbedded with fan gravels and embed a donkey mandible (*Equus asinus*, TMM 43543), dated by adjacent charcoal to 155 bp; bone collagen gave a similar AMS age (Table 1). The bed in question was subsequently cut and refilled with channel gravels, but even with several phases the minor inset cannot be older than a few centuries, much like analogous features at La Angostura.

A 90 cm drape of *colluvium* at the top of AG-4 profile comes down from the adjacent hillslope. It is an irregularly bedded sandy loam, with gravel stringers. The upper half has a humate date of 240 bp, which calibrates to roughly AD 1650 (see Table 1). This colluvium reflects a degraded ground cover, and is broadly contemporary with the minor inset.

The contemporary channel is sufficiently well defined to allow a range estimate of the paleohydrology linked to the minor inset. The Rotnicki–Manning equation (Rotnicki, 1983) was employed to estimate streamflow, and predicts a peak discharge of 107 m^3/s with a velocity of 3.2 m/s. On occasion this was a vigorous little stream, with a channel width of 32 m and hydraulic radius of 1.1 m. To "upgrade" this channel to account for the major inset would require a much larger channel, with a lower width to depth ratio (broad and shallow) and a hydraulic radius of 2.1. But that would greatly increase the peak discharge, although the more frequent bankfull discharge was unlikely to have significantly increased because meander wavelength did not substantially change (currently 160 m). Thus, this hydraulic simulation suggests that the major inset would have formed rapidly because of extreme floods, although baseflow was not significantly increased.

7.5. Late Holocene events in the Sierra Madre Occidental

To expand information on the Late Holocene, a number of other streams were sampled within the Sierra Madre Occidental (Fig. 1). The city of Durango lies adjacent to the large Guadiana valley, watered by the Río del Tunal, emerging from the mountains as a braided river. Along the southern margin is an 8 m alluvial body, originally described by Albritton (1958) as the Pueblito Formation and considered to be the youngest Quaternary unit in the area. We studied this feature at and around 23°57′49″ N, 104°38′43″ W (1878 m) (site TU), but our AMS ages of 7250, 7510 and 9270 bp are inconsistent, indicating reworking of charcoal during flood pulses. Most of the exposed beds are younger than ~7500 bp, and they close with two conspicuous paleosols, recalling the Pink Alluvium at La Angostura.

After this Early to mid-Holocene fill was abruptly entrenched by >8 m, a much younger, unconsolidated fill of 3.5 m was aggraded rapidly by three major floods. The first surge deposited a current-bedded loamy sand (>80 cm), with some shallow pockets of gravel, and an AMS date of 715 bp on charcoal. The second left a sand (80 cm) with some low-angle foreset beds, and a closing lens of rip-up clasts, mudballs, and charcoal with an 825 bp date. The third flood unit (55 cm) is identical, with a terminal date of 680 bp. Above that are unstratified loamy sands and sandy loams, dispersed pebbles, with more organic matter (twice the LOI level), representing a colluvial wash.

The 2σ calibrations overlap at AD 1260–1280, so that the paleofloods could have taken place within as little as 20 years. Significant is that after entrenchment the Tunal River rebounded almost immediately with rapid aggradation, as at Parras (see Fig. 15).

This is confirmed along the Ramos and Tepehuanes rivers, north of Papasquiaro, where Late Pleistocene fills are 8–10 m thick, and include volcanic tephra, while the Holocene unit is much lower, at 4 m. At La Loma (25°08′16″ N, 105°26′34″ W, 1698 m) (site LL) and Los Herrera (25°10′ N, 105°27′15″ W, 1684 m) (site LM), mid-Holocene sediments were partly eroded and the capping paleosol (as young as 620 bp) covered by a meter of uncompacted, current-bedded sandy loam, with gravel stringers. This package was again incised by 4 m, after which an inset of coarse-to-cobble-grade gravel was deposited to a similar level. Finally these were downcut by 4 m for a third time, before aggradation

of the modern floodplain, which links to gravel bars 1.5–2.0 m above low water of the Ramos. Although dating control is inadequate, two minor, post-entrenchment and Late Holocene alluvial bodies occur in the Papasquiaro district, within a frame of repeated cut-and-fill cycles, like at Parras, in a similar mountainous setting.

The major inset at Arroyo Grande post-dates the last major Holocene paleosol as well as major entrenchment, and may be related to catastrophic flood surges such as those of the Tunal River ~700 bp. Together with La Loma, El Tunal, and Parras, two periods of rapid entrenchment may have occurred in short order, rather than one, the course of events playing out differently at different sites, depending on the local threshold of disequilibrium and the sequence of weather perturbations.

8. Issues of interpretation

An unusually large database of some 40 major and minor stratigraphic profiles has been described and analyzed, and it remains to elaborate points of interpretation, before attempting a synthetic overview.

8.1. The terminal Pleistocene

In some sectors of Arroyo Grande the Holocene sequence rests directly on cemented gravels (at AG-3), and a charcoal age of 15,000 bp in AG.K (see Fig. 23) could be reworked from such conglomerates. But the end-Pleistocene contacts are more subtle.

At AG-5 the presumed base of Unit AG.A rests on a 50 cm calcrete and a 130 cm zone of prismatic structured and calcic sandy loam, with gravel and a high magnetic susceptibility (χ 88). The calcrete, although less lithified than at EP2 (Fig. 26), has a residual texture of silt loam, 60% CCE, and χ 52. The gravels only outcrop below this couplet.

At Encino de la Paz a conglomerate may be suballuvial, under >2.5 m of other, late Pleistocene beds. In the long Jaguey recording (Fig. 25) 4 m of clayey beds with two major paleosols are found below Unit 6b, and again no visible basal gravel. Here the major facies difference with EP2 is the carbonate recycling and resegregation into very large nodules, to leave less than 2% CCE in the matrix of Unit 5b or only 0.3% CCE in that of the mega-nodule horizon, Unit 1.

The conglomerate also fails to appear in a Late Pleistocene fill of 6 m at La Peña, 2.8 km downstream of Arroyo Grande (see Fig. 18), which is separated from the local Holocene units here by a hemicycle of downcutting. This older fill has four paleosols among white and gray muds, mainly with prismatic structure, above 2 m of interbeded, gleyed silt loams and sandy loams, with some gravel lines. Embedded within the basal interbeds at a depth of 5.1 m were the tibia and attached lateral cuneiform of an extinct Pleistocene horse (*Equus* sp., TMM 43545). Small aquatic snails and bivalves here point to a microhabitat with flowing water. The main, dark gray prismatic soil (at −2.2 m), with a charcoal AMS age of 15,990, rests on a partly decalcified calcrete. This mainly low-energy sequence recalls Unit VB at Puerto Ventanillas (between 16,150 and 9720 bp). The basal section at La Peña may, therefore, approach 20 ka in age.

Such scattered data points suggest a discontinuous accumulation of low-energy deposits ~16–10 ka bp (~19–11.5 ka BP) at La Peña, El Jaguey (Units 3–4?), Puerto Ventanillas, San Lorenzo, and Angostura. This would imply several, perhaps widely separated episodes of moisture. Prior to that, massive mobilization of carbonates formed petrocalcic horizons under semiarid conditions, some later partially dissolved as soil waters circulated freely (e.g., EP1; El Jaguey 1–2; AG-5; PV.A). Older still are basal conglomerates (AG-1, 2, 5; Puerto Cabrera ≥16.6 ka bp; San Lorenzo; UA; AG; petrocalcic fan at PV) that mark episodes of high-energy stream activity well back into MIS2.

These poorly understood events suggest end-Pleistocene climatic cycles of greater amplitude and longer wavelength, quantitatively different from those of the Holocene.

8.2. Stream entrenchment or deep gullying

Cut-and-fill cycles are a standard feature of historical, fluvial geomorphology. They may reflect little more that minor readjustments of channel slope and sediment load, but they can also point to significant interruptions of dynamic equilibrium, in response to climatic perturbations, human interference, or tectonic events. The record reviewed here includes a number of dramatic equilibrium shifts, observed over much of the study area, and accompanied by quantitative changes of sediment caliber.

The most incisive of these was the very rapid entrenchment that created the Angostura Badlands towards AD 1400 (cal.) (see Fig. 27). Some 6–12 m of channel downcutting affected the length of the Arroyo del Pueblo, from upstream of ENC to the northern exit from the Saltillo Basin. The semidesert arroyo at CSD, only indirectly connected to the axial river, also "crashed" at about the same time. Around Parras, two episodes of 11 m entrenchment occurred west of town, before and after ~AD 1400; at OA two spasms of downcutting are verified after ~AD 1240. The stratigraphy is quite precise, and even if some ^{14}C dates are faulty, a secure AD 1600 *terminus ante quem* is based on the age of the historical dam. At Durango (site TU) 8 m of entrenchment took place shortly before ~AD 1280, while at La Loma three episodes of downcutting, each by 4 m, followed a major soil with an age of ~AD 1340.

In short, the stratigraphy indicates a pattern of major entrenchment across North-Central Mexico, in one or two stages, completed before a dam structure dated historically to ~AD 1600, but after a cluster of median probability dates of about AD 1300 (see Fig. 27). Clearly one or more major climatic perturbations unleashed deluges of water that the streams were ill-equipped to handle. To accommodate the unprecedented discharge, streams abruptly entrenched their channels (compare Butzer 2005; Butzer and Helgren, 2005; Frederick, 2001).

The scale of this event can be roughly estimated. Today the main channel at Angostura typically averages 11.5 m deep and 40 m wide, bank to bank. During the last five centuries, this channel will have widened through bank undermining and collapse, and the channel deepened further. Notches in the walls of tributary channels suggest an early stage 7.5 m deep, and assuming that the channel has widened by over a third, an original width of perhaps 25 m suggests a cross-sectional area of 187 m^2 and a hydraulic radius of 4.675. With the largest accessible clasts (at depth) being ~4 cm in length, channel roughness (n) equals 0.0227. By the modified Manning equation, the channel forming velocity would be in the order of 11.8 m/s, and by the Rotnicki (1983) formula, peak formative discharge could be estimated at 2080 m^3/s. These are no more than gross orders of magnitude, which unrealistically assume a single event, because removal of so much sediment along the length of the stream, including the Pleistocene conglomerates at ENC, would have required many similar rainstorms. But clearly the Angostura Badlands were formed by some extreme "gully washers".

It is speculative to estimate peak discharge of the earlier channel but to do so is heuristically useful. The channel responsible for depositing the Pink Alluvium would have been broad, very shallow, and undulating, say 25 m wide and 0.75 m deep, yielding a hydraulic radius of 0.89. With a local gradient of 0.0093 and a channel roughness estimate of 0.01769, this would give a velocity of 5 m/s and a peak discharge of 85 m^3/s. The discharge responsible for cutting of the Angostura Badlands would then have been in the order of 25 times greater than that of previous major floods. This indeed was a phenomenal series of events unprecedented in the prior Holocene record.

8.3. Bedload eruptions

Although channels of sand, gravel or cobbles today are commonplace in North-Central Mexico, coarse bedload deposits are almost invisible in the Saltillo and Angostura records between the debris flow

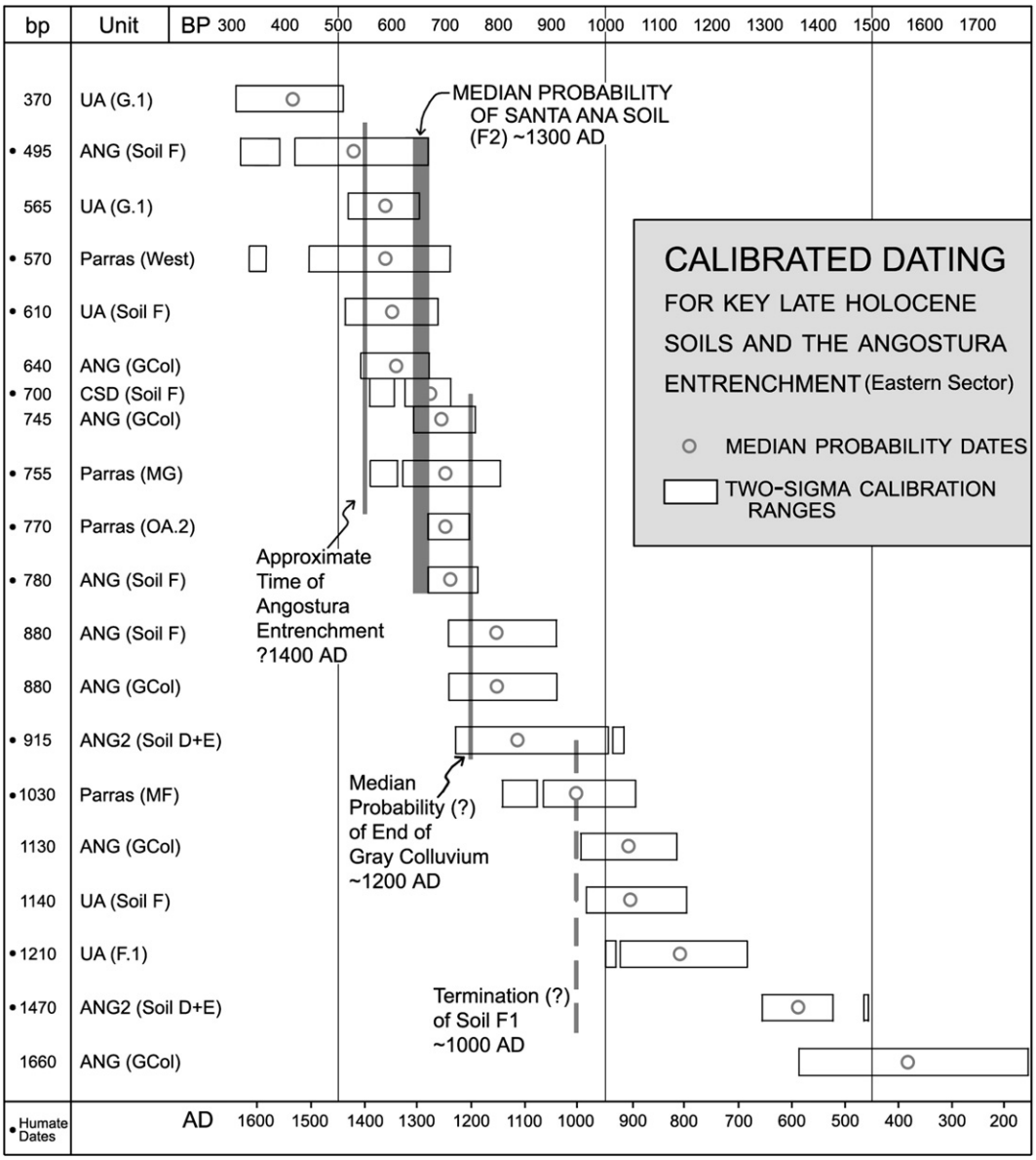

Fig. 27. Calibrated dating for key Late Holocene soils and the Angostura Entrenchment. See text for explanations and discussion.

at the base of LAD (?~7500 BP) and the gravel eruption in UA Unit E (~1600 BP), a span of perhaps 6 ka. Such high-energy aggradations are often integral to cut-and-fill cycles, but in the Early to mid-Holocene record they represent unusual and disruptive events.

During the Late Holocene, high-energy sedimentation attained greater recurrence, visibility and synchronicity. At Arroyo Grande two such episodes (in Unit AG.K) signal increasing instability during the final stages of fine-grained deposition between ~400 BC and perhaps AD 1000. At UA these events are recorded by two cobble horizons of Unit E (~AD 200 BC to ~300), and again at CSD (DG1-2). As a prelude to the Angostura Entrenchment, hydrological instability had been increasing across a millennium, in all likelihood in combination with spells of severe drought, deteriorating ground cover, and soil erosion (ANG, Gray Colluvium). These Medieval-age weather perturbations apparently coincided with a metastable equilibrium.

Since the time of bedload eruptions, streams have looked and responded much like they do today, with minor increases of energy triggering deposition of inset fills.

During the earlier Holocene, several episodes stand out: (a) activation of a gravelly small tributary at AG.5 before ~4000 BC; (b) the basal debris flow at LAD as well as channel cutting and massive cobble mobilization at El Jaguey, after ~6500 BC; (c) interbedding of lateral gravels with UA (Unit B, lower) after ~7000 BC, partly contemporary with stony slope wash at Parras (MC); (d) covering of a thin paludal Vertisol at Puerto Ventanillas by a gravel fan ~9200 BC; and (e) Coarse fluvial sands twice sweeping across marsh soils of Lake Tlahualilo, before and after ~11,500 BC. Such uncommon events draw attention to the high amplitude of periodic shifts in fluvial response, i.e. climatic oscillations affecting precipitation cycles.

The channel downcutting events and bedload eruptions that have remained visible in the records reviewed here can be ascribed to hydrological disequilibrium. As calibrated by median probability dates, identified and described in Table 1, this lithostratigraphic frame is presented in Fig. 28. It shows widely spaced, major disequilibria (average interval 1500 years) until about 500 BC, after which latent instability or rainfall variability increased dramatically.

8.4. Magnetic susceptibility

High readings of magnetic susceptibility (χ) in the study area are primarily from the concentration of magnetite derived in various stages from the rhyolites of the Western Sierra Madre, and now found

in the eolian sand sheets of the Mapimí or south of the Nazas River towards Villita (see Fig. 16). Magnetic sand grains are also carried by rivers, with the highest readings in eolian beds, reworked from channel sands, coming from the western drainages. On the other hand, the limestone catchments have next to no autochthonous magnetite. It is not surprising that readings of 25 to over 150 are found in almost all units of most western profiles, namely TU, LL, EP, Santa Fe, CA, FL, and Concordia. Consequently attention is directed to (a) profiles in the western drainage that have low values, and (b) sites in the eastern drainages where they only increase late in the record.

At Arroyo Grande, except for a high blip at ~4700 BC, readings fluctuate between 5 and 20, but at ~200 BC abruptly jump to between 30 and 55. Either no fluvial sand was entering a closed system, or allogenic eolian silt was not blowing in. At LM7 in the Mayran, susceptibility values remain below 10 throughout the column, suggesting that magnetite was not getting this far eastward. At LM2, CH30, San Lorenzo (upper SLA), and T7, readings are particularly high between ~7000 and ~4800 BC, possibly reflecting surges of Nazas flood silts.

The pattern is clearer in the local, limestone catchments. At Parras (MF, MG), values increase from under 10 to 35 at ~AD 1000, while near Saltillo (UA, F.2/G.1) these readings explode from less than 5 to more than 100 ~AD 1350. On the other hand, at Angostura, values rise from 15 to 30 with Soil D, and run near 40 in the Gray Colluvium, after about AD 1050. In these cases, eolian silts with fine magnetite particles are the only reasonable explanation, and we have observed a spring dust storm near AG. We suggest that eolian materials were being activated on a regional scale, beginning with disequilibrium after ~200 BC, and shallow dunes were advancing over the Mayran floor at LM4 ~AD 700. Even the most humid microhabitats were affected by the 14th century AD. It will require systematic mineralogical analysis and more sophisticated, magnetic susceptibility methods (as are being applied to the loesses of North China, Deng et al., 2005) to prove this interpretation, but it appears to support our contention of increasing periodicity and episodes of disequilibrium during the course of the Late Holocene.

8.5. Cumulic soils and wet floodplains

Abundant floodplain moisture is typically linked to low-energy channel response. Key criteria in the study area include cumulic soils, "banded" varieties of ponded channel beds, interlaminated tufas, and redox-modified subsoils. Greatest variety is found around Saltillo and at El Molino (Parras), linked to limestone bedrock and subchannel springs—artesian at the former, and compressional in the constricted bedrock channel at the latter. With sustained base flow and upwelling waters, fluctuating biotic activity and calcium bicarbonate concentrations can result in tufas interbedded with clays or organic mats alternating with algal chalks. Collectively these features imply higher

Table 2
Synoptic review of Holocene paleosols in North-Central Mexico

SOIL G.	*~AD 1500–1800.* Most recent humic soil, with texture and structure dominated by parent material and slope. Dating complicated by three or four calibration intercepts, but all younger than Angostura Entrenchment, in part forming on Inset Fills. Key examples: UA, ANG, TLA, AG. Reworking of alluvium as Inset Fills. Abrupt channel entrenchment during catastrophic rainfall event(s), creating Angostura Badlands and continuing ecological aridification by soil destruction and SOC loss. Approximate date AD 1400 (Fig. 27), and earlier than Colonial dam of AD 1600 at Parras. But older (~AD 1250) at Tunal, suggesting regional differences against background of metastable equilibrium.
SOIL F2.	*AD 1250–1400.* More distinctive soil with weak structure, representing partial slope stabilization. Key examples: ANG, CSD, Parras Slope soil erosion (Gray Colluvium, ANG, Figs. 9, 11) by high-intensity rains, probably following severe droughts that impaired groundcover ~AD 1050–1200. Onset of biological aridification.
SOIL F1.	*AD 750–1000.* A heavier soil with strong blocky structure, especially where there is no clear break between Soils F1 and E. Key examples: UA, ANG, and Parras (MF and lower OA.2) where there are interbedded tufas.
SOIL E	*AD 200–700.* More diversified soils with strong structure, including UA (unit F.1, and Soils E1 and E2) and A/Bkg soil at Parras (ME). Playa muds prominent in the Mayran (LM4, CH30), with humic soils in channels and overbank suites of the Nazas delta plain (SL, FL, Concordia, Santa Fe, Fig. 16), or a cumulic soil at AG. The first half of Soil E interbedded with or on top of high-energy bedload deposits (UA, AG), implying oscillating energy conditions and hydrological instability in both eastern and western Sierra Madre.
SOIL D2.	*1050–100 BC.* Three different facies document carbon sinks or smectite enrichment. In Saltillo Basin, humic pond muds alternate with algal chalks (UA, BWD, LAD, ANG). In upper Nazas, organic, black prismatic clays (AG), attain thickness of over 1.5 m (PC). In the Mayran, gray prismatic silty clays (LM7, CH30, also TLA). Fairly persistent wetlands at strategic locations, and low climatic periodicity. Two date clusters indicate two moisture peaks ~800 and ~250 BC. Hiatus of ~350 years suggests drier period without datable humic horizons.
Soil D1.	*~3000–1400 BC.* A long period of ~1500 years, half of which has no datable sedimentary record. Three clusters of dates (3000–2700, 2300–2100, 1800–1300 BC), with increasing two-sigma ranges, indicate intermittently wet-floodplain habitats in the east and the Mayran, but a record is missing in the western Sierras, where conditions were mainly dry. Entrenched channel at UA (Soil D1) with cumulic Mollisol; ponding in UA tributary; cumulic Alfisols with strong redox on alluvial terrace at LAD (Soil D); and modest soil at CSD. Prismatic silty clay at Parras (MD); several strongly structured soils in Mayran (LM2, CH30), but with indirect evidence of intermittent deflation. Hiatus of ~700 years indicates another dry period without humic horizons.
SOIL C.	*~5200–3700 BC.* Sustained redox conditions in the eastern watersheds, combined with brief periods of soil formation, ponding or tufa development (UA, LAD), but Ak soil at CSD. Slope screes interbedded with ponds and tufas at Parras (lower MD) imply both wet conditions and colluvial activity. In the Mayran, periodic flooding verified by playa muds or often thick soils with protracted redox, despite local gypsum (LM2, LM4, CH30). In upper Nazas, prismatic clays prone to redox highlight mainly wetter conditions. Dating tighter than for Soil D1. A hiatus of perhaps 600 years, with channel cutting at UA, debris flow at LAD, and cobble mobilization at El Jaguey.
SOIL B.	*~6600–5800 BC.* Core of period relatively wet, with up to three AB or ABk soils at UA (upper unit B), marked by prismatic structure, ferric rhizoliths, and tufa interbeds reflecting subchannel artesian vents and a high water table. At AG, Soil B records a seasonally very wet setting, with organic, prismatic clays and slickensides, in combination with redox features. But earlier at UA (lower unit B), alluviation proceeded between gravel bars, despite redox; at ANG "banded alluvium" implies rapidly changing energy conditions, following high-energy gravelly bed. Except for basal playa muds (CH30), absence of Mayran paleosols may indicate considerable Nazas diversion to TLA (major alternate channel at CA and T6, Fig. 16, ~6400 BC); such a diversion occurred ~AD 1770–1839 due to sediment blockage of main channel (E.K. Butzer, 1997). Hiatus of ~600 years.
SOILS A1 and A2.	*~9400–9100 BC and 8600–7200 BC.* Dates at UA inconsistent due to erosional reworking (loss of upper half of record) and channel squeeze-ups, but if grouped irrespective of stratigraphy, they cluster tightly. Both Soils A1 and A2, despite 500 year break, record channel-ponding, tufa interbedding, weak cumulic soils and variable redox; i.e. persistent base flow, high water tables, and artesian vents on wet floodplain. Semidesert stream at CSD (DD) argues for significant base flow, rich in $CaCO_3$, but at Parras (MB) a striking Bg/Bk profile, while at San Lorenzo (SLB) a sequence of B-horizons, a gley, repeated calcification, and interruptions by eolian activity. Redox and ferric concretions common in the Mayran, with wavy-laminated clays or k-horizons at LM7. A high playa stand recorded by prismatic clays with slickensides at Puerto Ventanillas. Nothing exposed at AG, but Bt pockets of Chromic Vertisol at El Jaguey penetrate deep into substrate. Much of Early Holocene was wetter than today in both east and west, with different hydrology recorded by subchannel spring activity, tufas, and ponding.

Chronostratigraphy inferred from graphic representation for clustering of median probability dates and two-sigma ranges (see Table 1, INTCAL 104.14c, and Reimer et al., 2004).

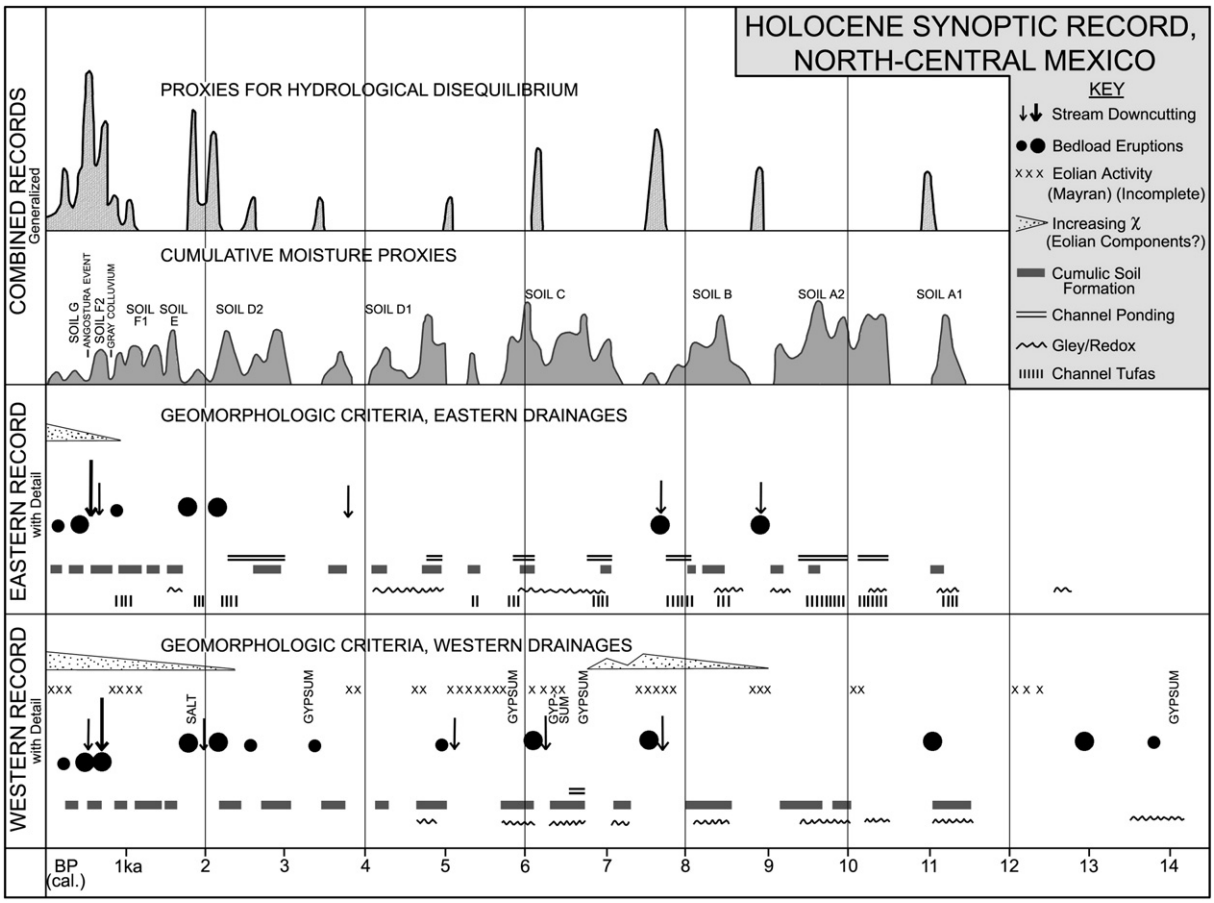

Fig. 28. Holocene synoptic record of disequilibrium and moisture proxies in North-Central Mexico. Compare with summary in Table 1.

water tables, greater floodplain productivity, a more equitable progression of the seasons, and more, effective rainfall.

At Saltillo (UA) the long-term water table would have been 8–10 m higher, while in the Mayran—where borrow pits strike the water table at a little below −4 m—in the order of 3 or 4 m higher. This all argues for substantial, "positive" changes of hydrology and a climate that was effectively wetter. Such features are the hallmark of what can be called "wet" cycles.

The information is presented as a data bank in Table 2 and complemented by the synoptic chart of Fig. 28. Neither type of presentation can practicably accommodate 2σ calibration spreads for 163 dates (158 on charcoal and humates, 5 on tufa or bone), so that median probability dates are used, calculated for each sample from its 2σ spread. The two tables and the chart (Fig. 28) explicitly serve a heuristic purpose.

9. Concluding discussion

The patterns and features examined in the preceding analysis and depicted in Figs. 27 and 28 warrant a synthetic, concluding commentary.

9.1. Converging and diverging patterns

(a) The criteria for moist floodplain conditions include paleosols, redox phenomena (indicative of higher water tables), channel-ponding (indicating sustained base flow), and interbedded tufas (mainly linked to calcite-rich subchannel springs). Given the absence of limestone aquifers in the upper Nazas drainage, ponding and tufas are rare in the west, but commonplace in the eastern floodplains, where wet microhabitats were reconstituted repeatedly.

(b) Compared with the end-Pleistocene record, such wet-floodplain features are prominent on the Holocene record, particularly during the time range of Soils A1, A2, and B. Equilibrium parameters were re-set with a climatic shift ~5800 BP, and subsequent moister cycles became shorter, more modest, and widely spaced. But the combined eastern and western records do not demonstrate a "dry" mid-Holocene.

(c) Bedload eruptions and channel cutting as indices of hydrological disequilibrium were relatively isolated during the Early Holocene, but became an increasing drumbeat after ~2500 BP and especially after ~1000 BP. They indicate growing hydrological and soil instability, which suggest greater seasonal or episodic concentrations of water, and of variance between "average" and "extreme" precipitation events.

(d) The western and eastern records are in phase and closely comparable in dynamics. Differences in detail probably relate to contrasts between the Pacific Ocean and Gulf of Mexico in terms of macro-sources of moisture. Differences also result from fewer criteria for "wet" cycles in environments with impermeable bedrock, but the larger number of cobble bedload activations in the west is significant and would imply a greater latent instability.

(e) Whether or not the episodes of gypsum or salt concentration (see Fig. 28) in parts of the Mayran had more general climatic implications is unclear. The incomplete record of eolian activity in the Mayran also requires further study, but is partly obscured by innumerable occasions of deflation and redeposition.

(f) Increasing magnetic susceptibility in the western catchment during the earlier Holocene and again the last 2200 years, or in the eastern sector since ~1000 BP, suggests coincidence with periods of instability; it would be promising to follow up on

whether more blowing dust did characterize the region during "drier" climatic trends.

(g) Although the end-Pleistocene record is highly incomplete and suggests climatic cycles with longer wavelengths, the millennia before ~14,000 BP must have been less humid. It is probable that Soil A at CSD is much older that its single date, to match the last activation of marginal alluvial fans at San Lorenzo and Puerto Ventanillas. This also implies that local precipitation around the Mayran and Nazas delta plain has been ineffective for geomorphological change during the last 18 ka. In other words, considerably more runoff debouched from lower elevation catchments earlier in MIS 2. But the notion that the end-Pleistocene was "wet" in northern Mexico, continuing thus into a "wet" Early Holocene, must be reconsidered.

9.2. Revisiting the black mucks

A large number of profiles with dark clayey paleosols have been evaluated above. Most of these appear to be cumulic, and probably the result of lateral translocation between a channel and a wet floodplain, complemented by transfer along the axial channel. In such cases the carbon and clays may be largely authigenic. But the Nazas watershed opens up other possibilities, with a large tract of black mucks still preserved on the upland piedmont that drains into the Arroyo Grande (see Fig. 21). Here, a possibility exists to link relict upland soils with valley paleosols, and to sketch a methodology to study the formation and attrition of soil organic carbon across a watershed during Holocene times.

The Chromic Haplustert at El Jaguey (see Fig. 25), with a terminal date of 8060 BP, developed on a substrate of slickensided clays. The original, prismatic, heavy clay soil must have formed over millennia, but was gradually eroded and reworked across the piedmont by shallow rills, to accumulate in gentle declivities. In this process, coarse materials will have diluted the clay fraction until a new cycle of pedogenesis favored humification and authigenic clay mineral formation, with an increasing component of smectite. With repeated incremental erosion and redeposition, Bt-horizons would have thinned, while cumulic processes thickened the increasingly organic and clayey A/AB-horizons. Eventually such profiles would resemble a cumulic Mollisol, but with vertic properties, as can be seen in the small basin at Puerta de Cabrera (2360–2800 BP).

The slickensides at the base of Soil B at AG probably reflect an early phase of attrition of the original watershed Vertisol, while at El Jaguey the younger Alfisol with strong illuvial features may represent a model for an intermediate condition. These questions of pedogenic evolution recall those surrounding the transformation of reddish, kaolinitic upland soils to black, smectite Vertisols in the poorly-drained savanna plains of Africa (see Thomas, 1974; Butzer,1976: ch.20).

The black mucks of the AG profile were, in part, periodically derived from the "bank" of black soils that formed and remained in storage on the watershed. Mobilization in the suspended load of the stream continued at intervals from before 8000 to about 1100 BP, and suggests interrelationships of soils and sediments that remain accessible in time and space.

It would be possible to sample representative grids of the various watershed soils, as well as the valley paleosols, for vertical sequences of organic components, $\delta^{13}C$ changes, micromorphology, clay minerals, and geochemistry. In combination with the forthcoming palynological results from AG, it should then be feasible to model SOC in storage, net productivity, and depletion (e.g., Peng et al., 1998). That will require a team of collaborating specialists, but an understanding of SOC flux during Holocene time would have important implications for the dynamics of the regional biota. It might also open new avenues to integrate fluvial and soils geomorphology within global investigations of the biosphere and its semiquantitative transformation.

9.3. Comparisons with the U.S. Southwest

The results of the Laguna Project do not stand in isolation, and can be compared with innovative external studies on the Late Holocene. For example, Ely (1997) examined a suite of flood deposits in Arizona and southern Utah and concluded that formative floods were also clustered in particular periods. Large floods were absent ~2200–400 BC, but increased thereafter, to a peak at ~AD 1000–1200, before a pronounced drop ~AD 1200–1400. After AD 1400, flood frequency exploded, unlike in North-Central Mexico.

Waters (1988) focused on a 20 km stretch of the Santa Cruz River south of Tucson. A salient feature here is the refilling of a deeply entrenched (~6.5 m) channel after AD 1400. This record, although very distant (900 km), has similar complexity and ages as the Late Holocene sequence of Fig. 28, even though hydrological and pedogenic expression varies in detail.

The features recorded by Nordt (2003) in the Casas Grandes and San Pedro valleys of northwestern Chihuahua have many similarities with those presented here, in particular some six paleosols dating roughly 9000–1350 BP. But his interpretations are radically different, and attribute paleosols to warmer and drier conditions, or alluvial fills to cooler and wetter climate with high-magnitude floods.

Basin-wide Late Holocene incision events during the time span between perhaps 1200 and 600 BP also have been noted by a number of researchers in the southern Great Plains (e.g., Hall,1990; Blum et al., 1994; Waters and Nordt, 1995; Nordt, 2004). Although the interpretation advanced for the climatic trigger varies, all of these authors agree that changes in climatic parameters were responsible for disrupting system equilibrium and initiating these widespread channel cutting events.

Constructional beach ridges in playa basins just south of the Mexico–New Mexico border indicate persistent high lake stands ~8500–8200 BP, ~6700–6100 BP, ~4250–3800 BP and (very briefly) ~200 BP, which are attributed to increased precipitation and cooler temperatures, following southward shifts in winter storm tracks (Castighia and Fawcett, 2006). These time spans resemble those of Soils B, C and D1 of the Laguna Project region, but no evidence exists of true lake formation in the Mayran, compared with these huge lakes and fluctuating depths of 5–20 m. In the Babícora Basin of northern Chihuahua, a 4.7 m core indicates a deep but fluctuating lake before 20,000 BP, but it dried out after 9500 BP; no Holocene pollen or diatom record is preserved (Metcalfe et al., 2002), with pollen also absent in the Holocene record of Cuatro Cienegas (Meyer, 1973), where renewed palynological investigation is now underway. Earlier work on surface exposures at Babícora appears to suggest lacustrine conditions during the Late Pleistocene (before 9600 bp), while the Holocene record is rich in organic matter as well as eolian sediments, that collectively are interpreted as paludal (Ortega-Ramírez et al., 1998); the inferences to warmer or cooler conditions are conjectural.

The Hueco Basin, near Chihuahua but on the Texas–New Mexico border, has been sampled for pedogenic carbonate development and stable carbon isotopes (Buck and Monger, 1999). Unfortunately the ^{14}C ages are from pedogenic carbonates. The carbonate morphology shows little or no consistent change, as in the Laguna profiles, but carbon isotopes show interesting variation, attributed to simple shifts between grasses and desert scrub on the basin floor.

Major potential resources for paleoecological evidence are the botanical remains from packrat middens. The problem is that the available ^{14}C ages are inadequate for the complexity of the cave or rock overhang stratigraphy, and the problem of disturbance by burrows appears to linger. Changes over time are glossed over in millennia. This caveat applies to such deposits at Puerto Ventanillas and near Torreón (see Fig. 16) (Van Devender, 1990), as well as a more recent study at the

Mexico–New Mexico border, where parallel but discordant pollen data are given (Holmgren et al., 2003). It appears that woodland was displaced by desert scrub by 10,000 BP, except for creosote, which arrived later, but at varying times.

Tree-ring studies have been carried out for long-lived Douglas fir at five sites in Durango (Cleaveland et al., 2003; D.W. Stahle, pers. comm.. 1996). The oldest record goes back to AD 1386, but this taxon is sensitive to winter precipitation and its measured variation shows no similarity to the historical Nazas or Mayran records (E.K. Butzer, 1997), which reflect summer discharge of the Nazas River in that time range.

But we can usefully draw on one explicit and nuanced tree-ring record, from El Malpaís Monument, New Mexico (Grissino-Mayer, 1995). Although dendroclimatology is a very different kind of proxy, and has superb chronological control, this 2100-year record relates to short-term trends or events, at a multidecadal scale or less, but embedded in century-scale cycles. That is also true for our soil-hydrology proxy record of the last 2 ka. The New Mexico tree-ring sequences identify an unusually long span of strong droughts ~AD 300–490, perhaps relevant to our bedload eruptions early during Soil E. More pertinent are high variances and alternations between very wet or very dry weather in central New Mexico ~AD 950–1400 (also Meko et al., 2007), a period of evident instability in North-Central Mexico. But for ~AD 1400–1800 the New Mexico record stands out by its remarkably low variability and generally dry conditions, compatible with the subdued change evident in the Laguna proxy record, but in contrast to the Arizona paleofloods of Ely (1997). Finally, statistical modification of the New Mexico dendroclimatology as a 30-year running mean identifies a unique peak of effective moisture ~AD 1400, coinciding with a similar peak in a foraminiferal record of the Gulf of Mexico (Poore et al., 2005). This would point to "monsoonal" linkages between the Gulf, North-Central Mexico, and New Mexico.

9.4. Ecological aridification versus human degradation

The Gray Colluvium at La Angostura points to a hydrological disequilibrium between Soils F1 and F2 that dates ~AD 1050–1200. It incorporates a good amount of SOC (steady LOI readings of ~4.0% through 1.6 m of sediment) and of disaggregated conglomeratic matrix, indicative of soil erosion attacking both A and C-horizons on the slopes. Ground cover was being destroyed, presumably as a result of alternating severe droughts and episodes of heavy rain. That attrition set the stage for the Angostura Entrenchment, after a brief and incomplete recovery (the Santa Ana soil zone). A deluge of water was unleashed by excessive rainstorms, that completely overwhelmed the existing channels, which responded by entrenchment and ongoing bank collapse. Downcutting would have begun downstream, moving headward (see Figs. 2 and 8), and upstream of Saltillo this process excavated a channel of similar dimensions at ENC (see Fig. 14), here cutting through tough, conglomeratic seams. Millions of tons of silt were entrained and swept downstream, so that the loss of SOC to the Saltillo Basin will have been immense.

Progressive attrition and then catastrophic entrenchment must have destroyed groundcover, riverine habitats, and soils. The resulting ecological aridification (rather than "desertification") is fully documented at ANG, and will have been replicated in other study areas around Saltillo, Parras, the upper Nazas and Ramos watersheds, and Durango. Subsequent recouping of SOC has been modest, and the biotic landscape has remained impoverished.

When the Spanish stockraisers, miners and missionaries arrived a century or so later (1577–1596), they already encountered a "degraded" countryside. While their activities may have exacerbated the situation, human forcing of environmental change played no role in the increasing variability of severe droughts and excessive rains in North-Central Mexico prior to AD 1600. That said, the question of whether and when human activity triggered Pre-Hispanic erosion near Lake Pátzcuaro (see O'Hara et al., 1993; Fisher et al., 2003) deserves to be reopened.

Returning for a moment to the northern Bajío, a variety of profiles in the Lajas and Puerto Nieto drainages provide two stratigraphic sequences (Frederick, 1995: Sections 4.3 and 5.4). Five basic units between ~12.5 ka BP and the present are represented in each. The oldest follows upon a strong vertic paleosol, and consists mainly of low-energy clays and muds, modified in turn by a weaker Vertisol. The next two units consist of loams and muds from the mid-Holocene, separated by modest paleosols, in part calcic. But the most striking is a highly organic complex of low-energy fills, ranging from massive overbank muds (2–3 m) to thin-bedded sandy deposits. Accumulation of this "cienega unit" began during the second millennium BC and terminated a little after AD 1000. Subsequently 4–6 m entrenchment followed. A final, higher energy unit (50–300 cm) includes strong colluvial components and was a response to Colonial landscape intrusion.

Although not well dated, the "cienega unit" suggests similar environmental inputs as Soils D2, E and F1 in North-Central Mexico, namely protracted ponding and soil formation. During this time span, no significant agricultural settlement existed in the wider Lajas drainage, despite separated, Classic to Early Postclassic, site clusters to the north (Villa de Reyes), west, and south. The impact of the Villa de Reyes settlement nucleus created a different, high-energy response (Frederick, 1995: 4.3.4, 5.3). Although Pre-Hispanic sedimentation along the Lajas after 2000 BC was related to climatic inputs, it also was coeval with accelerated sedimentation—attributed by various authors to soil degradation—in more than 10 small or large basins in Michoacan (see Frederick, 1995: Fig. 5.8).

The earliest period of landscape instability in Lake Pátzcuaro, with the appearance of maize pollen, is dated ~1900–1250 BC, the second ~600 BC to AD 650 (O'Hara et al., 1993), although population only increased significantly thereafter (Fisher et al., 2003). Depending on whether the small number of ^{14}C/AMS ages are accepted or not, major erosion set in either about AD 1200 or after 1520 (O'Hara et al., 1993 versus Fisher et al., 2003). A part of the problem also relates to different sampling strategies, namely dispersed sediment cores from several parts of the lake (by O'Hara), versus excavation and coring in one embayment with a concentration of settlement and landscape modification (by Fisher). More specifically, pointwise erosion was linked to disturbance at Pre-Hispanic archaeological sites, whereas Colonial intrusion apparently led to landscape-wide colluviation as a result of land abandonment (Fisher et al., 2003).

Recent detailed work in northern Guatemala, however, indicates that most rapid erosion occurred during initial land clearance (700 BC–AD 250), not at the time of greatest population density (Anselmetti et al., 2007; Beach et al., 2008, this volume), confirming the results of earlier work by Dunning et al. (2002). Against this one must interject that, just as in the Lajas Basin, there were ongoing climatic changes, documented by significant fluctuations of lake level between AD 120 and ~1200 (O'Hara et al., 1993; Fisher et al., 1999). Lake Pátzcuaro sedimentation may therefore have been controlled by *both* climatic impulses and land-use practices or changes.

This raises legitimate questions about the Pátzcuaro interpretation and that of other, adjacent basins. A mix of discriminating, geomorphic catchment studies and more precise, site-specific geoarchaeological investigation is called for. This must be accompanied by a robust chronology that includes OSL dates.

9.5. The Laguna project in global context

Explanation is a difficult but tempting arena for partial solutions that do not account for the record as a whole. The environmental history elaborated here includes: (a) a marked increase of precipitation in the eastern and western Sierra Madre at the very beginning of the Holocene; (b) a relatively wet Early Holocene at a time when sea-surface temperatures (SSTs) were lower and tropical cyclones fewer; (c) a basic distinction between effective rains that recharged aquifers versus excessive rainfall and runoff events that mobilized major floods

to remodel the fluvial geomorphology or surge into the Mayran playas; (d) an increasing variability and decreasing wavelength of alternating wet and dry perturbations during the course of the Holocene, although information on seasonality is lacking; (e) the probability that hurricanes or lingering tropical storms from the Gulf of Mexico and the Pacific Ocean had become major channel and slope-modifying forces by the later Holocene; and (f) a superposed cyclicity of landscape stability and instability, facilitated by or leading to changes of effective land or ground cover.

These points draw attention to some of the doubts and concerns a geomorphologist might have about universalizing, single explanations, not to mention bold hypotheses that shift atmospheric circulation belts to fit preconceived assumptions. Fortunately, the tide is turning, as paleoclimatic interpretations focus on multiscale variability and shorter time spans, illuminated by specific kinds of proxy records. Recent studies emphasize the role of centennial, multidecadal, and decadal oscillations, based on Greenland ice cores, deep-sea sediment columns, and tree-ring derived reconstructions (Gray et al., 2004; Poore et al., 2005; Richey et al., 2007). At this smaller scale, changes in the strength of the oceanic thermohaline circulation are one primary factor for SST oscillations that affect multiyear precipitation or temperature anomalies differently over various continents, and apparently modulate or confound linear ENSO global teleconnections (Gray et al., 2004; Brönnimann, 2007; Kerr, 2000). Atmospheric circulation anomalies, which favor storminess over the North Atlantic and Eurasia, drive the Loop Current in the Caribbean that carries warmer surface waters into the Gulf, accounting for a 3 °C difference in SST during the last 1400 years, between the Medieval Warm Period and the Little Ice Age (Richey et al., 2007). Interestingly, AD 1400 also marks an abrupt switch of circulation patterns over Greenland and Eurasia, apparently related to solar forcing and coupled ocean–atmosphere associations (Meeker and Mayweski, 2002). With cooler SSTs in the Gulf, fewer excessive rainfall events should be expected in North-Central Mexico.

At a larger scale, wavelet power-spectrum analysis of a Holocene ENSO record from Ecuador shows a fluctuating but dramatic increase of ENSO variability, that peaks after 2 ka (Moy et al., 2002; see also Magilligan et al., 2008, this volume); this event series is surprisingly homologous to the disequilibrium proxy record of our Fig. 28. Possibly this long-term trend of ENSO variance is tied to orbitally-induced changes of insolation (Moy et al., 2002). But more significant is the apparent link of our Mexico disequilibria to the "mechanics," rather than the linear manifestations of the ENSO.

Turning the analogs inside out, the moisture proxies of Fig. 28 provide a similar, discontinuous trace to that of Holocene Nile flood levels (reconstructed in K.W. Butzer, 1997), which have been (incorrectly, see Stager et al., 2007) claimed to be a linear ENSO proxy in earlier research. In effect, tropical and North Atlantic parallels to the Laguna Project record are apparent. But exactly how that works will require further study, including the role of solar irradiance.

For example, a greater incidence of hurricanes would not adequately explain the Mexico record. Hurricane Gilbert in 1988 was one of the most powerful rainstorms in well over a century, traveling far inland but bringing only 130 mm of rain to the rainshadow of Saltillo. Significant rainfall in the eastern half of the study area is often associated with moisture derived from Pacific storms. Perhaps if a Pacific hurricane first provides a thick plume of mid-to high-level moisture, followed directly by a strong Gulf hurricane, enough instability might develop to deliver extreme runoff events as far west as Parras, where flood debris of Hurricane Gilbert (1988) was found lodged in brush up to 4 m above channel-floor.

Directly or implicitly, current explanations are focused on summer rains, which will not be adequate for Early Holocene reconstructions. Large-scale flooding can also affect the Rio Grande valley during winter or the transitional seasons. This is likely to happen with quasi-stationary upper air troughs or cut-off lows over the Southwest, spinning off multiple cyclonic swirls into converging streams of Pacific and Gulf moisture. But these are more likely to be the "soaking" rains that sustain aquifers and wetlands. Such synoptic patterns are also related to tightly twisted (meridional) jet stream loops that are part of the repertoire of Atlantic multidecadal oscillations. Embedded within this interplay of tropical and subtropical dynamic categories, a switching between "summer" and "winter" storm categories may have occurred, with different impacts on the ground. That could help explain an earlier record with redox and high water tables, giving way to one with periodic, very heavy rains and greater landscape instability. The proxies suggest increasing variability and shorter wavelengths, but what may instead have changed could be the dominant, dynamic variables, that is, the synoptic patterns controlling the incidence and character of heavy rains.

The soil-geomorphology record of North-Central Mexico is primarily a history of changing "wet" cycles, rather than of wet or dry climates. These had major ecological impacts, which is also evident from the forthcoming palynological evidence. Given that paleoclimatic interpretation cannot yet be structured in a unifying theory, geomorphologists should react critically to oversimplifications of the systemic whole.

Acknowledgements

Elisabeth Butzer contributed at all stages to the historical and archival background to flooding in the Nazas Basin, and she is grateful to Luis Ferniza García, Enrique Fernández, Teresa Babún, and other local informants in San Pedro de las Colonias, and Virginia Rocha Saeñz of Parral del Hidalgo. Mariah F. Wade and William E. Doolittle (both UT Austin) helped prepare the field trip for the Conference of Latin–Americanist Geographers to northern Mexico (January 2000). Taylor Houston, John Geiselbrecht, and Alexandra Myers assisted in the laboratory work. Ernest W. Lundelius, Jr. (Texas Memorial Museum), identified the fossil bones, and Barbara Winsborough (Winsborough Consulting, Austin) investigated the diatoms and offered specialist insights on the organic accumulations. Troy Kimmel (UT Austin) offered advice on the synoptic patterns. M. Palacios-Fest (University of Arizona) tested a suite of samples for ostracods. Bruce M. Albert (Corinth, TX) invested much time and expertise on the palynological study, which will be published separately upon completion. David Helgren (San José State) provided critical feedback and information, as did Tim Beach (Georgetown), Nicholas Dunning (University of Cincinnati), and Paul Hudson (University of Texas). Rosemary Sherriff (University of Kentucky) gave suggestions on the Southwestern literature. The former University of Texas Radiocarbon Laboratory, the University of Arizona Laboratory of Isotope Geochemistry, the University of Arizona AMS Facility, the National Ocean Sciences AMS Facility (Woods Hole, MA), and Stafford Research Laboratories provided the ^{14}C and AMS dates; we are particularly appreciative of close collaboration with Sam Valastro (Austin) and Chris Eastoe and Austin Long (Tucson). Mark Bateman (Sheffield University) made available OSL ages, details which will be published separately. The Laguna Project was supported by the Texas Higher Education Coordinating Board, Advanced Technology Program Grant 003658-473, and by the endowment of the R.C. Dickson Centennial Professorship of Liberal Arts.

References

Anselmetti, F.S., Hodell, D.A., Ariztegui, D., Brenner, M., Rosenmeier, M.F., 2007. Quantification of soil erosion rates related to ancient Maya deforestation. Geology 35, 915–918.

Albritton, C.C., 1958. Quaternary stratigraphy of the Guadiana Valley, Durango, Mexico. Geological Society of America Bulletin 69, 1197–1216.

Beach, T., Luzzadder-Beach, S., Dunning, N., Cook, D., 2008. Human and natural impacts on fluvial and karst depressions of the Maya lowlands. Geomorphology.

Benham, H.W., 1847. The field of Buena Vista corrected by Lieut. Benham. Pencil manuscript, Univ. of Texas at Arlington Libraries, Henry W. Benham Family Papers, Collection AR 388, Map Annex 108/1.

Blum, M.D., Toomey, R.S., Valastro, S., 1994. Fluvial response to Late Quaternary climatic and environmental change, Edwards Plateau, Texas. Palaeogeography, Palaeoclimatology, Palaeoecology 108, 1–21.
Brönnimann, S., 2007. Impact of El Niño-Southern Oscillation on European climate. Review of Geophysics 45 (3), RG3003.
Buck, B.J., Monger, H.C., 1999. Stable isotopes and soil-geomorphology as indicators of Holocene climate change, northern Chihuahuan Desert. Journal of Arid Environments 43, 357–373.
Butzer, E.K., 1997. Archival documentation of extreme climatic events, Northern Mexico (16th–19th centuries). Abstracts, Assoc. of Amer. Geog., Annual Meeting Fort Worth, TX, p. 35.
Butzer, K.W., 1997. Sociopolitical discontinuity in the Near East c. 2200 BCE: Scenarios from Palestine and Egypt. In: Dalfes, N., Kukla, G., Weiss, H. (Eds.), Third Millennium B.C. Abrupt Climatic Change and Old World Social Collapse. NATO ASI Series, Springer, pp. 245–295.
Butzer, K.W., 1976. Geomorphology from the Earth. Harper Row, New York.
Butzer, K.W., 1999. Technología de irrigatión tlaxcalteca: Mito o realidad? In: Monroy Castillo, M.I. (Ed.), Constructores de la nacion: La migración tlaxcalteca en el norte de la Nueva España. Biblioteca Tlaxcalteca, El Colegio de San Luís, San Luís Potosí, pp. 135–140.
Butzer, K.W., 2005. Environmental history in the Mediterranean world: cross-disciplinary investigation of cause-and-effect for degradation and soil erosion. Journal of Archaeological Science 3, 1773–1800.
Butzer, K.W., Butzer, E.K., 1997. The 'natural' vegetation of the Mexican Bajío: archival documentation of a 16th-century savanna environment. Quaternary International 43/44, 161–172.
Butzer, K.W., Harris, S.E., 2007. Geoarchaeological approaches to the environmental history of Cyprus: explication and critical evaluation. Journal of Archaeological Science 34, 1932–1952.
Butzer, K.W., Helgren, D.M., 2005. Livestock, landcover, and environmental history: the Tablelands of New South Wales, Australia, 1820–1920. Annals Association of American Geographers 95, 80–111.
Butzer, K.W., Stuckenrath, R., Bruzewicz, A.J., Helgren, D.M., 1978. Late Cenozoic paleoclimates of the Gaap Escarpment, Kalahari Margin, South Africa. Quaternary Research 10, 310–339.
Byrne, R., Horn, S.P., 1989. Prehistoric agriculture and forest clearance in the Sierra de las Tuxtlas, Vera Cruz, Mexico. Palynology 13, 181–193.
Castighia, P.J., Fawcett, P.J., 2006. Large Holocene lakes and climate change in the Chihuahuan Desert. Geological Society of America Bulletin 34, 113–116.
Cleaveland, M.K., Stahle, D.W., Therrell, M.D., Villanueva-Díaz, J., Burns, B.J., 2003. Tree-ring reconstructed winter precipitation and tropical teleconnections in Durango, Mexico. Climatic Change 59, 369–388.
Cullen, H., de Menocal, P., Hemming, S., Hemming, G., Brown, F.H., Guilderson, T., Sirocko, F., 2000. Climate change and the collapse of the Akkadian empire: evidence from the deep sea. Geology 28, 379–382.
Deng, C., Vidic, N.J., Verosub, K.L., Singer, M.J., Liu, Quingsong, Shaw, J., Zhu, Rixiang, 2005. Mineral magnetic variation of Jiaodao Chinese loess/paleosol sequence and its bearing in long-term climatic variability. Journal of Geophysical Research 110, B03103. doi:10.1829/2004aJB00 3451.
Dunning, N.P., Luzzadder-Beach, S., Beach, T., Jones, J., Scarborough, V., Culbert, T.P., 2002. Arising from the Bajos: the evolution of a Neotropical landscape and rise of Maya civilization. Annals of the Association of American Geographers 92, 267–283.
Drysdale, R., Zanchetta, R., Hellstrom, J., Maas, R., Fallik, A., Pickett, M., Cartwright, I., Piccini, L., 2006. Late Holocene drought responsible for the collapse of Old World civilizations is recorded in an Italian cave flowstone. Geological Society of America Bulletin 34, 101–104.
Ely, L.L., 1997. Response of extreme floods in the southwestern United States to climatic variations in the Late Holocene. Geomorphology 19, 175–201.
Fisher, C.T., Pollard, H.P., Frederick, C., 1999. Intensive agriculture and socio-political development in the Lake Pátzcuaro Basin, Michoacán, Mexico. Antiquity 73, 642–649.
Fisher, C.T., Pollard, H.P., Israde, I., Garduño, V., Banerjee, S.K., 2003. A reexamination of human-induced environmental change within the Pátzcuaro Basin, Michoacán, Mexico. Proceedings National Academy of Sciences. doi:10.1073/pnas 0630493100.
Frederick, C.D., 1995. Fluvial response to Late Quaternary climate change and land use in Central Mexico. Ph.D. Dissertation, Univ. of Texas Austin.
Frederick, C.D., 2001. Evaluating causality of landscape change: examples from alluviation. In: Goldberg, P., Holliday, V., Ferring, R. (Eds.), Earth Sciences and Archaeology. Kluwer Academic, New York, pp. 55–76.
Gray, S.T., Graumlich, L.J., Betancourt, J.L., Pederson, G.T., 2004. A tree-ring based reconstruction of the Atlantic Multidecadal Oscillation since 1567 AD. Geophysical Research Letters 31, LI2205. doi:10.1029/2004GLO19932.
Grissino-Mayer, H. D., 1995. Tree-ring reconstructions of climate and fire history at El Malpaís National Monument, New Mexico. Ph.D. Dissertation, Univ. of Arizona, Tucson.
Hall, S.A., 1990. Channel trenching and climate change in the Southern U. S. Great Plains; with Suppl. Data 90-89. Geology 18, 342–345.
Holmgren, C.A., Peñalba, M.C., Rylander, K.A., Betancourt, J.L., 2003. A 16,000 14C yr B.P. packrat midden series from the USA–Mexico borderlands. Quaternary Research 60, 319–329.
Kerr, R.A., 2000. A North Atlantic climatic pacemaker for the centuries. Science 288, 1984–1986.
Liu, J., et al., 2007. Complexity of coupled human and natural systems. Science 317, 1513–1516.
Magilligan, F.J., Goldstein, P.B., Fisher, G.B., Bostick, B.C., Manners, R.B., 2008. Late Quaternary hydroclimatology of a hyper-arid Andean watershed: Climate change, floods, and hydrologic responses to the El Niño-Southern Oscillation in the Atacama Desert. Geomorphology 101, 14–32.
Meeker, L.D., Mayweski, P.A., 2002. A 1400-year high-resolution record of atmospheric circulation over the North Atlantic and Asia. The Holocene 12.3, 257–266.
Meko, D.M., Woodhouse, C.A., Baisan, C.A., Knight, T., Lukas, J.J., Hughes, M.K., Salzer, M.W., 2007. Medieval drought in the upper Colorado River Basin. Geophysical Research Letters 34, L10705. doi:10.1029/2007GL029988.
Metcalfe, S., Say, A., Black, S., McCulloch, R., O'Hara, S., 2002. Wet conditions during the Last Glaciation in the Chihuahuan Desert, Alto Babícora Basin, Mexico. Quaternary Research 57, 91–101.
Meyer, E.R., 1973. Late Quaternary paleoecology of the Cuatro Cienegas Basin, Coahuila, Mexico. Ecology 54, 982–995.
Moy, C.M., Seltzer, G.O., Rodbell, D.T., Anderson, D.M., 2002. Variability of El Niño/Southwestern Oscillation activity at millennial timescales during the Holocene epoch. Nature 420, 162–165.
Muhs, D.R., Reynolds, R.L., Been, J., Skipp, G., 2003. Eolian sand transport pathways in the southwestern United States: importance of the Colorado River and local sources. Quaternary International 104, 3–18.
Nelson, B.A., 1997. Chronology and stratigraphy of La Quemada, Zacatecas, Mexico. Journal of Field Archaeology 24, 85–109.
Nordt, L.E., 2003. Late Quaternary fluvial landscape evolution in desert grasslands of northern Mexico. Geological Society of America Bulletin 115, 596–606.
Nordt, L.E., 2004. Late Quaternary alluvial stratigraphy of a low-order tributary in central Texas, USA and its response to climate and sediment supply. Quaternary Research 62, 289–300.
O'Hara, S., Street-Perrott, F.A., Burt, T.P., 1993. Accelerated soil erosion around a Mexican highland lake caused by Prehispanic agriculture. Nature 362, 48–51.
Ortega-Ramírez, J.R., Valiente-Banuet, A., Urrutia-Fucugauchi, J., Mortera-Gutiérrez, C.A., Alvarado-Valdez, G., 1998. Paleoclimatic changes during the Late Pleistocene–Holocene in Laguna Babícora, near the Chihuahuan Desert, Mexico. Canadian Journal of Earth Sciences 35, 1168–1179.
Peng, C.H., Guiot, J., Van Campo, E., 1998. Estimating changes in terrestrial vegetation and carbon storage: the use of regression analyses. Quaternary Science Reviews 17, 719–735.
Poore, R.Z., Pavich, M.J., Grissino-Mayer, H.D., 2005. Record of the North American southwest monsoon from Gulf of Mexico sediment cores. Geology 3, 209–212.
Reimer, P.J., et al., 2004. IntCal04 terrestrial Radiocarbon age calibration 0–26 cal kyr BP. Radiocarbon 46, 1029–1058.
Richey, J.N., Poore, R.Z., Flower, B.P., Quinn, T.M., 2007. 1400 yr multiproxy record of climate variability from the northern Gulf of Mexico. Geology 35, 423–426.
Rotnicki, K., 1983. Modelling past discharges of meandering rivers. In: Gregory, K.J. (Ed.), Background to Paleaohydrology. Wiley, New York, pp. 321–354.
Schulte, E.E., Hopkins, B.G., 1996. Estimation of soil organic matter by weight-loss-on-ignition. Soil Organic Matter: Analysis and Interpretation. Soil Science Society America Special Publication Number, vol. 46, pp. 357–373.
Sirocko, F., Sarnthein, M., Erlenkeuser, H., Lange, H., Arnold, M., Duplessy, J.C., 1993. Century-scale events in monsoonal climate over the past 24,000 years. Nature 364, 322–324.
Smith, J.H., 1919. The War with Mexico. Macmillan, New York.
Stager, J.C., Ruzmaikin, A., Conway, D., Verburg, P., Mason, P.J., 2007. Sunspots, El Niño, and the levels of Lake Victoria, East Africa. Journal of Geophysical Research 112 (D15). doi:10.1029/2006JD008362.
Thomas, M.F., 1974. Tropical Geomorphology: A Study in Weathering and Landform Development in Warm Climates. Macmillan, London.
USDA, 1999. Soil Taxonomy: A Basic System of Making and Interpreting Soil Surveys. United States Department of Agriculture, Washington, DC.
Van Devender, T.R., 1990. Late Quaternary vegetation and climate of Chihuahuan Desert, United States and Mexico. In: Betancourt, J.L., Van Devender, T.R., Martin, P. (Eds.), Packrat Middens: The Last 40,000 years of Biotic Change. Univ. Arizona Press, Tucson, pp. 105–133.
Waters, M.R., 1988. Holocene alluvial geology and geoarchaeology of the San Xavier reach of the Santa Cruz River, Arizona. Geological Society of America Bulletin 100, 479–491.
Waters, M.R., Nordt, L.G., 1995. Late Quaternary floodplain history of the Brazos River in east–central Texas. Quaternary Research 43, 211–319.